A ROLE FOR THE CRL4-WDTC1 E3 LIGASE IN THE SUPPRESSION OF ADIPOGENESIS

Beezly Sultana Groh

A dissertation submitted to the faculty of the University of North Carolina at Chapel Hill in partial fulfillment of the requirements for the degree of Doctor of Philosophy in the Department of Biochemistry and Biophysics.

Chapel Hill
2013

Approved by:

Yue Xiong

William F. Marzluff

Henrik G. Dohlman

Robert J. Duronio

Michael B. Major

ABSTRACT

Beezly Sultana Groh: A Role For The CRL4-WDTC1 E3 Ligase In The Suppression Of Adipogenesis
(Under the direction of Yue Xiong)

Excess lipid accumulation in fat tissues underlies obesity and a myriad of associated pathologies that range from type 2 diabetes to cancer. Lipid synthesis in adipocytes, the primary cells of fat tissues, is regulated via extracellular and intracellular mechanisms. *WDTC1* encodes an evolutionarily conserved suppressor of lipid accumulation in multicellular organisms. Decreased *WDTC1* expression is associated with obesity in mice and humans. Yet, the molecular mechanism underlying its anti-obesity function remains elusive. WDTC1 is a candidate DWD protein (DDB1 binding WD40 repeat protein) that potentially functions as a substrate specificity factor for a cullin 4 E3 ligase (CRL4) complex. I hypothesized that WDTC1 mediates its anti-adipogenic effect through targeting substrates for ubiquitylation by the CRL4 complex. In this dissertation, I aim to understand the molecular function of WDTC1 in adipogenesis. I demonstrate that WDTC1 is indeed a CRL4 substrate receptor and its interaction with a CRL4 complex is central to its function. Using 3T3-L1 cell culture model of adipogenesis, I show that WDTC1 mutations disrupting its interaction with CRL4 impair the suppression of lipid accumulation and increase adipogenic gene expression. Rescue experiments demonstrate that the WDTC1 knockdown phenotypes can be rescued by ectopic expression of wild-type but not CRL4 binding mutants, underscoring the critical importance of the CRL4-WDTC1 interaction to the observed adipogenic suppression. In addition, I found that *Cul4a* knockout mice exhibit defects analogous to those reported in *Wdtc1*$^{+/-}$ mice, such as adipocyte hypertrophy and poor metabolic parameters. Mechanistically, I examined whether WDTC1 plays a role in transcriptional control. I provide

evidence that the $CRL4^{WDTC1}$ complex promotes histone H2AK119 monoubiquitylation, an epigenetic modification that is associated with transcriptional silencing. Hence, I propose that $CRL4^{WDTC1}$ E3 ligase may mediate its anti-adipogenic effect, at least in part, by repressing a subset of proadipogenic genes through histone H2AK119 monoubiquitylation. I also describe proteomic screens in 3T3-L1 cells to identify WDTC1 interacting proteins via mass spectrometry. Collectively, this work reveals a function of the $CRL4^{WDTC1}$ complex in adipogenesis and provides a potential mechanism by which WDTC1 suppresses lipid accumulation in adipocytes.

To my Mommi and Bappi, Mom and Dad Groh, Kristopher, Jack and family

ACKNOWLEDGEMENTS

I would first like to thank my mentor, Dr.Yue Xiong, for his support and guidance throughout my dissertation research. I am thankful for the confidence he had in my scientific ability, which gave me this amazing opportunity to independently design and pursue my own research project. Most of all, I am thankful for all the ways he challenged me to meet my individual potential as a scientist. I also thank members of my committee Drs. Henrik Dohlman, Robert Duronio, Ben Major and Bill Marzluff, for their helpful suggestions, encouragement and support over the years. I especially thank Dr. Bill Marzluff for supporting me from the beginning and meeting with me whenever research aims became intractable. Lastly, I thank past and present members of the Xiong laboratory. I had the rare opportunity to work with not only some very talented scientists, but also genuinely wonderful people.

On a personal note, the unconditional love of my parents continues to shape the person I am—words fail me, but you two have loved and supported me all my life and I am beyond grateful for everything. I am also eternally thankful for the love and support of my parents-in-laws. To my brother Rezai, members of my family and friends, thank you for being there for me with great understanding and support. My Jack's playfulness always reminds me to live in the now. Lastly, my love Kris' infinite inspiration and outstanding patience gave me the courage to pursue this goal. Thank you for always helping me find the parts of me that would not give up when things got impossibly tough.

TABLE OF CONTENTS

LIST OF TABLES

LIST OF FIGURES

LIST OF ABBREVIATIONS

CAND1	Cullin-associated Nedd8-dissociated 1
CDT	Chromatin licensing and DNA replication factor
CRL	Cullin RING E3 ligase
CSA	Cockayne syndrome gene A
CSB	Cockayne syndrome gene B
CSN	COP9 signalosome
CUL	Cullin
DCAF	DDB1-CUL4 associated factors
DDB	Damaged DNA Binding
DUB	Deubiquitinating enzyme
DWD	DDB1-binding WD40 protein
E1	Ubiquitin activating enzyme
E2	Ubiquitin conjugating enzyme
E3	Ubiquitin ligase
EV	Empty vector
FAS	Fatty acid synthase
HA	Hemagglutinin
HDAC	Histone deacetylase
HECT	Homologous to the E6AP Carboxyl Terminus
IB	Immunoblot
IP	Immunoprecipitation
kDa	Kilodalton

LC-MS	Liquid chromatography–mass spectrometry
MEF	Mouse embryonic fibroblast
NEDD8	Neural precursor cell expressed, developmentally downregulated 8
NER	Nucleotide excision repair
PCNA	Proliferating Cell Nuclear Antigen
PRC	Polycomb repressive complex
RING	Really interesting new gene
RNAi	Ribonucleic Acid (RNA) interference
ROC	RING of cullins
SDS-PAGE	Sodium dodecyl sulfate-polyacrylamide gel electrophoresis
shRNA	Small hairpin RNA
siRNA	Small interfering RNA
TPR	Tetratricopeptide repeat
Ub	Ubiquitin
UBE1	Ubiquitin-activating enzyme 1
UBE2D3	Ubiquitin-conjugating enzyme E2 D3
WCE	Whole cell extract
WD40	Tryptophan-aspartic acid domain-40 amino acid residues
WDTC1	WD40 and tetratricopeptide repeats 1
XPC	Xeroderma pigmentosum C group protein

CHAPTER 1: INTRODUCTION

Summary

Protein posttranslational modification constitutes a key regulatory mechanism to control the function and composition of the proteome and thereby, underlies all biological processes. Proteins can be modified by the addition of small chemical groups such as phosphate, methyl and acetyl groups or by the addition of small proteins such as ubiquitin, SUMO1 and NEDD8. Of particular interest is protein modification with ubiquitin, a highly conserved 76 amino acid (8.5 KDa) protein that is ubiquitously present in all eukaryotes but absent in bacteria and archaea. Ubiquitin can be covalently attached to substrate protein or to another ubiquitin through sequential enzymatic activities, a process termed ubiquitylation. Since its discovery nearly 40 years ago in the covalent modification of histone H2A, ubiquitylation has emerged as a widely utilized modification to alter properties of a protein, including stability, activity, localization and interactions. As such, protein ubiquitylation has a critical role in essentially all cellular processes.

Protein post translational modification with ubiquitin

In mammals, ubiquitin is encoded by four different genes (*UBB*, *UBC*, *UBA52* and *RPS27A*). While *UBB* and *UBC* encode several copies of ubiquitin in a tandem configuration, *UBA52* and *RPS27A* encode a single copy of ubiquitin fused to ribosomal proteins L40 and S27a, respectively (Varshavsky, 2006). Accordingly, ubiquitin is initially synthesized as an inactive precursor. Specific isopeptidases called deubiquitinases (DUBs) cleave precursor ubiquitin fusion proteins at their C-termini into conjugation competent monomeric units (Jonnalagadda et al., 1989). Ubiquitin possesses two key functional features, a conserved C-terminal diglycine motif (G75 and G76) and seven lysine residues (K6, K11, K27, K29, K33, K48 and K63). The diglycine motif is required for ubiquitin conjugation since the carboxyl group of G76 is the site of covalent conjugation to substrate lysine or lysine residue of another ubiquitin (Pickart and Eddins, 2004). All seven internal lysine residues, as well as the N-terminal methionine (M1), of the ubiquitin monomer are cellular substrates for conjugation to the G76 carboxyl group of a donor ubiquitin, which yield ubiquitin polymers or polyubiquitin chains (Kulathu and Komander, 2012).

Although many mechanistic details of ubiquitylation are still impending, much of the identification and characterization of the enzymes involved in the catalysis of the chemical steps were carried out by the Hershko laboratory in the early 1980s. Ubiquitylation proceeds through a concerted enzymatic cascade comprising an E1 ubiquitin activating enzyme, an E2 ubiquitin conjugating enzyme, and an E3 ubiquitin ligating enzyme (Hershko, 1983; Pickart, 2004) (Figure 1.1A). E1 and E2 enzymes catalyze the ATP-dependent activation and conjugation of ubiquitin, while E3s confer reaction specificity through substrate recruitment and facilitate ubiquitin transfer by bridging the interaction between substrates and E2s.

Ubiquitylation is initiated by the activation of conjugation competent ubiquitin via a two-step reaction catalyzed by the E1 activating enzyme (Kerscher et al., 2006; Pickart, 2001a). By coupling ATP hydrolysis, E1 first adenylates the C-terminal carboxyl group of ubiquitin, leading to the formation of a high energy ubiquitin-adenylate intermediate. This

intermediate is subsequently the substrate for attack by the sulfhydryl group of the E1 catalytic cysteine, and thus resulting in the formation of a thioester linkage between E1 and ubiquitin (E1-Ub). Formation of the E1-Ub complex induces structural changes that expose cryptic E2 binding sites in E1, promoting its binding to an E2 conjugating enzyme (Ye and Rape, 2009). In the second step of the ubiquitylation reaction, ubiquitin is transferred from the E1-Ub to E2 through a transthiolation reaction involving the C-terminus of ubiquitin and the E2 catalytic cysteine, resulting in the formation of the E2 and ubiquitin thioester complex (E2-Ub). In the final enzymatic step of the ubiquitin conjugation reaction, charged E2-Ub can directly transfer ubiquitin to a substrate protein, but more commonly, E2-Ub combines with an E3 ligase which recruits a specific protein for ubiquitylation. Lastly, ubiquitin is conjugated to a lysine residue in target protein or acceptor ubiquitin through the formation of an isopeptide bond between the C-terminal glycine carboxyl group of ubiquitin and the target lysine ε-amino group of substrate. Although noncanonical, the N-terminal α-NH2 group of the substrate can also be modified by ubiquitin, as well as serine and threonine hydroxyl and cysteine thiol groups of target proteins (McDowell and Philpott, 2013).

Substrates can be monoubiquitylated through the conjugation of a single ubiquitin monomer, mulitiply monoubiquitylated, or polyubiquitylated through repeated reactions that generate polymeric ubiquitin chains of distinct or mixed linkages (Komander and Rape, 2012; Ye and Rape, 2009) (Figure 1.1B). Polyubiquitylation generally targets proteins for proteolytic degradation via the 26S proteasome, while monoubiquitylation is linked to nonproteolytic functions ranging from protein trafficking to chromatin regulation (Hicke, 2001; Pickart, 2001b). Modification of substrate lysine without further modification to ubiquitin itself, referred to as the specificity of the monoubiquitylation reaction, is thought to be determined by a number of factors including structural constraints imposed by a particular substrate-E3 complex or specificity might be encoded by the distinct E2 or E3 pairings (Komander and Rape, 2012). Monoubiquitylation may be confined to a specific lysine residue as in the case of K119 in histone H2A or across a defined domain—the DNA binding domain of p53

transcription factor, for example. Polyubiquitylation can either proceed through either homotypic or heterotypic linkages (Kulathu and Komander, 2012). Polyubiquitin chains are homotypic when the donor ubiquitin is successively conjugated to the same residue in each acceptor ubiquitin (M1, K6, K11, K27, K29, K33, K48 or K63) during elongation. By contrast, polyubiquitin chains are referred to as heterotypic (branched and nonbranched) when assembled by mixed linkages or an array of atypical linkages. Although K48 and K63 linkages remain best characterized, all possible linkage types have been detected in mammalian cells and presently, their regulated assembly and biological significance is a subject of intensive research.

Ubiquitylated substrates are recognized by a large number of proteins that contain ubiquitin-binding domains (UBDs), which bind discreet interaction surfaces on ubiquitin (Husnjak and Dikic, 2012; Komander and Rape, 2012). UBDs may be broadly classified into α-helix based, zinc-finger based, plekstrin homology-like and ubiquitin conjugating (UBC)-like domains. Many UBDs preferentially bind a specific type of ubiquitin conjugate and can thus "decode" information encoded by differentially ubiquitylated substrates into the appropriate cellular response—the ubiquitin signal encoded by monoubiquitin versus polyubiquitin chains of specific and mixed linkages, for example. Similar to the reversal of phosphorylation by protein phosphatases, a family of DUBs (~95 in humans) cleaves conjugated ubiquitin from substrates, thus rendering ubiquitylation a highly dynamic and reversible posttranslational modification (Kulathu and Komander, 2012). Collectively, the type of ubiquitin modification, the ubiquitin binding proteins that decode the signal carried by a distinct conjugate and the DUBs that dynamically regulate the ubiquitylated proteome constitute the "ubiquitin code" and determine the functional outcome of substrate ubiquitylation (Husnjak and Dikic, 2012; Komander and Rape, 2012).

Enzymes of the ubiquitylation cascade

The ubiquitin conjugation system is hierarchically organized with the mammalian genome encoding 2 E1s, 28 active E2s and a large array of E3 ligases that is estimated to exceed 600 (Deshaies and Joazeiro, 2009; Groettrup et al., 2008; Pickart, 2001a). This organizational hierarchy is predicted to increase specificity through additional regulation and generate functional diversity in the ubiquitin system. Examples illustrating this include the exquisite linkage specificity achieved by several E2 enzymes through differential positioning of ubiquitin in their active sites or when the specific E2-E3 interactions dictate substrate monoubiquitylation versus polyubiquitylation (Komander and Rape, 2012).

The canonical cascade for protein ubiquitylation involves ubiquitin activation by the E1 UBE1. However, the recent identification of a second E1 enzyme UBE1l2 (Chiu et al., 2007; Jin et al., 2007; Pelzer et al., 2007), a dual system of ubiquitin activation, adds an unexpected level of regulation in the ubiquitin pathway. The two E1s exhibit different specificities towards E2s, partly owing to subtle differences in their ubiquitin fold domains which recruit E2s. While all E2s except USE1 can be charged by UBE1, UBE1l2 charges a small cohort of E2s but specifically charges USE1 with ubiquitin. Consistent with the notion that UBE1l2 promotes a discreet subset of ubiquitylation reactions, UBE1l2 mice are embryonic lethal likely due to altered neuronal development (Chiu et al., 2007; Lee et al., 2013).

The 28 E2 ubiquitin conjugating enzymes (UBE2s) can be grouped into monoubiquitylating, chain initiating or chain elongating E2s (Kulathu and Komander, 2012). A common feature shared by all active E2s is a core ubiquitin-conjugating domain (UBC) comprising ~150 residues, which binds E1s and includes the catalytic cysteine as well as a conserved asparagine residue at the active site. Although E2 enzymes are critical to ubiquitylation reactions, their substrate affinity in the absence of an E3 is too low for efficient and specific ubiquitylation (Rodrigo-Brenni et al., 2010). Most E2s engage a number of different E3s to ubiquitylated substrates (UBE2D, for example), but a few exclusive

physiological E2-E3 pairs have been characterized (such as APC/C and UBE2S) (Ye and Rape, 2009). While some E2s dictate structure of the ubiquitin modification (mono- vs polyubiquitylation) and confer linkage specificity to polyubiquitin chains, substrate specificity is largely dictated by the E3 ligase. Nevertheless, E2s add functional versatility to the ubiquitin system by modulating the type of ubiquitin modification, and therefore the biological outcome of substrate ubiquitylation.

The large number of E3 ligases is thought to reflect the specific targeting of an even larger number of cellular proteins by the ubiquitin system (Pickart, 2001a). In addition to conferring substrate specificity, E3s generally serve a scaffolding role to bridge the interaction between a substrate lysine and the E2-Ub intermediate to facilitate efficient ubiquitylation. As such, a shared property of all E3 ligases is distinct substrate and E2 binding domains, which may be included in a single protein or comprise distinct subunits. There are two mechanistically distinct classes of E3 ligases: HECT (homology to E6AP C-terminus) domain and RING (really interesting new gene) domain families (Figure 1.1A). To note, there are at least two other subfamilies of E3s: the U-box (*U*FD2 homology) which is structurally similar to RING E3s and the recently classified RBR (RING-in-between-RING) E3s which are RING/HECT hybrids (Kulathu and Komander, 2012).

Named after the founding member E6AP protein, the mammalian genome encodes ~30 HECT domain E3 ligases (Metzger et al., 2012). Substrate ubiquitylation by HECT E3s follows a covalent mechanism. Their C-termini contain the conserved ~40 kDa (~350 amino acids) HECT domain, while variable N-termini mediate substrate recognition. The HECT domain has a bilobal architecture consisting of an E2 interacting N-lobe and a C-lobe that harbors the active site cysteine. Ubiquitylation proceeds through an obligate transfer of ubiquitin from E2-Ub to the catalytic cysteine of HECT E3 by a transthiolation reaction. Following the formation of the HECT E3-Ub thioester intermediate, ubiquitin is directly conjugated to a target substrate. Nearly a third of the HECT E3s belong to the NEDD4 family

and among their diverse functions, HECT E3s regulate the trafficking of many receptors, transporters and channels (Rotin and Kumar, 2009).

The RING family comprises the vast majority of E3 ligases with the mammalian genome potentially encoding over 600 RING proteins (Deshaies and Joazeiro, 2009). Unlike HECT E3s, RING E3s do not transfer ubiquitin directly to substrate. Instead, RING E3s minimally function in "catalysis by proximity" by simultaneously binding the targeted substrate and the E2-Ub conjugate (Pickart and Eddins, 2004). The catalytic step involves a nucleophilic attack by the substrate lysine ε-amino group on the E2-Ub reactive thioester bond, resulting in isopeptide bond formation between substrate and ubiquitin. In addition to its scaffolding role, RING E3s may induce subtle conformational changes in E2s to stabilize the transition state intermediate (an oxyanion) of the ubiquitin conjugation reaction (Deshaies and Joazeiro, 2009; Ye and Rape, 2009). Structurally, RING E3s share a domain (~70 amino acids) of distinctively spaced histidine and cysteine residues which coordinate two zinc cations, forming a 'cross-brace' structure termed the RING domain. RING E3s either possess an intrinsic RING domain or contain a separate RING domain subunit. The RING domain binds the E2-Ub conjugate while a separate domain or subunit mediates specific recruitment of diverse substrates. As such, RING E3s can function as monomers or in the context of multisubunit complexes. The cullin family of RING E3 ligases typify multisubunit assemblies and is the subject of remaining discussion on E3 ligases.

The cullin family of RING E3 ligases

The evolutionarily conserved cullin RING ligases (CRLs) represent the largest known family of E3 ligases (Deshaies and Joazeiro, 2009; Petroski and Deshaies, 2005; Sarikas et al., 2011). The CRL enzymatic core contains a cullin protein which functions as a molecular scaffold to assemble a substrate targeting module and a ubiquitin conjugation module into a single multisubunit complex. Among their diverse functions, CRLs have key roles in cell cycle control, signal transduction, development, and DNA replication, repair and transcription.

Mammals encode six canonical (CUL1, CUL2, CUL3, CUL4A, CUL4B and CUL5) and three distantly related (CUL7, CUL9 and APC2) cullin proteins. With the exception of CUL7 and CUL9—which evolved more recently in the common chordate ancestor, cullin orthologs are present in *Drosophila melanogaster* (5), *Caenorhabditis elegans* (6), *Arabidopsis thaliana* (5) and yeast (3). Structurally, cullins are characterized by three key features: a highly conserved C-terminal cullin-homology domain, an N-terminal domain containing a series of cullin repeats along with divergent sequences and a conserved lysine residue proximal to the cullin-homology domain (Figure 1.2). The following discussion will focus on the canonical cullins.

Although cullins do not possess an intrinsic RING domain, the CRL catalytic core includes ROC1 (for RING of cullins; also known as RBX1/HRT1), a zinc-binding RING-H2 domain subunit (Kamura et al., 1999b; Ohta et al., 1999; Seol et al., 1999; Tan et al., 1999). A notable exception is the CUL5-based complexes which preferentially include the related RING subunit ROC2 (discussion will refer to ROC1 for clarity). A highly conserved C-terminal globular domain in cullins harbors the cullin homology domain (~180 amino acids). At this domain, cullins bind ROC1 through an interlocking mechanism that tightly integrates the RING domain (Sarikas et al., 2011). ROC1 in turn recruits E2-Ub to form the active CRL conjugation apparatus. This modular assembly of a catalytic core is one of two defining structural features of CRL complexes, the substrate targeting module being the other.

On the basis of the crystal structures of CRL1 and CRL4 complexes (Angers et al., 2006; Zheng et al., 2002b), cullins have a arched but rigid stalk-like N-terminal domain that consists of three helical cullin repeats (CR1-CR3). This rigid architecture presumably positions the ROC1 bound E2-Ub at a proper distance from the substrate to promote efficient ubiquitin transfer. Indeed, inserting a linker in CUL1 to render flexibility to its N-terminal domain abolished CRL1 activity in vitro (Zheng et al., 2002b). Despite the anticipated structural conservation among cullin proteins, the very N-terminal sequences in each cullin is quite divergent. The latter provides a structural explanation for the most striking feature of

cullins proteins—they each assemble distinct substrate targeting modules at their N-termini in a combinatorial manner to recruit structurally diverse substrates to a common catalytic core. The substrate targeting module comprises an interchangeable substrate receptor that binds substrate and thus dictates the substrate specificity of its cognate CRL complex and in most cases, a distinct adaptor protein that links the substrate receptor to the core complex. The multisubunit organization of the CRL complexes is shown schematically in Figure 1.3.

CUL1 is the founding member of the CRL E3 ligase family. Independent genetic studies on cell cycle control in *C. elegans* and *S. cerevisiae* led to the identification of CUL1 and the cullin gene family (Kipreos et al., 1996; Mathias et al., 1996), and set the stage for the subsequent discovery of the CUL1-based CRL1 complexes (also known as SCF complexes) (Feldman et al., 1997; Skowyra et al., 1997). CRL1 complexes are composed of four subunits: CUL1 scaffold, ROC1 RING subunit, SKP1 adaptor and F-box containing proteins as variable substrate receptors. The F-box domain (~40 amino acid motif named after cyclin F where it was first identified) in the substrate receptor mediates binding to SKP1, which in turn links it to the CRL1 catalytic core (Bai et al., 1996). The human genome encodes 69 F-box proteins while the number of F-box proteins in other organisms ranges from 20 in *S. cerevisiae* to an astonishing 700+ in *A. thaliana* (Gagne et al., 2002; Skaar et al., 2009). The different combinations of F-box proteins generate a multitude of distinct CRL1 complexes and thereby greatly expand the diversity in substrate targeting by the CRL1 E3 ligase. This general principle applies to other CRLs (discussed below).

CUL2- and CUL5-based CRLs both utilize Elongin C as the adaptor, which binds the two cullins as a heterodimeric complex with Elongin B (Kamura et al., 2004). Although they share the same adaptor, CUL2 and CUL5 each assemble distinct complexes by interacting with two separate classes of substrate receptors. Elongin C binds proteins with two similar motifs: von Hippel-Lindau (VHL)-box and suppressor of cytokine-signaling (SOCS)-box. Yet, structural determinants within the VHL-box and SOCS-box direct their interaction with either CRL2 or CRL5, respectively, to differentially recruit substrates to cognate complex (Sarikas

et al., 2011). Examples of differential substrate recruitment by VHL-box and SOCS-box proteins includes proteolytic targeting of hydroxylated HIF-1α transcription factor by $CRL2^{VHL}$ complex (Ivan et al., 2001) and of antiviral protein APOBEC3G by the virally subverted $CRL5^{VIF}$ complex (Yu et al., 2003). CUL3-based CRL complexes uniquely omit an adaptor protein, instead binding directly to a class of substrate receptors through their Broad complex, Tramtrack, Bric-a-brac (BTB) domains (Furukawa et al., 2003; Geyer et al., 2003; Pintard et al., 2003; Xu et al., 2003). Although this direct binding may implicate that nearly all BTB proteins potentially assemble into CRL3 complexes, as is the apparent case for all three *S. cerevisiae* BTB proteins, this has yet to be experimentally verified for the large number of BTB proteins present in higher organisms (humans encode over 400) (Pintard et al., 2004). CUL4-based CRLs employ a similar multisubunit assembly with the specific adaptor DDB1 and a distinct class of DDB1-binding substrate receptors (CRL4 complexes are discussed in detail in separate sections). Given their relatively recent discovery and the extraordinary number of diverse complexes that cullins potentially assemble in the cell (estimated 300-500 distinct CRLs), future research should be able to better define the functional repertoire of CRL E3 ligases.

Regulation of CRL RING E3 ligases

Despite the diversity in subunit composition and cellular function, the assembly and ubiquitin ligase activity of CRL complexes are similarly regulated by a regulatory cycle involving several mechanisms. All cullins are covalently modified by the ubiquitin-like protein NEDD8 (~60% identity with ubiquitin) at a conserved lysine residue in their C-termini, proximal to the cullin homology domain (Hori et al., 1999). The NEDD8 conjugation (termed neddylation) drives the formation of active CRL E3 complexes and is essential for their function in mammalian cells (Bosu and Kipreos, 2008). Underlying the activating function, neddylation induces a conformation change in cullins such that it optimally reorients the ROC1 bound E2-Ub at the C-terminus towards the N-terminally bound substrate, thereby

facilitating ubiquitin transfer across a ~50 Å gap (Duda et al., 2008; Saha and Deshaies, 2008). Indeed, cullins appear to be the primary substrates of the NEDD8 conjugation pathway. Similar to ubiquitylation, neddylation comprises an enzymatic cascade which includes the NEDD8-activating E1 enzyme NAE (NAE1/UBA3 heterodimer) and the NEDD8-conjugating E2 enzymes UBE2M/UBE2F. Although not essential for in vivo neddylation reactions, DCN1 interacts with cullin bound ROC1 and possibly functions as a NEDD8 E3 ligase (Kamura et al., 1999a; Kurz et al., 2008; Yang et al., 2007). Demonstrating the importance of neddylation to CRL4 activity, a small molecule inhibitor of NAE, MLN4924, was recently developed to disrupt CRL function in human tumor cells and is currently in clinical trials (Soucy et al., 2009).

Analogous to deubiquitylation, cullin neddylation is reversed by the multisubunit COP9 signalosome (CSN) complex (termed deneddylation), thus converting active CRLs into inactive complexes (Lyapina et al., 2001). The CSN5 subunit encodes a critical metalloprotease active site for the isopeptidase activity towards neddylated cullins (Cope et al., 2002). Another key player in the regulation of CRL complexes is CAND1 (or TIP120A), which interacts with unneddylated cullins and in a mutually exclusive manner with cullin substrate receptors (Hwang et al., 2003; Liu et al., 2002; Min et al., 2003; Oshikawa et al., 2003; Zheng et al., 2002a). Mechanistically, CAND1 was proposed to inactivate cullins through a sequestration based mechanism. Indeed, the crystal structure of CAND1-CUL1-ROC1 complex shows that CAND1 forms an inhibitory complex with CUL1 that simultaneously masks the neddylation site and the adaptor binding site (Goldenberg et al., 2004). In this regulatory cycle, cullin neddylation displaces bound CAND1 and prevents re-association, thus enabling CRL activation and substrate recruitment by associated substrate receptors.

While biochemical and structural studies demonstrated that CSN and CAND1 negatively regulate CRL4 complexes, a more complicated and even seemingly paradoxical picture emerged from genetic studies. First, genetic ablation of CSN components

phenocopies the loss of cullin function in multiple organisms and despite the increase in neddylated cullins, CSN inactivation impairs the activity of CUL1, CUL3 and CUL4-based complexes (Bosu and Kipreos, 2008; Petroski and Deshaies, 2005). Similarly, CAND1 inactivation in *Arabidopsis* and human cells suggested it is a positive regulator of cullin function. To reconcile these disparate findings, a number of models have been proposed (Bosu and Kipreos, 2008). First, a cycle of neddylation/deneddylation prevents proteolytic degradation of substrate receptors, which are frequently autoubiquitylated by their cognate CRL after ubiquitylation of target substrate is completed. In this view, sustained neddylation of cullins may promote 'instability' of select substrate receptors and thereby limit their availability. Consistent with this model, depletion of CSN5 resulted in both a failure to deneddylate CUL1 and the accumulation of CRL1 substrates, presumably from decreased stability of substrate receptors (Cope and Deshaies, 2006). Second, assembly of functionally distinct CRL complexes must require regulated substrate receptor exchange. A recent study suggests CAND1 facilitates assembly of new and rare CRL1 complexes by promoting the dissociation of pre-existing or high affinity F-box substrate receptors in exchange for new or less abundant F-box proteins (Pierce et al., 2013). It should be noted that an alternative model favors that substrate receptor abundance drives neddylation and the formation of active CRL complexes, and suggests neddylation-CSN-CAND1 cycle accounts for a minor fraction of CRL regulation (Bennett et al., 2010). Clearly, multiple layers of regulation are present to control the assembly of distinct CRL complexes to dynamically respond to cellular conditions.

CRL4 complexes

The core CRL4 complex comprises either CUL4A or CUL4B as the scaffold (collectively referred to as CUL4), ROC1 as the RING subunit in trans and DDB1 (DNA damage binding 1) as the CUL4 specific adaptor. DDB1 is evolutionarily conserved from *Arabidopsis* to humans, and it is essential in mammals and *Drosophila* but not in organisms

with DDB1 orthologs, such as *A. thaliana and S. pombe*. DDB1 was first characterized as a DNA damage sensor that functions in a heterodimeric complex with DDB2 to recognize UV-induced DNA lesions in the nucleotide excision repair (NER) pathway (Chu and Chang, 1988). A decade later, in an attempt to characterize DDB1-DDB2 interacting proteins, DDB1 was found to interact with CUL4A (Shiyanov et al., 1999). The pleiotropic effects uncovered by genetic studies of DDB1 mutants in model organisms implicated that DDB1 is a multifunctional protein with roles beyond DNA damage repair (Jackson and Xiong, 2009). Finally, the presence of DDB1 in several distinct CUL4 complexes including those containing DDB2 and CSA established a role for DDB1 as the adaptor for CUL4 E3 ligases (Groisman et al., 2003; Hu et al., 2004; Sugasawa et al., 2005; Wertz et al., 2004), and thus accounted for its pleiotropic effects.

Structurally distinct, DDB1 is a large protein (127 kDa) containing three β-propeller domains (BPA-BPC; spanning 100 Å) compared with the small size and structural complexity of all other cullin adaptors (<20 kDa) (Li et al., 2006). Additionally, cullin adaptors (SKP1, Elongin C or BTB substrate receptors) share sequence homology with each other and share a common structural element termed the SKP1/BTB/POZ fold to interact with their cognate cullin N-terminus (Sarikas et al., 2011). DDB1 does not contain this recognition fold. The flexibly linked BPB domain of DDB1 binds the N-terminus of CUL4, while the BPA-BPC domains form a rigid double propeller fold (resembling a clam shell) and was initially believed to function in substrate presentation (Li et al., 2006). The structural complexity and variation in cullin-adaptor interaction seen with CUL4-DDB1 possibly reflect the requirement for multiple interaction surfaces to accommodate structurally diverse receptors, or to bind cofactors for efficient CRL4 activity, or both.

Despite DDB1 firmly established as the adaptor for CRL4 complexes, substrate recruitment mechanism for CUL4-based complexes remained elusive. It was reasonably anticipated that like other CRLs, CRL4 complexes are assembled with its own class of substrate receptors. The discovery that two separate DDB1 binding proteins, WD40 proteins

DDB2 and CSA, assembled into identical CRL4 complexes strongly hinted at this possibly (Groisman et al., 2003). Further supporting this proposition were the findings that XPC and CSB were substrates of $CRL4^{DDB2}$ and $CRL4^{CSB}$ complexes, respectively (Groisman et al., 2006; Sugasawa et al., 2005). A pattern emerged that suggested the involvement of a shared structural motif when a third WD40 protein, CDT2, was reported to target replication licensing factor CDT1 for CRL4-mediated proteolysis (Higa et al., 2006a; Ralph et al., 2006; Sansam et al., 2006). Ultimately, combined proteomic, structural and biochemical approaches to systematically search for specificity factors led to the identification of a diverse family of WD40-repeat proteins as putative substrate receptors of CRL4 complexes (Angers et al., 2006; He et al., 2006; Higa et al., 2006b; Jin et al., 2006). These four independent studies collectively identified 52 DDB1 binding WD40 proteins (referred to as DWDs hereafter; also referred elsewhere as DCAFs for DDB1-CUL4 associated factors or CWDs for CUL4-DDB1 associated WDRs).

WD40 repeats are structural motifs of ~40 amino acids that are characterized by the frequent occurrence of a glycine-histidine (GH) dipeptide and a tryptophan-aspartic acid (WD) dipeptide at the end of the repeat. WD40 domain proteins typically contain several tandem or intervening WD40 repeats that often fold into a circular β-propeller structure. Search for a signature motif that defines DWDs led to the identification of a submotif within WD40 repeats, termed “WDXR”; comprises the WD dipeptide followed an X (any residue)-arginine/lysine dipeptide. More extensive sequence analyses yielded the “DWD-box”, a 16 residue stretch terminating in the WDXR motif (He et al., 2006). Most DWD proteins contain at least one, frequently two tandem and rarely, three DWD boxes. A disease derived mutation in the WDXR of DDB2 (R273H) impairs its DDB1 binding (Rapic-Otrin et al., 2003; Shiyanov et al., 1999), underscoring the importance of this arginine in WDXR. Surprisingly, the crystal structure of the *D. rerio* DDB1-DDB2 complex revealed that the corresponding residue (R309) did not directly contact DDB1 but it may contribute to DNA binding and stabilize a propeller blade in DDB2 (Scrima et al., 2008). Although the WDXR is important for

the interaction between many DWD proteins and DDB1, not all DWDs contain a WDXR motif (Jin et al., 2006). Moreover, mutational analysis revealed that while many DWDs interact with DDB1 though its BPC domain, different BPC surfaces are utilized (Jin et al., 2006). These observations highlight the possibly that multiple sequence and structural elements determine the association between DWDs and DDB1. Indeed, the H-box, a recently discovered structural motif found in seven DWD proteins, is likely to be important for their association with DDB1 but this has yet to be experimentally tested for all H-box containing DWDs (Li et al., 2010).

Results from the four studies clearly demonstrated that only a subset of the ~300 WD40 proteins encoded by the human genome interacts with DDB1. Database searches of the DWD box motif estimated ~90 unique DWD proteins are present in human cells (He et al., 2006). Besides WD40 domain, the array of presumptive functional domains in DWDs, ranging from bromodomain to tetratricopeptide, predicts the versatility of the CRL4 core complex. The interaction between DDB1 and the 52 DWDs has been confirmed, but primarily through transient overexpression followed by immunoprecipitation experiments. Importantly, the functional interaction between CRL4 and DWDs remains unexplored for the vast majority of them. As such, a key question regards whether all or most DWDs function as substrate receptors for CRL4 complexes to specify ubiquitylation of distinct substrates. Systematic validation of the putative substrate receptors will certainly require linking specific CRL4 complexes to biological processes and identifying the physiological substrates through combined genetic, proteomic and biochemical approaches. Nevertheless, given the extraordinary number of distinct CRL4 complexes that may be assembled in the cell, it is reasonable to anticipate that these DWDs potentially extend the functional range of the CRL4 catalytic core. Elucidating the molecular function of one DWD protein, WDTC1 (also known as DCAF9), is the primary focus of my dissertation research.

Chromatin related functions of CRL4 complexes

Besides the well established role for DDB1 in DNA repair, early genetic analysis of CUL4 deletion mutants in several organisms overwhelmingly implicated a role for CUL4 in chromatin regulation (Jackson and Xiong, 2009). Deleting *cul4* (or *pcu4*) in *S. pombe* resulted in a viable but slow growth phenotype and two obvious phenotypes: abnormally elongated cells and decondensed chromatin (Osaka et al., 2000). The later discoveries that *S. pombe* cul4 interacts with Clr4 histone H3K9 methyltransferase to maintain heterochromatin and is required for S-phase destruction of Cdt1 at least partially accounts for the decondensed chromatin and growth retarded phenotypes of *Δcul4* cells, respectively (Horn et al., 2005; Jia et al., 2005; Ralph et al., 2006). RNAi-mediated inactivation of *cul4* in *C. elegans* causes growth arrest at the L2 larval stage and severe polyploidy arising from massive re-replication of the genome (Zhong et al., 2003). A failure to effect S phase-coupled degradation of CDT1 (replication licensing factor) explained the re-replication in *cul4* RNAi cells. Known CRL4 substrates are listed and those related to chromatin based processes are indicated in bold (Table 1.1). The following discussion with focus on reports that directly link CUL4 to chromatin related functions: DNA damage repair, replication and transcriptional regulation.

CRL4 in the maintenance of genome integrity

At least two substrate receptors of CRL4 complexes are mutated in human hereditary diseases: DDB2 in xeroderma pigmentosum E group (XPE) and CSA in Cockayne syndrome, both diseases are associated with a defect in NER. In response to UV-induced helix-distorting DNA damage, DDB2 and CSA each function in separate NER pathways, global genome repair (GGR) and transcription coupled repair (TCR), respectively. In GGR, $CRL4^{DDB2}$ is rapidly recruited to site of damage following UV. In turn, DDB2 recruits repair factor XPC to chromatin where both are polyubiquitylated by CRL4, but undergo different fates (Sugasawa et al., 2005). DDB2 ubiquitylation decreases its affinity for damaged DNA

(and presumably CRL4 as well), displaces it from chromatin and targets it for degradation (El-Mahdy et al., 2006). In contrast, XPC ubiquitylation increases its DNA binding affinity and is protected from degradation to carry out repair. Additionally, $CRL4^{DDB2}$ also have reported roles in histone H2A, H3 and H4 monoubiquitylation following UV irradiation to facilitate GGR, possibly through recruitment of repair factors (Kapetanaki et al., 2006; Wang et al., 2006). In TCR, $CRL4^{CSA}$ complex is recruited to chromatin through its interaction with CSB, but in a CSN bound inactive state (Groisman et al., 2006). The precise mechanism and order of events are still unclear but CSB is thought to link the DNA damage signal, marked by stalled RNAPII, to the recruitment of NER repair factors. Although it is unknown how $CRL4^{CSA}$ is activated following repair, CSB degradation is critical for restoring transcription post-TCR.

To maintain genome integrity, DNA replication must be restricted to only once per cell cycle. Of the checkpoint mechanisms evolutionarily conserved from *S. pombe* to humans, includes $CRL4^{CDT2}$-mediated degradation of CDT1 after S phase initiation to prevent re-replication and in response to DNA damage to prevent replication before damage repair. An interesting requirement of the $CRL4^{CDT2}$-mediated degradation of CDT1 is that only PCNA bound CDT1 is ubiquitylated (Arias and Walter, 2006; Jin et al., 2006). Through mutational analysis, sequences in CDT1 that specify its interaction with PCNA was identified and termed the “PIP-box” (for PCNA-interacting motif). Similar to CDT2 depletion, mutating the PIP-box results in a loss of $CRL4^{CDT2}$ chromatin recruitment, CDT1 stabilization and re-replication, indicating that the PCNA-CDT1 interaction is critical for $CRL4^{CDT2}$ recruitment to chromatin (Arias and Walter, 2006). Following this discovery, the PIP-box was demonstrated to be critically important for targeted degradation of other $CRL4^{CDT2}$ substrates including p21 CDK inhibitor, E2F1 transcription factor and SET8 histone methyltransferase (Abbas et al., 2010; Nishitani et al., 2008; Shibutani et al., 2008). As no other CRL4 complexes have been reported to require PCNA, this feature may be unique to $CRL4^{CDT2}$ substrates. It remains to be seen if other PIP-box proteins are also $CRL4^{CDT2}$ substrates and if the PCNA interaction is a shared mechanism for recruiting $CRL4^{CDT2}$ to chromatin.

CRL4 complexes in transcriptional regulation

Apart from directly targeting transcriptional regulators, recent reports indicate a role for CRL4 complexes in the direct regulation of chromatin dynamics—histone lysine methylation, in particular. Early studies in *S. pombe* showed that Cul4 recruits histone H3K9 methyltransferase Clr4 to maintain heterochromatin silencing (Horn et al., 2005; Jia et al., 2005). Although Cul4 ubiquitin ligase activity is evidently important for H3K9 methylation as neddylation defective Cul4 mutant cannot restore heterochromatin silencing, the activity linking Cul4 and Clr4 remains unknown. In mammalian cells, at least three DWD proteins have established roles in histone methylation: WDR5 and RBBP5 are core components of the MLL histone H3K4 methyltransferase complex (activates transcription) and EED is a component of EZH2 containing PRC2 H3K27 methyltransferase complex (silences transcription). One study reported that WDR5/RBBP5 and EED are functionally linked to CRL4 as depletion of DDB1 or CUL4A leads to a dramatic loss of H3K4 and H3K27 methylation (Higa et al., 2006b). However, the idea that CRL4-WDR5 functionally interact to promote H3K4 methylation is challenged by the finding that WDR5 itself is the ubiquitylation target of CRL4B and that rather than decreasing, the loss of CRL4B increases H3K4 trimethylation (H3K4me3) with the concomitant activation of gene transcription (Nakagawa and Xiong, 2011).

A recent study finally shed some light on a probable link between CRL4 activity and transcriptional regulation through direct alteration to chromatin structure. Histone H2AK119 and H2BK120 are the nucleosomal substrates of ubiquitylation, however, while H2AK119ub is associated with gene silencing, H2BK120ub activates transcription and is a prerequisite modification for H3K4me3 (Hammond-Martel et al., 2012). Polycomb complex PRC1 was once believed to be the sole E3 ligase for H2AK119; however, recent findings challenge this premise. Indeed, $CRL4B^{RBPB4/7}$ directly catalyzes H2AK119ub to silence transcription of a set of genes, including the tumor suppressor genes *PTEN* and *CDKN2A* (*p16*) (Hu et al., 2012). Additionally, this study shows that $CRL4B^{RBPB4/7}$-dependent H2AK119ub leads to PRC2

recruitment and H2K27me3 enrichment, revealing a crosstalk mechanism to tightly enforce gene silencing. In this example, the RBPB4/7 DWD protein is speculated to recruit CRL4B to chromatin and functions in the downstream recruitment of PRC2, thus connecting two distinct enzymatic activities on chromatin.

WDTC1 (Adipose), an anti-obesity factor and a putative CRL4 substrate receptor

More than half a century ago, Dr. Winifred W. Doane hypothesized that environmental conditions with marked nutrient shortage may select for mutations that enhance fat storage capacity. The rationale being that although deleterious under normal conditions, such alleles could provide a survival advantage in nutrient deprived conditions. During course of her doctoral dissertation work at Yale University, she isolated such a mutation in a wild *D. melanogaster* population from Sub-Saharan Kaduna, Nigeria. The most obvious phenotype she observed was massive hypertrophy of the fat body (fly fat organ) accompanied by “enormous oil globules”, and thus named the mutant “*adipose*” (*adp*) (Doane, 1960a). Not surprisingly, *adp* mutants exhibit a selective advantage in starvation survival tests (Doane, 1960b).

About forty years after characterizing the *adp* mutant phenotype, Dr. Doane collaborated with research groups in Germany to identify the *adp* gene (Hader et al., 2003). Comparative sequence analysis of open reading frames (ORFs) was performed between mutant and wild-type sequences within a 70 kb candidate region. Compared to the wild-type, a frameshift-causing 23 bp deletion was identified in one single ORF, the candidate *adp* gene. This deletion is expected to cause premature termination of the Adp protein; induces a stop codon one amino acid following the frameshift. Transgenic expression of the candidate wild-type *adp* ORF in mutant files completely rescued the mutant phonotype and firmly established the identify of the *adp* gene. The *adp* gene is evolutionarily conserved from plants to mammals and encodes a protein with a novel architecture (discussed in detail in

Chapter 2). The fly Adp protein shares 37% sequence identity to human Adp but functional conservation was unknown.

To elucidate whether the anti-obesity function of *adp* is conserved in vertebrates, the Graff laboratory generated transgenic mice to study the loss and gain of function phenotypes of the mammalian *adp* homolog (referred to as *Wdtc1* hereafter) (Suh et al., 2007). Because *Wdtc1*$^{-/-}$ mice are partially embryonic lethal and enough mice could not be generated, the authors evaluated *Wdtc1* heterozygous mice. The loss of a single *Wdtc1* allele yielded a clear obese phenotype, indicating evolutionary conservation of WDTC1 function and dose sensitivity. The *Wdtc1*$^{-/+}$ mice were obese based on appearance, total body weight and fat content, histological assessment of adipocyte size and plasma analysis of metabolites. Quite strikingly, transgenic overexpression of *Wdtc1* in mature adipocytes produced mice that were leaner and showed improved metabolic profiles compared to their wild-type littermates. The 3T3-L1 cell culture adipogenic model was then utilized to explore potential molecular function of WDTC1. WDTC1 overexpression also inhibited 3T3-L1 adipogenesis. Additionally, nuclear exclusion of WDTC1, by attaching a nuclear export signal, mimicked the WDTC1 RNAi phenotype, suggesting WDTC1 may have a nuclear function. Following this lead, WDTC1 was shown to bind histones and HDAC3 histone acetyltransferase in coimmunoprecipitation experiments. Suh and colleagues speculated that WDTC1 may function in transcriptional regulation through regulating chromatin structure. The molecular mechanism underlying the anti-obesity function of WDTC1 remains unknown.

Of the four studies reporting the discovery of DWD proteins, the human WDTC1 protein (676 amino acids) was first reported to interact with CRL4 components in two separate studies (Angers et al., 2006; Jin et al., 2006) and predicted in another through sequence analyses with the DWD box (He et al., 2006). In the Angers et al. study, tandem affinity purification followed by mass spectrometry identified WDTC1 in DDB1 and CUL4A complexes. The reciprocal analysis of WDTC1 complexes confirmed the association, including interaction with CUL4B and reported an interaction with histone proteins. Like the

vast majority of DWD proteins, the functional interaction between CRL4 and WDTC1 remain uncharacterized.

Research summary

The main goal of my dissertation research was to study the molecular mechanism underlying the anti-adipogenic function of WDTC1. In Chapter 2 (modified from a first author manuscript currently in revision), I characterized the functional interaction between CRL4 and WDTC1 and I elucidated a potential mechanism, histone H2AK119 monoubiquitylation, by which $CRL4^{WDTC1}$ complex suppresses adipogenesis. In Chapter 3, I describe the data obtained from screening for WDTC1 interacting proteins via mass spectrometry and include characterization of a putative $CRL4^{WDTC1}$ substrate, fatty acid synthase. Finally, in Chapter 4, I provide perspective on the outstanding questions in WDTC1 research and discuss future prospects for investigating WDTC1 cellular function.

FIGURES AND TABLES

Figure 1.1. The ubiquitin conjugation system and the types of ubiquitin linkages.
Figure and modified figure legend from Husnjak and Dikic, 2012.

(A) The E1-E2-E3 enzymatic cascade is required for ubiquitin conjugation to target protein (ubiquitylation). The catalytic activities of HECT and RING E3 ligases, and deubiquitinases (DUBs; enzymes that reverse ubiquitylation) are shown schematically. Substrates can be modified by a single ubiquitin monomer (monoubiquitylation) or multiple ubiquitin monomers (multi-monoubiquitylation) or by the sequential addition of multiple ubiquitin monomers to one of eight residues (M1, K6, K11, K27, K29, K33, K48, or K63) of a previously conjugated ubiquitin (polyubiquitylation).

(B) Summary of the various types of ubiquitylation and the major cellular processes regulated by specific linkages.

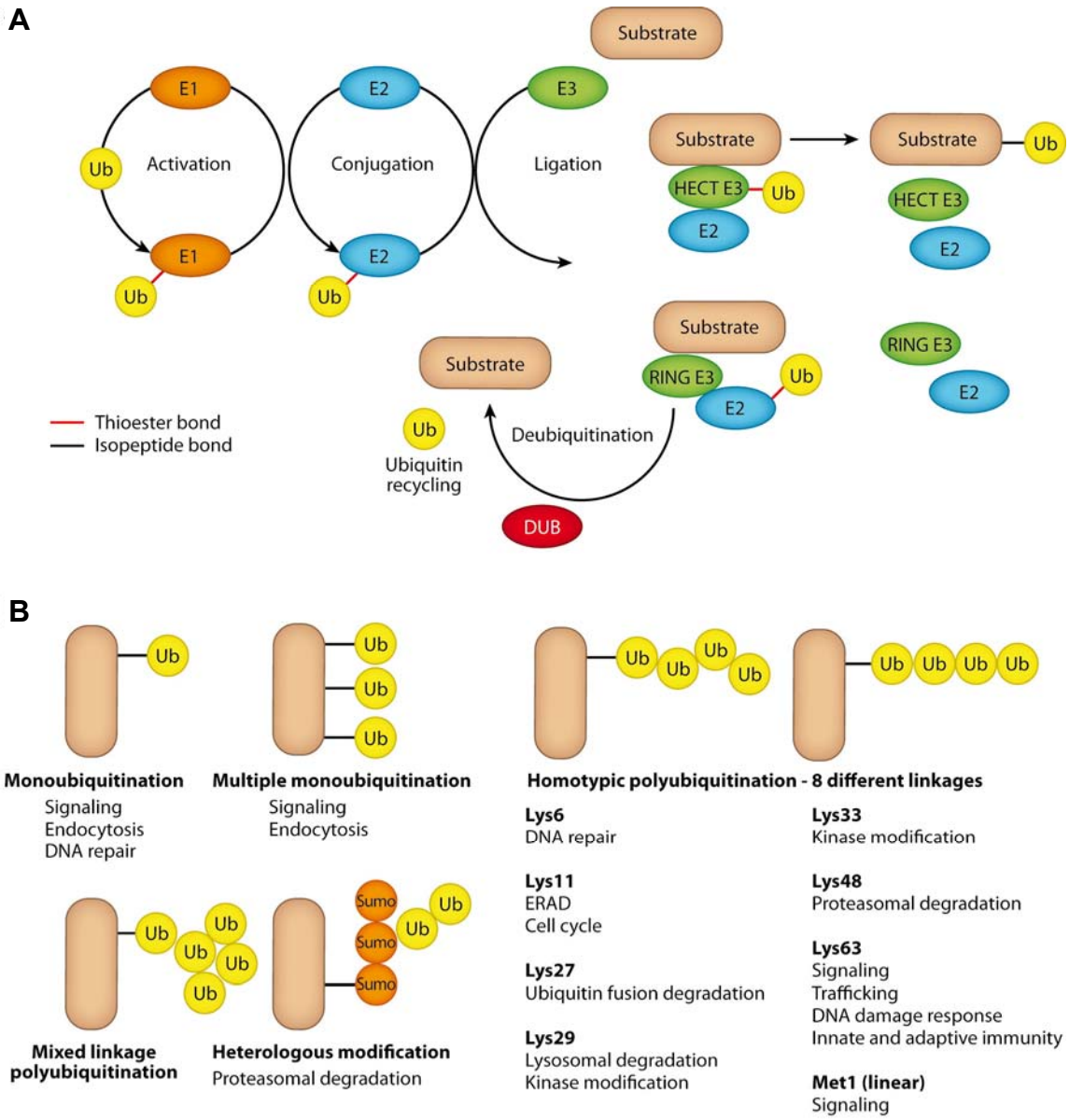

Figure 1.2. Schematic representation of cullin protein domain organization.
Figure and modified figure legend from Sarikas et al., 2011.

The N-terminal Cullin repeat 1 (CR1) binds a specific adaptor and the C-terminal cullin homology domain (CH) binds the RING subunit ROC1/2. The neddylation site is indicated by the red vertical line; CUL7 and CUL9 neddylation site has not been experimentally determined; based on consensus sequence analyses.

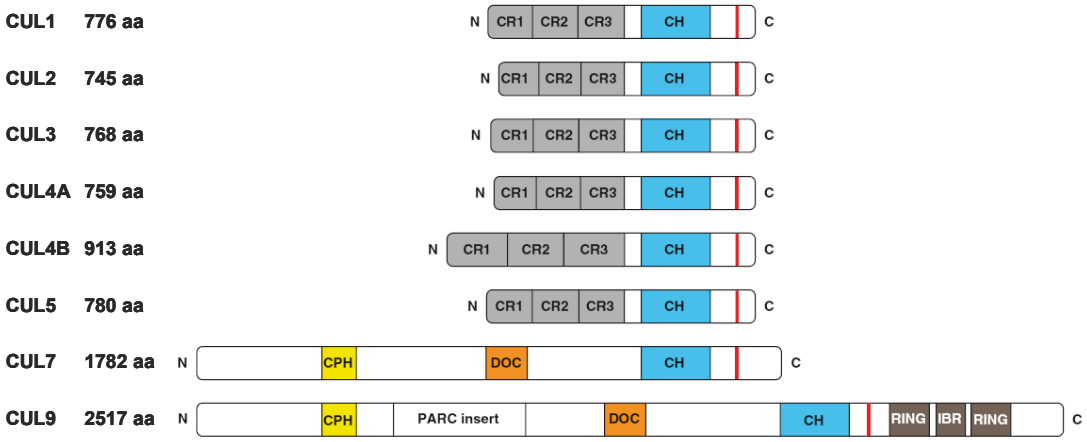

Figure 1.3. Composition of multisubunit CRL E3 ligase complexes.

Each cullin protein functions as a molecular scaffold to assemble distinct complexes via interchangeable substrate receptors, which recruit diverse substrates to a common catalytic core. Specific composition of the different complexes is described in text. Cullins either directly interact (CUL3) or bind a specific adaptor protein at their N-termini (light blue) to interact with a family of substrate receptors that share a common sequence motif (dark blue). At their C-termini, cullins assemble the conjugation apparatus with ROC1/2 RING subunit (light grey) which recruits E2 enzymes for substrate ubiquitylation. Cullins are activated by neddylation (ND8). Abbreviations: Elon, Elongin; BC-box, Elongin-BC interacting VHL-box or SOCS-box proteins.

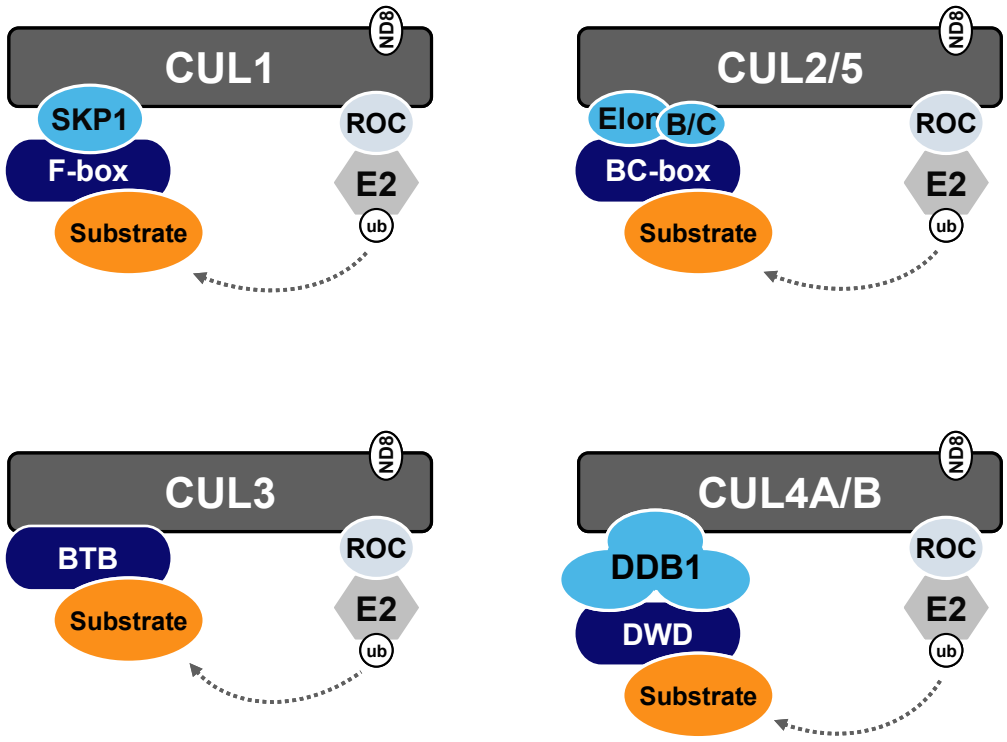

Table 1.1. Substrates of CRL4 E3 ligase complexes.
Table adapted and modified from Jackson and Xiong, 2009.

Receptor	Substrate	Substrate function	Reference
BRWD3	**dCRY1**	Transcriptional repressor of circadian genes	(Ozturk et al. 2013)
CDT2	**CDT1**	DNA replication licensing factor	(Higa et al., 2003, 2006; Hu et al., 2004; Arias and Walter, 2005, 2006; Hu and Xiong, 2006; Jin et al., 2006; Nishitani et al., 2006; Sansam et al., 2006; Senga et al., 2006; Zhong et al., 2003)
CDT2	**SET8**	Histone methyltransferase	(Abbas et al. 2010)
CDT2	**E2F1**	Transcription factor	(Shibutani et al. 2008)
CDT2	**p21**	CDK inhibitor	(Nishitai et al. 2008; Kim et al. 2008; Abbas et al., 2008)
CDT2	**p53**	Transcription factor	(Banks et al. 2006)
CDT2	**MDM2**	E3 ligase	(Banks et al. 2006)
CDT2	**PCNA**	Translesion DNA synthesis	(Terai et al. 2010)
CDT2	CHK1	Cell cycle checkpoint	(Huh and Piwnica-Worms 2012)
CDT2	**Pol η**	Translesion DNA polymerase	(Kim and Michael 2008)
CSA	**CSB**	Nucleotide excision repair (TCR)	(Groisman et al. 2006)
DDB2	**XPC**	Nucleotide excision repair (GGR)	(Sugasawa et. al. 2005)
DDB2	**DDB2**	Nucleotide excision repair (GGR)	Sugasawa et. al. (2005)
DDB2	**H2A**	Chromatin function	(Kapetanaki et. al. 2006)
DDB2	**H3, H4**	Chromatin function	(Wang et al. 2006)
FBXW5	TSC2	Inhibitor of mTOR signaling	(Hu et al. 2008)
RbAp46/48	**H2A**	Chromatin function	(Hu et al. 2012)
β-TrCP	REDD1	Inhibitor of mTOR signaling	(Katiyar et al. 2009; Regazzetti et al. 2012)
TRPC4AP	**N-Myc, C-Myc**	Transcription factor	(Choi et al. 2010)
VprBP	**RORα**	Nuclear hormone receptor	(Lee et al. 2012)
VprBP	**MCM10**	DNA replication initiation and elongation factor	(Kaur et al. 2012)
WDR5	**WDR5****	Subunit of SET1 histone methyltransferase	(Nakagawa and Xiong 2011)
WDR23	**SKN-1**	Transcription factor	(Choe et al. 2009)
AhR (TBL3?)	**ER-α****	Estrogen receptor	(Ohtake et al. 2007)
DET1*	**c-Jun**	Proto-oncogenic transcription factor	(Wertz et al. 2004)
HOXB4*	**Geminin**	Inhibitor of DNA replication	(Ohno et al. 2010)
HOXA9*	**Geminin**	Inhibitor of DNA replication	(Ohno et al. 2013)
Not required?	GRK5	Kinase for desensitizing GPCR signaling	(Wu et al. 2012)
Not required?	RASSF1A	Inhibitor of Ras signaling	(Jiang et al. 2011)
Unknown	**Cyclin E****	Cell cycle progresion	(Higa et al. 2006; Zou et al. 2009)
Unknown	**Dacapo/p27**	CDK inhibitor	(Higa et al. 2006)
Unknown	**HOXA9**	Tanscription factor	(Zhang et al. 2003)
Unknown	PRDX3**	ROS scavenger	(Li et al. 2011)
Unknown	**Topo I**	DNA topoisomerase	(Kerzendorfer et al. 2010)

Proteins in bold indicate chromatin related substrates

*Not a WD40 domain protein

**CRL4B specific

CHAPTER 2: BIOCHEMICAL ANALYSIS OF WDTC1 IN ADIPOGENESIS

SUMMARY

WDTC1, an anti-adipogenic gene product and a putative substrate receptor of a cullin 4 RING E3 ligase (CRL4), suppresses adipogenesis by an unknown mechanism. I hypothesized that the anti-adipogenic function of WDTC1 is mediated through CRL4 activity. In this study, I characterized the interaction between WDTC1 and CRL4, and delineated the molecular function of WDTC1 using 3T3-L1 cell culture model of adipogenesis. I demonstrated that WDTC1 mutations that disrupt DDB1 binding mimic the loss of function defects observed in WDTC1 knockdown cells, impaired suppression of triglyceride accumulation and increased adipogenic gene expression. Rescue experiments showed that WDTC1 RNAi defects can be restored by wild-type WDTC1 but not CRL4 binding mutants, confirming that the CRL4 interaction is critical for WDTC1 function. Furthermore, I found that *Cul4a* knockout mice exhibit adipocyte hypertrophy and metabolic defects, these phenotypes are analogous to *Wdtc1* heterozygous mice. Mechanistically, $CRL4^{WDTC1}$ complex promotes H2AK119 monoubiquitylation, an epigenetic modification linked to transcriptional repression. Collectively, the results in this chapter identify $CRL4^{WDTC1}$ E3 ligase as a suppressor of adipogenesis and implicate a role for this complex in transcriptional repression during adipogenesis.

BACKGROUND

Over 50 years ago, Dr. Winifred Doane isolated and extensively characterized a naturally-derived *D. melanogaster* mutant, which she termed *adipose (adp)* (Doane, 1960a; Doane, 1960b). The most obvious mutant phenotype observed was hypertrophy of the fly fat organ due to excessive lipid storage (Doane, 1960a). Recently, Doane and colleagues identified the fly *adp* gene, which is evolutionarily conserved from files to humans as a single copy gene (Hader et al., 2003). The mammalian *adp* ortholog is WD40 and tetratricopeptide repeats 1 (*WDTC1*), encoding a protein that contains WD40 repeat and TPR repeat domains. Specifically, the fat suppressive function of *Wdtc1* is evolutionarily conserved in mammals (Suh et al., 2007). Loss of a single *Wdtc1* allele results in obese mice with poor metabolic parameters, and conversely, transgenic *Wdtc1* expression in fat cells yields skinnier mice (Suh et al., 2007). Further, population studies have recently linked intronic *WDTC1* single nucleotide polymorphic gene variants (Lai et al., 2009) and reduced *WDTC1* gene expression (Galgani et al., 2013) to human obesity. Despite the strong genetic evidence linking *WDTC1* to anti-adipogenic function, its molecular function remains elusive.

In eukaryotic cells, covalent attachment of the 76 amino acid protein ubiquitin to substrate proteins, known as ubiquitylation, has a critical role in virtually all cellular processes. Perturbations in this system have been linked to diseases ranging from cancers to neurodegeneration (Petroski, 2008). Proteins can be polyubiquitylated, which typically targets it for proteolytic degradation, or monoubiquitylated, which regulates the property and thus the function of the protein (Hicke, 2001; Pickart, 2001b). Ubiquitylation proceeds via an enzymatic cascade where E1 and E2 enzymes catalyze the activation and conjugation of ubiquitin, while E3s confer reaction specificity through substrate recruitment (Hershko, 1983; Pickart, 2004). Belonging to the largest family of E3 ligases—the cullins, cullin 4-RING ubiquitin ligases (CRL4s) are a large subclass of multisubunit E3 enzymes. The core complex comprises either CUL4A or CUL4B paralog as the scaffold, the E2 interacting RING domain protein ROC1 (RBX1/HRT1) and the adaptor protein DDB1 (Jackson and Xiong,

2009). Substrate targeting to the catalytic core typically requires the interaction between DDB1 and substrate receptors. As recently elucidated, a subset of DDB1 binding WD40 repeat (DWD) proteins likely function as substrate receptors for CRL4 complexes (Angers et al., 2006; He et al., 2006; Higa et al., 2006b; Jin et al., 2006). The human genome encodes ~90 DWD proteins (He et al., 2006), but their function remain vastly unexplored. CRL4 E3 ligases are strongly linked to chromatin-related processes through ubiquitylation of histones and factors controlling DNA repair, replication and transcription protein (Jackson and Xiong, 2009; O'Connell and Harper, 2007).

Indeed, WDTC1 (DCAF9) is a DWD protein and as such, a putative substrate receptor of CRL4 E3 ligases (Angers et al., 2006; He et al., 2006; Jin et al., 2006). However, the in vivo interaction between WDTC1 and CRL4 has not yet been explored. I hypothesized that WDTC1 functions as a substrate receptor of the CRL4 E3 ligase to mediate its anti-adipogenic activity. The aim of this chapter is to examine the functional significance of the WDTC1 and CRL4 interaction, and elucidate the molecular mechanism underlying the anti-adipogenic function of WDTC1. I demonstrated that WDTC1 functions as part of a CRL4 complex to suppress adipogenesis. I also uncovered a function of the $CRL4^{WDTC1}$ E3 complex in promoting histone H2AK119 monoubiquitylation, a modification associated with transcriptional repression and thus a potential mechanism by which WDTC1 suppresses adipogenesis.

RESULTS

WDTC1 is a substrate receptor of CRL4 E3 ubiquitin ligases

To begin to characterize the interaction between WDTC1 and CRL4, I compared a few key structural and sequence elements. *WDTC1* encodes a protein with a novel structure, and its linear domain organization is predicted to be conserved from mammals to *Arabidopsis* (Figure 2.1A, top). The modeled human WDTC1 structure depicts the unique combination of a classic seven-bladed β-propeller with antiparallel α-helices of the TPR

repeats which are spatially separated by unstructured regions (Figure 2.1B). Of note, the structural basis of the interaction between WDTC1 and DDB1 is predicted to include a short N-terminal α-helical motif termed the H-box (Li et al., 2010). Although not strictly conserved at the primary sequence level, the H-box is a shared structural feature among a few DWD proteins, and surprisingly, several viral proteins that hijack the CRL4 complex. The alignment of H-box sequences revealed substantial sequence homology among vertebrates, consistent with their shared mode of DDB1 interaction (Figure 2.1A, bottom left). Additionally, the signature motif present in nearly all DWD proteins is the DWD box, a highly conserved 16 residue sequence positioned within WD40 repeats (He et al., 2006). Similar to most DWD proteins, WDTC1 contains two tandem DWD boxes with conserved WDXR submotifs (Figure 2.1A, bottom right). Interestingly, although the H-box of the DWD protein DDB2 makes a large contribution to DDB1 binding (Jin et al., 2006; Li et al., 2010), the importance of the arginine in the WDXR of DDB2 is indicated by its mutation (R273H) in some human XPE patients and its loss of DDB1 binding (Rapic-Otrin et al., 2003; Shiyanov et al., 1999). In fact, this arginine in WDXR submotifs is critically important for the interaction between many DWD proteins and DDB1 (Higa and Zhang, 2007). These observations therefore underscore the presence of multiple binding determinants for the functional interaction between DWD proteins and CRL4 complexes.

To experimentally confirm the prediction that WDTC1 and CRL4 interact in vivo, endogenous CUL4A or CUL4B complexes were immunoprecipitated from HEK293T cells, and the presence of WDTC1 in the immunoprecipitates was determined by immunoblot analysis. I found that WDTC1 forms both CUL4A and CUL4B endogenous complexes (Figure 2.2A). While in vitro binding assays suggested that the H-box of WDTC1 is the key determinant of binding to DDB1 (Li et al., 2010), this has not been experimentally verified in cells. Additionally, in line with the aim to characterize WDTC1 molecular function, I sought to determine the contribution of the tandem WDXR motifs in WDTC1 to CRL4 complex assembly. I generated two WDTC1 mutants, one deleted the N-terminal 25 amino acid

residues spanning the H-box (referred to as ΔH) and the other substituted the arginine residues in the tandem WDXR motifs to alanines (referred to as RARA). I first confirmed their expression and determined that their relative stability is similar by cycloheximide chase (Figure 2.2B). I then examined their effect on binding CRL4 components by coimmunoprecipitation assays.

As expected, wild-type (WT) Flag-tagged WDTC1 (Flag-WDTC1-WT) coimmunoprecipitated all CRL4 proteins tested (Figure 2.2C, lane 6). Consistent with the reported importance of the H-box, its deletion in WDTC1-ΔH completely ablated complex formation (lane 7). Interestingly, WDTC1-RARA mutant showed a marginal decrease in DDB1 binding but its interaction with CUL4 and ROC1 was markedly reduced (lane 8), indicating that the WDXR motifs in WDTC1 are required for forming stable CRL4 complexes. A superimposed structure of WDTC1 is shown in complex with CRL4 (Figure 2.2D). WDTC1 is anchored through its H-box into the DDB1 BPC domain. As in the case of DDB2-DDB1 binding (Fischer et al., 2011), the tandem WDXR residues of WDTC1 are not predicted to make direct contact with DDB1 but are solvent-exposed on the bottom surface of the propeller fold.

Besides DDB2 (Nag et al., 2001; Sugasawa et al., 2005), the Xiong laboratory recently reported the second example of a DWD protein, WDR5, that is ubiquitylated by its cognate CRL4B complex and targeted for proteolysis (Nakagawa and Xiong, 2011). I therefore tested whether WDTC1 is a CRL4 substrate by an in vivo ubiquitylation assay. I found that although WDTC1 was extensively ubiquitylated, its ubiquitylation status was unchanged by either DDB1 knockdown or ΔH mutation that disrupts DDB1 binding (Figure 2.2E). Finally, the steady state levels of transiently expressed Flag-WDTC1 protein are largely unaltered by knockdown of DDB1 or either CUL4A or B (Figure 2.2F), indicating that CRL4 does not regulate WDTC1 protein stability. Although DDB1 depletion resulted in a slight decrease in WDTC1 protein (lane 2), this is possibly due to instability arising from the loss of its primary binding partner. Together, these results demonstrate that WDTC1 is a

component of CRL4 complexes and likely functions as a substrate receptor of CRL4 E3 ligases.

The interaction of WDTC1 with CRL4 is critical for WDTC1-mediated adipogenic suppression

To determine the biological significance of the CRL4-WDTC1 interaction, I hypothesized that the fat suppressive role of WDTC1 is mediated through CRL4. I first confirmed expression of CRL4 proteins in adipose tissues out of a panel of adult mouse tissues (Figure 2.3A). In addition to adipose tissues, WDTC1 protein appears to be broadly expressed, in agreement with a previous report on *Wdtc1* mRNA expression pattern (Suh et al., 2007). To test my hypothesis, I assayed the adipogenic differentiation of 3T3-L1 preadipocytes, the best characterized and most extensively used cell culture model to study adipogenesis. Originally derived from mouse embryonic fibroblasts (Green and Meuth, 1974), 3T3-L1 adipogenesis is thought to closely recapitulate adipogenesis in mice. Treating 3T3-L1 cells to an adipogenic media triggers transcriptional activation of the terminal differentiation program and morphological changes following lipogenic accumulation of triglycerides (MacDougald and Lane, 1995).

I first confirmed the endogenous interaction between WDTC1 and CRL4 subunits during the course of 3T3-L1 differentiation, which I monitored by phenotypic changes (data not shown) and Fatty Acid Synthase (FAS) protein induction. WDTC1 was immunoprecipitated from cells collected at specific time points and the presence of CRL4 proteins in the immunoprecipitates was determined by immunoblot analysis (Figure 2.3B). Although anti-WDTC1 antibody shows low immunoprecipitation efficiency, the results show that WDTC1 forms both CUL4A and CUL4B endogenous complexes. The levels of CRL4 proteins remained relatively constant during differentiation (Figure 2.3B, input lanes), consistent with the notion that CRL4 has diverse roles in the process of 3T3-L1 proliferation, differentiation and lipid accumulation. Unexpectedly, WDTC1 protein levels also remained

constant during differentiation, although its mRNA expression was reported to be downregulated in differentiated 3T3-L1 cells (Suh et al., 2007). It is unclear whether WDTC1 activity is downregulated during adipogenesis to enable cells to acquire and maintain the adipocyte phenotype via lipid accumulation. I predict an as yet unknown upstream factor suppresses WDTC1 activity to promote adipogenesis.

A substrate receptor role for WDTC1 would predict that disruption of CRL4 binding would affect adipogenic suppression by WDTC1. I therefore evaluated the effects of disrupting the CRL4-WDTC1 interaction on WDTC1 function during adipogenesis. For this purpose, I generated stable cells that expressed a vector control (EV), Flag-WDTC1-WT or -ΔH and -RARA mutants of WDTC1. I confirmed that ectopically expressed WDTC1 forms CRL4 complexes in these cells (Figure 2.3C; lane 6) and confirmed the expected total disruption and reduced binding of the WDTC1 mutants with CRL4, although ΔH and RARA expression is lower than WT (lanes 7 and 8). When these cells were adipogenically induced, WDTC1-WT suppressed adipogenesis as assessed by Oil Red O staining (ORO) (Figure 2.3D), consistent with previous reports on the anti-adipogenic function of WDTC1 (Hader et al., 2003; Suh et al., 2007; Teague et al., 1986). In striking contrast, WDTC1-ΔH expression enhanced adipogenesis compared to EV, suggesting that it may function as a dominant negative form of WDTC1. Further, the expression of the WDTC1-RARA mutant, partially defective in binding DDB1, also promoted adipogenesis, but at a lower efficiency than WDTC1-ΔH. Consistent with the phenotypes assessed by ORO, ectopic expression of WDTC1-WT suppressed triglyceride accumulation, while expression of the WDTC1-ΔH (3.5 fold) and WDTC1-RARA (2.4 fold) mutants resulted in significantly higher triglyceride levels compared to control cells (Figure 2.3E). Finally, consistent with its role as a suppressor of adipogenesis, expression of WDTC1-WT resulted in decreased adipogenic marker expression but this decrease is absent in the WDTC1-RARA expressing cells while marker expression is significantly increased in WDTC1-ΔH cells (Figure 2.3F). Together, these

results support the idea that CRL4 interaction is critically important for WDTC1 function in the suppression of adipogenesis.

CRL4 binding mutants of WDTC1 cannot rescue WDTC1 function

To further validate the functional link between WDTC1 and CRL4 in the suppression of 3T3-L1 adipogenesis, I attempted to generate DDB1, CUL4A or CUL4B stable knockdown cells by RNAi. I failed to obtain DDB1 knockdown cells, but was able to generate stable CUL4A and CUL4B knockdown cells (Figure 2.4A). However, I was unable to make clear phenotypic assessment of the adipogenic capacity of CUL4A or B knockdown cells. This is not surprising considering the expected pleiotropic effect of the CRL4 core components (Jackson and Xiong, 2009) and as speculated earlier, their potential involvement in multiple processes associated with 3T3-L1 adipogenesis. Specifically, given the well established role of CRL4 complexes in cell cycle regulation, depletion of CUL4A resulted in a cell proliferation defect while depletion of CUL4B resulted in a cell cycle defect. CUL4A depletion enhanced 3T3-L1 proliferation rate (Figure 2.4B) but cell cycle distribution, as determined by flow cytometry analysis following propidium iodide staining of DNA, appeared to be normal (Figure 2.4C). The faster proliferation rate of CUL4Ai cells was unexpected since CUL4A depletion in MEFs impedes cell cycle progression through the S and early M phases, leading to slow proliferation rate (Kopanja et al., 2009). In contrast, the proliferation rate of CUL4Bi cells appeared to be normal when compared to control cells (Figure 2.4B), but analysis of DNA content indicated drastic alteration of the cell cycle; >2N in G1 phase and >4N in S phase (Figure 2.4C). When adipogenically induced, CUL4A depletion promoted adipogenesis, and on the contrary, CUL4B depletion suppressed adipogenesis (Figure 2.4D). Although I interpret these data cautiously, it is unclear exactly why knockdown of CUL4A and CUL4B have the opposite effect on 3T3-L1 adipogenesis. As CUL4A and CUL4B paralogs are not completely redundant, I speculate that this may relate to additional nuclear role of CUL4B protein and its impact on cell cycle control.

To counter limitations discussed above, I designed a rescue experiment to demonstrate the specificity of the WDTC1-CRL4 interaction in adipogenic suppression. Utilizing a lentiviral knockdown-rescue vector strategy developed by James Bear's laboratory (Uetrecht and Bear, 2009), I generated 3T3-L1 stable cell lines that simultaneously knockdown endogenous *Wdtc1* mRNA and replace WDTC1 protein expression to near endogenous levels with shRNA refractory open reading frames encoding either WDTC1-WT, WDTC1-ΔH or WDTC1-RARA (Figure 2.5A). Consistent with the reported RNAi phenotype of WDTC1 (Suh et al., 2007), WDTC1 knockdown dramatically enhanced 3T3-L1 adipogenesis as assayed by ORO (Figure 2.5B), triglyceride quantitation (Figure 2.5C) and adipogenic marker expression (Figure 2.5D). While the addition of WDTC1-WT almost completely rescued the loss of adipogenic suppression in cells depleted of endogenous WDTC1 in all three assays, both CRL4 binding mutants failed to fully rescue the RNAi phenotype. The phenotype and the adipogenic marker expression of the WDTC1-RARA rescue cells were an intermediate between control cells and shWDTC1 cells, indicating partial rescue. In sharp contrast, WDTC1-ΔH rescue expression closely mimicked the RNAi phenotype, demonstrating that the loss of adipogenic suppression is primarily due to the loss of CRL4 binding. Considering the genetic evidence indicating that *adp/Wdtc1* exhibits dose sensitivity (Doane, 1960a; Suh et al., 2007), I interpret the WDTC1-RARA mutant to represent a hypomorphic form of WDTC1. Collectively, these findings demonstrate a remarkable parallel between $CRL4^{WDTC1}$ complex formation and WDTC1 function in the negative regulation of adipogenesis.

Cul4a$^{-/-}$ mice exhibit adipocyte hypertrophy and poor metabolic profiles

I next sought genetic evidence to support an in vivo role of CRL4 in adipogenic regulation. *Cul4b*, *Ddb1* and *Roc1* knockout mice are embryonic lethal (Cang et al., 2006; Jiang et al., 2012a; Tan et al., 2009). Additionally, an adipose specific conditional mouse knockout model has not yet been reported for any of the CRL4 subunits. Although it is

interesting to note that central obesity is frequently observed in X-linked mental retardation (XLMR) patients carrying *CUL4B* mutations (Tarpey et al., 2007), but the basis for this apparent association is unclear. However, *Cul4a* systemic knockout mice are viable and display no detrimental developmental defects throughout their lifespan with the exception of mice being sensitive to liver toxins and having enhanced UV-induced DNA damage response (Kopanja et al., 2009; Liu et al., 2009). The availability of this reagent therefore provided an exciting but preliminary opportunity to investigate a potential role of CUL4A in mammalian adipocyte biology. To this end, I focused on the visceral gonadal white adipose tissue (GWAT) and the subcutaneous inguinal white adipose tissue (IWAT) fat depots of normally fed mice. To rule out the possibility that genetic ablation of the *Cul4a* gene leads to altered expression of WDTC1 or its paralog CUL4B, I checked their protein expression in wild-type (WT) and *Cul4a*$^{-/-}$ mice fat pads by immunoblotting (Figure 2.6A).There was no obvious change in either WDTC1 or CUL4B expression, thus permitting a clearer phenotypic assessment of *Cul4a*$^{-/-}$ mice. Visually, WT and *Cul4a*$^{-/-}$ mice were similar in appearance and there were no significant differences in their body weight (Figure 2.6B).

Despite the similarity in body weight, I observed that the *Cul4a*$^{-/-}$ mice had noticeably larger GWAT and IWAT fat depots compared to their wild-type counterparts (Figure 2.6C), and as expected, these tissues weighed significantly more while the weights of other organs were unchanged (Figure 2.6D). Importantly, histological analyses revealed a striking adipocyte hypertrophy phenotype in both fat depots of *Cul4a*$^{-/-}$ mice (Figure 2.6E). I noted that the number of adipocytes was similar between wild-type and *Cul4a*$^{-/-}$ mice by nuclei counting. Therefore, adipocyte hypertrophy (increase in cell size), but not adipocyte hyperplasia (increase in total adipocytes), accounted for the overall increase in adiposity or fat mass. Lastly, serum levels of glucose, triglycerides, insulin and leptin in overnight fasted mice were measured. *Cul4a*$^{-/-}$ mice had significantly elevated levels of these metabolites (Figure 2.6F), with the exception of insulin, although it followed the same trend. Adipocyte hypertrophy and altered metabolic parameters of the *Cul4a*$^{-/-}$ mice are remarkably

comparable to the phenotypes observed in *Wdtc1*$^{+/-}$ mice (Suh et al., 2007), consistent with these proteins functioning in the same molecular pathway.

CRL4^{WDTC1} promotes histone H2AK119ub in a lineage specific manner

To gain insight into the mechanism by which CRL4^{WDTC1} suppresses adipogenesis, I considered a potential role for this complex in transcriptional repression. This is an intriguing possibility since the only example of WD40 and TPR domains functioning collectively is in transcriptional corepression by the well characterized yeast Tup1-Ssn6 heterodimer (Malave and Dent, 2006). In fact, based on three observations reported by Suh et al., 2007, a transcriptional repressor function leads the suggested role for WDTC1. First, WDTC1 expression is associated with reduced adipogenic marker expression (confirmed by me) and inhibition of PPARγ reporter gene transcription. Second, its adipogenic suppressive function is lost upon nuclear exclusion. Third, WDTC1 physically interacts with ectopically expressed histones and HDAC3, a component of many corepressor complexes. Separately, despite the established role for CRL4 in transcriptional regulation, a direct role in transcriptional repression has been demonstrated only recently for the CRL4B$^{RBBP4/7}$ complex (Hu et al., 2012), raising the possibility that other DWD proteins may have similar biochemical function.

I first examined the distribution of Flag-WDTC1 in subcellular fractions by immunoblotting (Figure 2.7A), and its cellular localization by immunoflourescence microscopy in 3T3-L1 cells (Figure 2.7B). I found that while WDTC1 is primarily recovered in the cytosolic fraction, it is also present in the nuclear fractions, and importantly, the MNase-digested chromatin fraction (Figure 2.7A, lane 4). Although WDTC1 is expected to bind histones, it is unclear whether it binds nucleosomal histones (Angers et al., 2006; Suh et al., 2007). I therefore performed a nuclear immunoprecipitation with soluble chromatin extracts from HEK293T cells transiently expressing Flag-WDTC1 and HA-tagged core histones. All core histones except histone H4 were recovered in Flag-WDTC1 immunoprecipitates, indicating that WDTC1 binds nucleosomal histones (Figure 2.7C). I noted that WDTC1

interacted with histone H2A, but not the presumably ubiquitylated form of H2A (lane 3), which prompted me to test whether $CRL4^{WDTC1}$ regulates histone H2A ubiquitylation, a modification linked to transcriptional repression (Kouzarides, 2007).

Because WDTC1-ΔH disrupts DDB1 binding and thus disrupts probable ubiquitylation activity, and appears to functionally antagonize WDTC1 during adipogenesis, I took advantage of this mutant to investigate the effect of WDTC1 expression on histone H2A ubiquitylation. Histone H2A monoubiquitylated at the highly conserved K119 residue (H2AK119ub) represents the primary form of ubiquitylated H2A in cells, although polyubiquitination of H2A has been reported (Goldknopf and Busch, 1977; Nickel and Davie, 1989). I first examined the global level of H2AK119ub in preadipocyte and induced 3T3-L1 cells stably expressing either a vector control (EV), Flag-WDTC1-WT or -ΔH by immunoblotting with a H2AK119ub specific antibody. I did not detect any significant changes in H2AK119ub levels among these cell lines in the preadipocyte state (Figure 2.7D). In contrast, expression of WDTC1-WT resulted in a modest, but significant increase in H2AK119ub while WDTC1-ΔH expression resulted in a slight decrease. However, ectopic expression of either WDTC1-WT or WDTC1-ΔH in two non-adipogenic cell lines, HEK293T and HCT116, had no detectable effect on H2AK119ub levels whether DDB1 was depleted or not (Figures 2.7E and 2.7F). Minimally, this suggests WDTC1 promotes H2AK119ub in an adipocyte-linage specific manner. The global change in H2AK119ub in 3T3-L1 induced cells was modest, implicating that perhaps $CRL4^{WDTC1}$ regulates H2AK119ub locally at a subset of genes rather than globally. Nevertheless, WDTC1-mediated increase of H2AK119ub is dependent on the CRL4 interaction. I speculated that perhaps WDTC1 recruits CRL4 to specific targets to monoubiquitylate H2A, similar to CRL4B recruitment by RBBP4/7 DWD proteins to target promoters (Hu et al., 2012). I tested the interaction between WDTC1 and endogenous histones by chromatin coimmunoprecipitation assays, confirming nucleosomal histone binding at physiologic levels (Figure 2.7G). Supporting the recruitment hypothesis, I

found that while ΔH deletion in WDTC1 abolishes CRL4 binding, this mutant retained histone binding activity (lane 3).

Finally, to test weather H2A is a direct target of $CRL4^{WDTC1}$ E3 ligase, I performed in vitro ubiquitylation assays. I affinity purified Flag-WDTC1-WT or Flag-WDTC1-ΔH complexes from HEK293T cells and confirmed the presence of CRL4 components in WT, but not in ΔH, eluted fraction by immunoblotting and Coomassie Blue staining (Figure 2.8A). Recombinant histone H2A protein was incubated with either purified WDTC1-WT or WDTC1-ΔH complexes in a reaction mix containing ubiquitin, recombinant E1, E2-UBE2D3 and ATP. Reaction products were resolved by SDS-PAGE and detected by H2AK119ub specific antibody. The results show that H2A is robustly ubiquitylated by WDTC1 in a CRL4 dependent manner (Figure 2.8B; compare lanes 1 and 2), demonstrating that H2A was a specific substrate of $CRL4^{WDTC1}$ in this in vitro system. Multiple H2AK119 ubiquitylated species were detected, but their identity has not been determined and I suspect that they represent non-specific ubiquitylation at additional sites, perhaps reflecting the high efficiency of H2A ubiquitylation in vitro. Shorter exposure of the blot showed that the primary reaction product is the monoubiquitylation detected by the H2AK119ub antibody (Figure 2.8C). To determine whether K119 residue is the primary target of $CRL4^{WDTC1}$, wild-type H2A and its mutants, H2AK118R and H2AK119R, were tested in in vitro ubiquitylation assay. While purified Flag-WDTC1-WT enhanced wild-type H2A ubiquitylation compared to control, disrupting the K118 residue had very little effect (Figure 2.8D; compare lanes 2 and 3). In contrast, K119R mutation resulted in a substantial loss of H2A ubiquitylation, indicating that K119 is the primary $CRL4^{WDTC1}$-dependent ubiquitylation site (lane 4). These results collectively suggest $CRL4^{WDTC1}$ promotes H2AK119ub in vitro, and in vivo in an adipocyte lineage specific manner.

CRL4^{WDTC1}-mediated H2AK119ub is linked to altered levels of H3K4me3

Referred to as crosstalk, H2AK119ub is typically combinatorial with other transcription repressive modifications such as H3K27 and H3K9 trimethylation, and acts dominantly over modifications linked to gene activation such as H3K4 trimethylation (Vissers et al., 2008; Zhang, 2003). Although the mechanistic details are not entirely clear, crosstalk is a probable mechanism by which H2AK119ub-enriched chromatin is rendered transcriptional silent. To expand on the finding that CRL4^{WDTC1} promotes H2AK119ub, I considered the effect of WDTC1 expression on other histone modifications—histone trimethylation (me3), in particular. After adipogenic induction, I prepared chromatin extracts from 3T3-L1 cells stably expressing EV control, Flag-WDTC1-WT or -ΔH and examined the global level of various histone modifications by immunoblotting with modification specific antibodies.

As expected, WDTC1-WT expression, but not WDTC1-ΔH, resulted in a global increase in H2AK119ub but had no apparent effect on H2BK120ub, the primary site of histone H2B monoubiquitylation (Figure 2.9A). While no obvious change in H3K9me3 was observed, a slight decrease in H3K27me3 was detected in cells expressing WDTC1-ΔH. Because H3K27me3 is thought to be upstream of H2AK119ub in Polycomb-mediated gene repression (Cao et al., 2005) and WDTC1-WT had no apparent effect on this modification, the significance of this decrease is not immediately clear but implies decreased gene silencing in WDTC1-ΔH cells. The most obvious change concomitant with the increase in H2AK119ub was the marked decrease in H3K4me3 in WDTC1-WT expressing cells. I confirmed this finding in cells depleted of WDTC1 proteins by two independent shRNAs, which resulted in decreased H2AK119ub but a considerable increase in H3K4me3 levels (Figure 2.9B). Together, these results demonstrate that WDTC1, through its function as a CRL4 E3 ligase component, promotes H2AK119ub during adipogenesis and that reduced WDTC1 function is associated with reduced H2AK119ub and increased H3K4me3.

DISCUSSION

The primary goal of this study was to elucidate the molecular mechanism underlying WDTC1 anti-adipogenic function. In this chapter, I showed that WDTC1 functions as a component of a CRL4 E3 ligase to suppress adipogenesis, possibly through epigenetic regulation of transcription via H2AK119ub. First, the interaction of WDTC1 with CRL4 is essential for its function in suppressing adipogenesis. Disruption of WDTC1-DDB1 binding results in defects in 3T3-L1 cell adipogenesis similar to that observed in WDTC1 deficient cells. Second, I sought genetic evidence supporting a role for CRL4 in adipocyte biology. I found that *Cul4a* knockout mice develop phenotypes in fat tissues that are very similar to that reported in *Wdtc1*$^{+/-}$ mice. Finally, I showed that CRL4^{WDTC1} complex regulates histone H2AK119 monoubiquitylation during adipogenesis and is likely to function as adipocyte lineage specific E3 ligase for histone H2AK119.

Representing one of the most abundant modifications in higher eukaryotes (5-15% of total H2A), H2A was the first protein identified to be ubiquitylated with the site mapped to the highly conserved K119 residue (Goldknopf and Busch, 1977; Goldknopf et al., 1975). The most extensively characterized H2A E3 ligase is the RING1B of PRC1 complex which plays a critical and evolutionarily conserved role in developmental control in flies and mammals (Schuettengruber and Cavalli, 2009). While RING1B has been found in additional protein complexes besides PRC1 (Zhou et al., 2009), it has been conceptually unclear how a single E3 ligase regulates different biological processes that involve epigenetic silencing. More specifically, considering the abundance of H2AK119ub in cells, it is intriguing as to whether RING1B singularly catalyzes H2AK119ub or distinct E3 ligases exist for H2AK119. Two reports support the latter possibility. First, 2A-HUB (DZIP3/hRUL138) mediates selective repression of a specific set of chemokine genes in macrophages through functional interactions with a histone deacetylase complex (Zhou et al., 2008). Second, CRL4B$^{RBBP4/7}$ collaborates with PRC2 to repress various target genes involved in cell growth and migration (Hu et al., 2012). Both 2A-HUB and CRL4B$^{RBBP4/7}$ appear to be devoid of an association with

PRC1 subunits. The results presented in this study suggest $CRL4^{WDTC1}$ is a novel and lineage specific H2AK119 E3 ligase. This supports the notion that in addition to the iconic PRC1, multiple H2AK119 E3 ligases that function in epigenetic repression may exist. It is interesting to note that this study and the study by Hu et al. identify two homologous H2AK119 E3 ligases, $CRL4^{WDTC1}$ and $CRL4B^{RBBP4/7}$, which only differ in the substrate recognition DWD subunit. Given the ~90 estimated DWD proteins in mammalian cells (He et al., 2006), it is tempting to speculate that additional DWD proteins may target H2AK119ub through CRL4 E3 ligases, a notion that is consistent with the observed function of *CUL4* gene in chromatin regulation.

Studies on transcriptional regulation of adipogenesis have traditionally focused on a cascade of sequentially expressed transcriptional factors (Rosen and MacDougald, 2006), but epigenetic regulation is emerging as a critical regulator of adipogenesis, especially on the control of such key adipogenic factors as PPARγ and C/EBP family members (Cristancho and Lazar, 2011). Specifically, the genome-wide changes of multiple histone acetylation and methylation marks, many of which are involved in transcriptional activation, have been detected and some functionally linked to adipogenesis. By contrast, epigenetic repression of adipogenesis remains poorly understood. The $CRL4^{WDTC1}$-dependent correlation between increased H2AK119ub and decreased H3K4me3 levels uncovered in this study has functional implication in adipogenic transcriptional repression. In vitro evidence indicates that H2AK119ub blocks transcription initiation by inhibiting H3K4 di- and trimethylation by MLL3 histone methyltransferase (Nakagawa et al., 2008), a recently characterized positive regulator of adipogenesis in mice (Lee et al., 2008). To the best of my knowledge, WDTC1 represents the first factor that links H2AK119ub, which has long been associated with gene silencing, to adipogenesis. Collectively, the results in this chapter suggested a model in which WDTC1 recruits the CRL4 complex at a subset of adipogenic genes to monoubiquitylate H2AK119, which consequently prevents H3K4me3, and thus repressing transcriptional activation of adipogenic genes (Figure 2.10). I predict transcriptional control of

these genes is dynamically regulated by the action of $CRL4^{WDTC1}$ E3 ligase and upstream signals that prevent $CRL4^{WDTC1}$ activity. Conceivably, transcriptional activation of these promoters requires coordinated action of histone deubiquitinases and methyltransferases. Undoubtedly, identifying $CRL4^{WDTC1}$ target genes through future genome-wide studies is the critical next step in exploring an in vivo role for $CRL4^{WDTC1}$ in transcriptional repression.

EXPERIMENTAL PROCEDURES

WDTC1 cloning and plasmids

The human *WDTC1* (NM_015023.4) coding sequence was PCR amplified from a HepG2 cDNA library and cloned into pENTR™/D-TOPO (Invitrogen) to generate a WDTC1 entry vector for Gateway cloning or conventional subcloning. The DDB1 binding deletion mutant WDTC1-ΔH was subcloned from pENTR-WDTC1 and WDTC1-RARA was generated by sequential QuikChange site-directed mutagenesis (Stratagene) to pENTR-WDTC1. To generate expression constructs, WDTC1 entry vectors were recombined with Gateway adapted destination vector p3XFLAG for transient and pMX-FLAG-puro for stable expression (destination vectors were a gift of Dr. K. I. Nakayama). HA-tagged ubiquitin expression plasmid has been described previously (Nakagawa and Xiong, 2011). Mouse *Wdtc1*, *Cul4a* and *Cul4b* shRNA sequences were designed using BLOCK-IT RNAi tool (Invitrogen) and cloned into pMKO.1-puro retroviral vector (Addgene plasmid 8452) for stable knockdown of respective mRNAs in 3T3-L1 cells. To generate WDTC1 knockdown-rescue vectors, shRNA sequences targeting mouse *Wdtc1* and shRNA refractory human *WDTC1* coding sequences were cloned into a bicistronic lentiviral vector, pLL-5.5-IRES-EGFP (a gift of Dr. J. Bear), as described previously (Cai et al., 2007; Uetrecht and Bear, 2009). A minimum of 2-3 shRNA constructs were screened and 1 or 2 were selected based on knockdown efficiency; shRNA sequences are listed in Table 2.1. All plasmids were sequence verified.

Cell culture and adipocyte differentiation

HEK293T cells and 3T3-L1 preadipocytes were cultured in DMEM supplemented with 1X penicillin-streptomycin solution (Corning) and 10% (v/v) fetal bovine serum (FBS) or fetal calf serum (FCS), respectively. HCT116 cells were cultured in McCoy's 5A FBS media; supplemented as above. 3T3-L1 cells were differentiated with modifications to protocol described previously (Student et al., 1980). To induce differentiation, 2 day post confluent 3T3-L1 cells (day 0) were treated with an induction media containing 1 mM dexamethasone,

0.5 mM isobutylmethylxanthine, and 1 µg/ml insulin (all from Sigma) in 10% FBS supplemented DMEM. Two days later, induction media was replaced with 1 µg/ml insulin only for the duration of the experiment and media was changed every 2 days. A schematic summarizing 3T3-L1 differentiation with time points indicated for different experimental procedures is shown (Figure 2.11).

Transfections, retroviral and lentiviral infections

HEK293T cells were transfected at 1:3 plasmid to reagent ratio using Fugene 6 transfection reagent (Promega) for transient overexpression or transfected with 50 nM of siRNA for knockdown using Lipofectamine 2000 reagent (Invitrogen) according to manufacturers' protocol. In experiments requiring both plasmid and siRNA transfections, siRNA transfection was preceded by plasmid transfection to counter differential transfection efficiencies of siRNA knockdown cells. Cells were incubated for 72 h for knockdown by siRNA; siRNA sequences were described previously (Hu et al., 2004) and listed in Table 2.1. For retroviral or lentiviral production, HEK293T cells were cotransfected with various plasmids for viral packaging as described (Kotake et al., 2007). Viral media was collected 48 h posttransfection at two 12 h intervals, syringe filtered through 0.45 µm filter and polybrene (8 µg/ml) supplemented. Preconfluent 3T3-L1 preadipocytes were infected with the viral media twice within a 24 h interval. Cells were split to maintain preconfluency. Retrovirally transduced cells were selected with 4 µg/ml puromycin and maintained in selection media until adipogenic induction. Infection of 3T3-L1 cells by the lentivirus encoding pLL-5.5-IRES-EGFP WDTC1 knockdown-rescue constructs was assessed by real-time qPCR and immunoblotting.

Antibodies, immunoprecipitation and immunoblotting

Our laboratory made two separate attempts to generate an antibody against WDTC1 but failed to obtain a high affinity WDTC1-specific antibody. I later obtained an anti-WDTC1 rabbit monoclonal antibody (Abcam) and an anti-WDTC1 polyclonal antibody (Abgent) that

gave WDTC1 specific signals. The polyclonal antibody appeared to be limited to immunoblotting and showed within lot variations in detecting WDTC1 protein; therefore, most experiments utilized the monoclonal antibody. DDB1, CUL4A and ROC1 antibodies were generated by our laboratory as described previously (Hu et al., 2004), a commercially available antibody was used for the detection of mouse CUL4A and all other antibodies used in this study were from commercial sources and listed in Table 2.2. For preparing cell extracts, cells were lysed on ice in NP-40 lysis buffer [50 mM Tris (pH 8.0), 150 mM NaCl, 10% glycerol, 1 mM EDTA and 0.1% NP-40] supplemented with Halt^{TM} (Thermo Sci.) protease/phosphatase inhibitor cocktail (PPIC). For immunoprecipitation experiments, clarified cell extracts were immunoprecipitated by overnight incubation with primary antibody at 4 °C. For nuclear immunoprecipitation, Triton X-100 insoluble nuclear fractions were treated with deoxyribonuclease (DNase) to prepare soluble chromatin extracts essentially following method described previously (Day et al., 2010). Immunoprecipitates were washed 3-5 times in lysis buffer with rotation, eluted by boiling in Laemmli buffer, resolved by SDS-PAGE, transferred to PVDF membrane (Millipore) and detected by immunoblotting with indicated antibodies. Immunoblotting was performed following standard protocols and blots were developed using ECL reagent (GE Amersham). Protein band densitometry analyses were performed using ImageJ software (U.S. National Institutes of Health).

Oil Red O staining and triglyceride assay

To stain lipid droplets, differentiated cells were fixed in 3.7% buffered paraformaldehyde for 0.5 h and stained with 0.3% Oil Red O stain (ORO) in isopropanol for 1 h. After staining, cells were washed in distilled water and photographed using a digital camera and a dissecting microscope. Intracellular triglyceride levels were measured in induced cell lysates with an enzymatic assay using the Triglyceride Quantitation Kit and manufacturer's protocol (BioVision). Triglyceride levels are normalized to sample protein concentrations by a BCA assay (Thermo Sci.).

Real-Time quantitative PCR

Total RNA was isolated from cells using Trizol (Invitrogen) and further purified to remove residual phenol/chloroform using RNAeasy Mini cleanup (Qiagen). First strand cDNA was synthesized with 800 ng of RNA using Superscript II reverse transcriptase kit (Invitrogen). Quantitative PCR (qPCR) was performed in duplicate or triplicate using 1 µl of cDNA and SYBR Green PCR master mix (Applied Biosystems) in an Applied Biosystems 7900HT Fast Real-Time PCR system. Gene expression was normalized to *TPB* levels and analyzed by the $\Delta\Delta C_t$ method. qPCR primers for *WDTC1* and *SREBP1c* was designed using Primer-BLAST (NCBI) and all other primers were described previously (Choi et al., 2010) and listed in Table 2.2.

Animal experiments

C57BL/6 control and *Cul4a* conventional knockout mice were a gift of Dr. P. Raychaudhuri. All animal experiments were performed in accordance with University of North Carolina (UNC) animal care and use committee. Total body weight was measured for approximately age matched control and *Cul4a*$^{-/-}$ adult male and female mice (~1 year old); all other experiments utilized male mice aged 6-12 months old. Mice were fed a regular fat diet (10% kcal fat; Research Diets) *ad libitum*. Mouse tissues were harvested and weighed before formalin fixation and paraffin embedding. For histological analyses, 8 µm sections were hematoxylin and eosin (HE) stained. For analyses of metabolites, overnight fasted mice were euthanized and blood was collected by cardiac puncture and kept on ice until serum was separated by centrifugation and stored at -80 °C until analysis. Serum glucose, triglycerides, insulin and leptin levels were measured at the UNC Animal Clinical Chemistry Core Facility. Insulin and leptin levels were measured by metabolism multiplex immunoassay (Millipore).

Subcellular fractionation and chromatin extraction

Cells were fractionated and soluble chromatin extracts were prepared by micrococcal nuclease (MNase) digestion as described previously (Mendez and Stillman, 2000). Pelleted

3T3-L1 cells (8 x 10^6) were resuspended and incubated on ice for 5 min in 200 µl buffer A [10 mM HEPES (pH 7.9), 10 mM KCl, 1.5 mM MgCl2, 0.34 M sucrose, 10% glycerol, 1 mM DTT and Halt™ PPIC] plus 0.1% Triton X-100. Nuclei were recovered in pellet 1 (P1) after centrifugation (4 min, 1,300 g, 4 °C), and the supernatant (S1) was further clarified by centrifugation to obtain cytosolic fraction (S2). For nucleoplasmic fraction, P1 pellet was washed once in buffer A and lysed in 100 µl buffer B (3 mM EDTA, 0.2 mM EGTA, 1 mM DTT and Halt™ PPIC), centrifuged and the supernatant was recovered (S3). For chromatin enriched fraction, P1 pellet was resuspended in buffer A and treated with 2 U MNase (1 min, 37 °C) and centrifuged; treated nuclei were then lysed in 100 µl buffer B and the chromatin fraction was recovered in the supernatant (S3) of MNase treated nuclei.

In vivo ubiquitylation assays

For the detection of ubiquitylated proteins in vivo, HEK293T cells were first transfected with HA-ubiquitin and split ~10 h later. HA-ubiquitin transfected cells were transfected again with various combinations of plasmids 24 h and then siRNAs 32 h post HA-ubiquitin transfection to minimize variations in HA-ubiquitin expression across cells. At 67 h post siRNA transfection, cells were treated with MG132 (10 uM) and collected 5 h later. Cells were lysed under denaturing conditions in 1% SDS buffer [50 mM Tris (pH 7.5), 0.5 mM EDTA, 1% SDS, 1 mM DTT] by boiling for 10 min and then sonicating at 15% amplitude for 15” (0.5” pulse on/2” pulse off). Extracts were clarified by centrifugation and immunoprecipitated in 0.1% SDS by 10-fold dilution with NP-40 buffer as described previously (Hu et al., 2008). Flag-tagged WDTC1 was immunoprecipitated by anti-FLAG M2 agarose beads, resolved by SDS-PAGE and ubiquitylated WDTC1 proteins were detected by immunoblotting with anti-HA antibodies.

In vitro ubiquitylation assays

In vitro ubiquitylation assays were performed according to manufacturer’s protocol (Enzo Life Sci.) and as described previously (Hu et al., 2012). WDTC1 immunocomplexes were

immunoaffinity purified from transfected HEK293T cells expressing either Flag-WDTC1-WT or Flag-WDTC1-WT-ΔH. Flag-WDTC1 proteins were immunoprecipitated with anti-FLAG M2 agarose beads overnight at 4 °C. Immunocomplexes were washed three times in lysis buffer and twice in TBS followed by elution with molar excess of FLAG peptide (Sigma). In 50 µl reaction volume, 100 nM of either WDTC1-WT or WDTC1-ΔH immunocomplexes (source of E3) and 200 nM of human recombinant histone H2A substrate (New England Biolabs) were combined with a ubiquitylation buffer containing 100 nM E1 (UBE1), 1 uM E2 (UBE2D3), 1 uM human recombinant ubiquitin Mutant No K (Boston Biochem), 1 U inorganic pyrophosphatase, 1 mM DTT and 5 mM Mg-ATP. Reactions were incubated at 37 °C for 30 min and terminated by addition of SDS sample buffer. Reaction products were resolved by SDS-PAGE and detected by immunoblotting with anti-H2AK119ub or anti-ubiquitin antibodies.

Molecular modeling

Modeling was performed at the UNC R. L. Juliano Structural Bioinformatics Core facility. Suitable templates for the H-box, WD40 and TPR domains of WDTC1 were identified using HHpred (Soding, 2005). The Hbox and WD40 domains were modeled simultaneously using the Modeller software package (Fiser and Sali, 2003) and two template structures. One template was of the WDTC1 H-box in complex with DDB1 [PDB ID 3I7N; (Li et al., 2010)], and the second template was of the H-box and WD40 domains of DDB2 in complex with DDB1, CUL4A and ROC1 [PDB ID 4A0K; (Fischer et al., 2011)]. The TPR domains were modeled separately based on the template structure of Sgt2, a TPR structure from *Aspergillus fumigatus* [PDB ID 3SZ7 (Chartron et al., 2011)]. The model of the CRL4-WDTC1 complex was based on the structure of the CRL4-DDB2 complex (PBD 4A0K) with WDTC1 superimposed based on its H-box (PBD 317N) and then replacing DDB2. The TPR domains were manually moved to a location near their insertion within the β-propeller. Models were rendered using Pymol.

Statistical analyses

The data are expressed as means ± SD or means ± SEM from the number of experiments indicated in figure legends. Statistical significance of differences between control and experimental samples was analyzed by two-tailed *t* tests using GraphPad Prism 5.1 Software.

FIGURES AND TABLES

Figure 2.1. *WDTC1* encodes a DWD protein with a novel structure.

(A) Domain structure of human WDTC1 with locations of the H-box motif and tandem WDXR residues indicated (top). Alignment of WDTC1 H-box motifs in different species (bottom left; boxed in grey) and bolded orange represents key residues contacting DDB1 as revealed by co-crystal structure of DDB1 and human WDTC1 H-box motif. Alignment of DWD boxes in different DWD proteins (bottom right) with WDXR submotif indicated and tandem DWD boxes are shown only for WDTC1 (indicated by a -1 or -2).

(B) Modeled structure of the human WDTC1 protein. WD40 repeats form a classic seven-bladed β-propeller (light blue) with protruding antiparallel α-helices of the TPR motifs (green) linked by unstructured regions (dashed lines). The solvent-exposed arginine residues of tandem WDXRs, rendered in dark blue ball-and-sticks, are located on the bottom surface of the propeller fold. WDTC1 modeling was based on DDB2 (PDB 4A0K), Sgt2 (PDB 3SZ7) and the WDTC1 H-box (PDB 3I7N) structural templates. The structure was color coded according to the linear domain organization presented in (A).

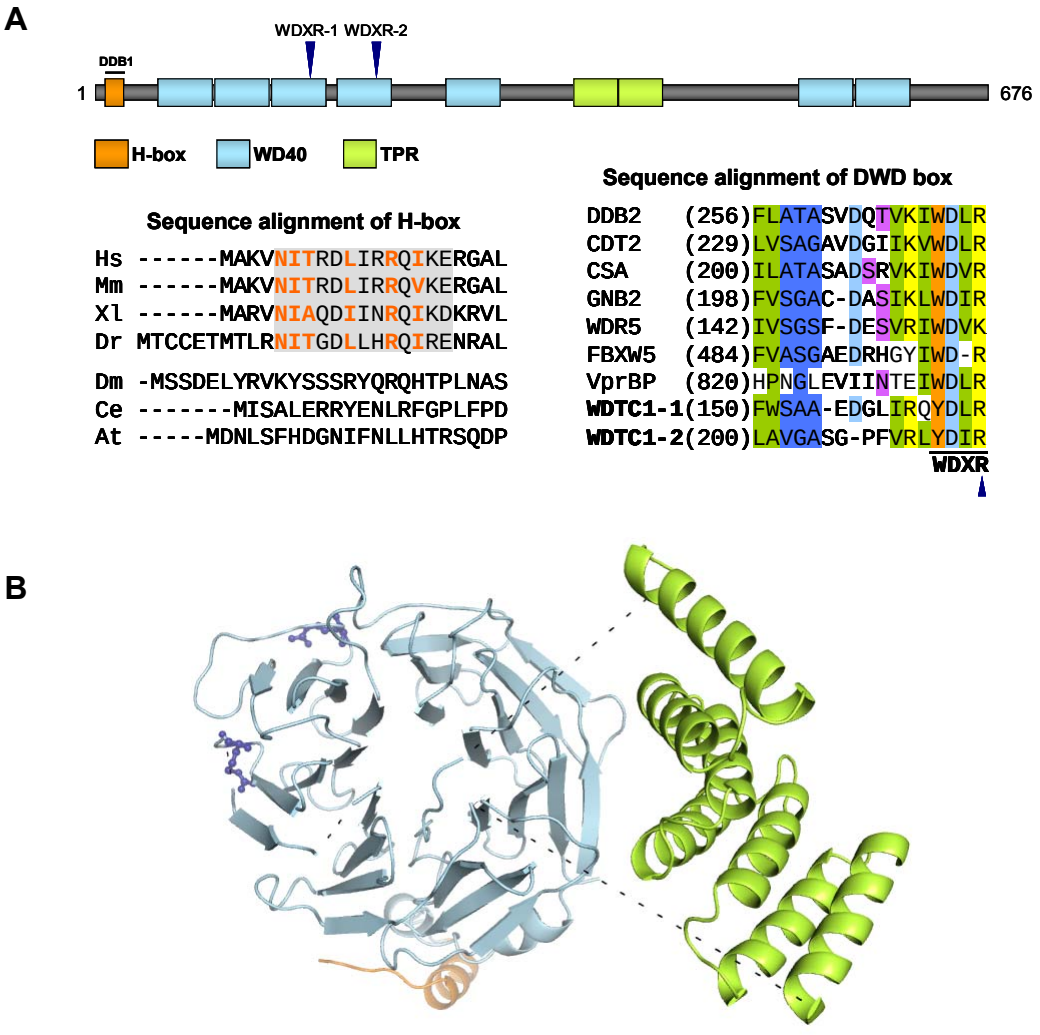

Figure 2.2. WDTC1 is a substrate receptor of CRL4 complexes.

(A) Endogenous CUL4A and -B complexes were isolated from HEK293T cell lysates by immunoprecipitation (IP) with CUL4A or CUL4B antibodies and associated proteins were detected by immunoblotting (IB) with indicated antibodies; IgG, control antibodies.

(B) Flag-tagged wild-type and mutant WDTC1 proteins were transiently expressed in HCT116 cells. Cells were treated with 50 μg/ml protein synthesis inhibitor cycloheximide (CHX) for 0, 2, 4 and 8 hours. Cells lysates were prepared and protein levels were analyzed by immunoblotting as indicated (top) and quantified by normalizing to α-tubulin and plotted as relative to 0 h (bottom).

(C) Flag-tagged wild-type and mutant WDTC1 proteins were transiently expressed in HEK293T cells. Flag-WDTC1 complexes were isolated from cell lysates by immunoprecipitation with anti-FLAG and their associated proteins were detected by immunoblotting as indicated; EV, empty vector control.

(D) Top, the modeled structure of WDTC1 in complex with CRL4 (PDB 4A0K): DDB1 (dark blue), CUL4A (grey) and ROC1 (pink). WDTC1 structure is described in Figure 2.1B. WDTC1 superimposition was based on its H-box structural template (PDB 3I7N). Bottom, schematic representation of wild-type and mutant WDTC1 summarizing the results presented in (C). Binding of WDTC1 proteins to CRL4 is indicated by +; –, binding not detected.

(E) HEK293T cells transfected with HA-ubiquitin plasmid along with various combinations of Flag-WDTC1-WT or Flag-WDTC1-ΔH plasmid and scramble (–) or DDB1 siRNA were lysed under denaturing conditions and immunoprecipitated with anti-FLAG. The levels of WDTC1 ubiquitylation were evaluated by immunoblotting with indicated antibodies.

(F) HEK293T cells transiently expressing Flag-WDTC1 were transfected with scramble (scrm) siRNA or siRNAs against DDB1, CUL4A or CUL4B. Flag-WDTC1 protein levels and knockdown efficiency were assessed by immunoblotting with indicated antibodies. Lysates were also immunoblotted with p21 and cyclin E antibodies to validate the functional depletion of CUL4A or CUL4B, respectively.

Figure 2.2. (continued)

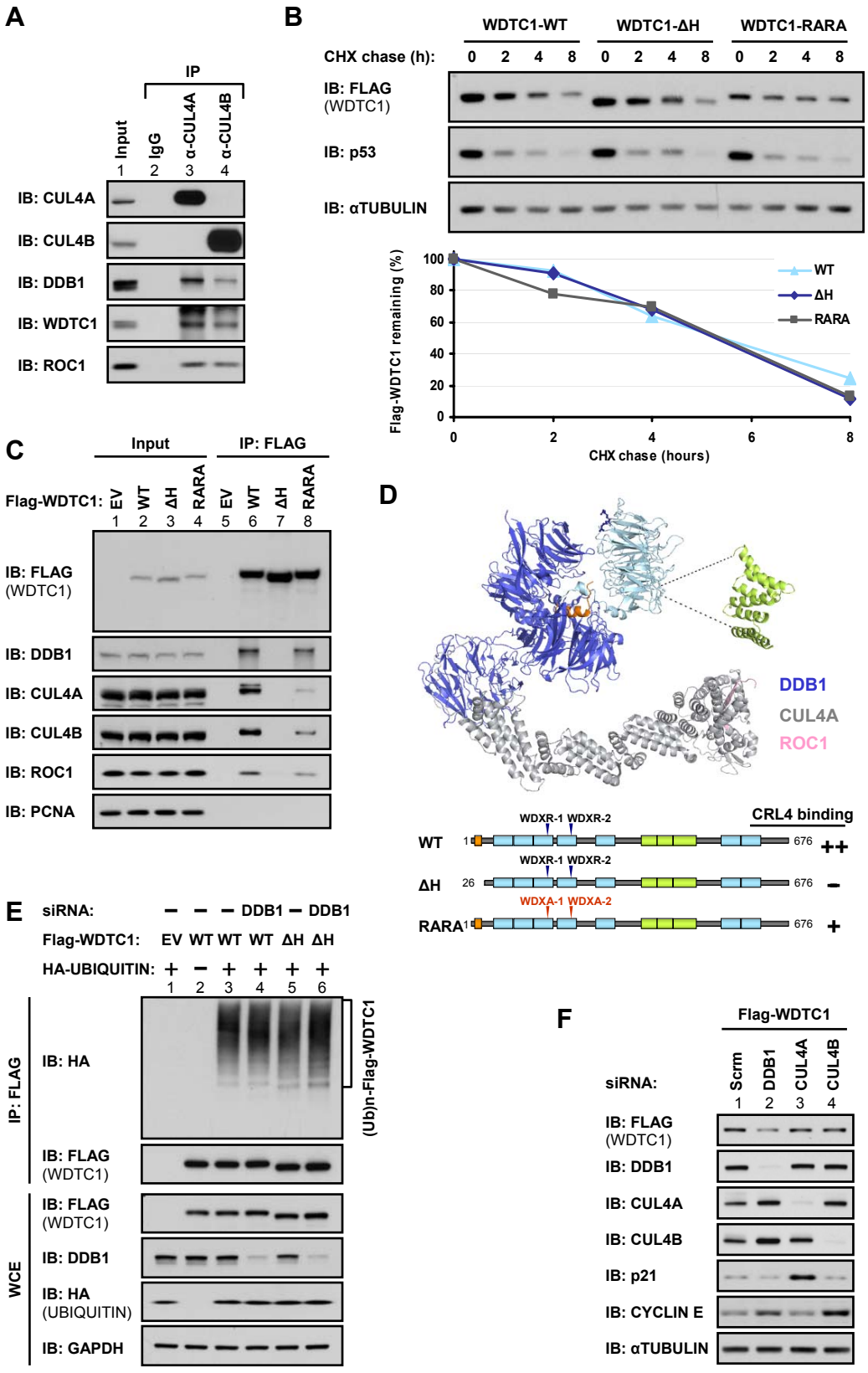

Figure 2.3. WDTC1 suppresses adipogenesis in a CRL4-dependent manner.

(A) Expression of CRL4 and WDTC1 proteins in a panel of adult mouse tissues was assessed by immunoblotting with indicated antibodies; brown adipose tissue (BAT), inguinal white adipose tissue (IWAT), mesenteric white adipose tissue (MWAT) and gonadal white adipose tissue (GWAT).

(B) 3T3-L1 preadipocytes were adipogenically induced and lysates were prepared from cells collected at indicated days post induction, including an uninduced (0D) control. Endogenous WDTC1 interaction with CRL4 subunits was evaluated by immunoprecipitation with anti-WDTC1 followed by immunoblot analyses with indicated antibodies.

(C) 3T3-L1 preadipocytes were retrovirally transduced to generate stable cell lines expressing vector control (EV) or Flag-tagged wild-type (WT) and mutant WDTC1 proteins. Protein expression and CRL4 binding were confirmed by immunoprecipitation followed by immunoblotting with antibodies as indicated.

(D-F) 3T3-L1 stable cells described in (B) were adipogenically induced. Their adipogenic potential was assessed by Oil Red O (ORO) staining (D); plate view (top) and microscopic view (bottom). (E) Triglyceride levels were quantified by an enzymatic assay. (F) Adipogenic gene expression was evaluated by real-time qPCR analysis. The data in (E) and (F) were derived from three replicate experiments and plotted relative to EV control levels (mean ±SEM, *P< 0.05, **P< 0.005 for cells expressing WDTC1 proteins, compared with EV).

Figure 2.3. (continued)

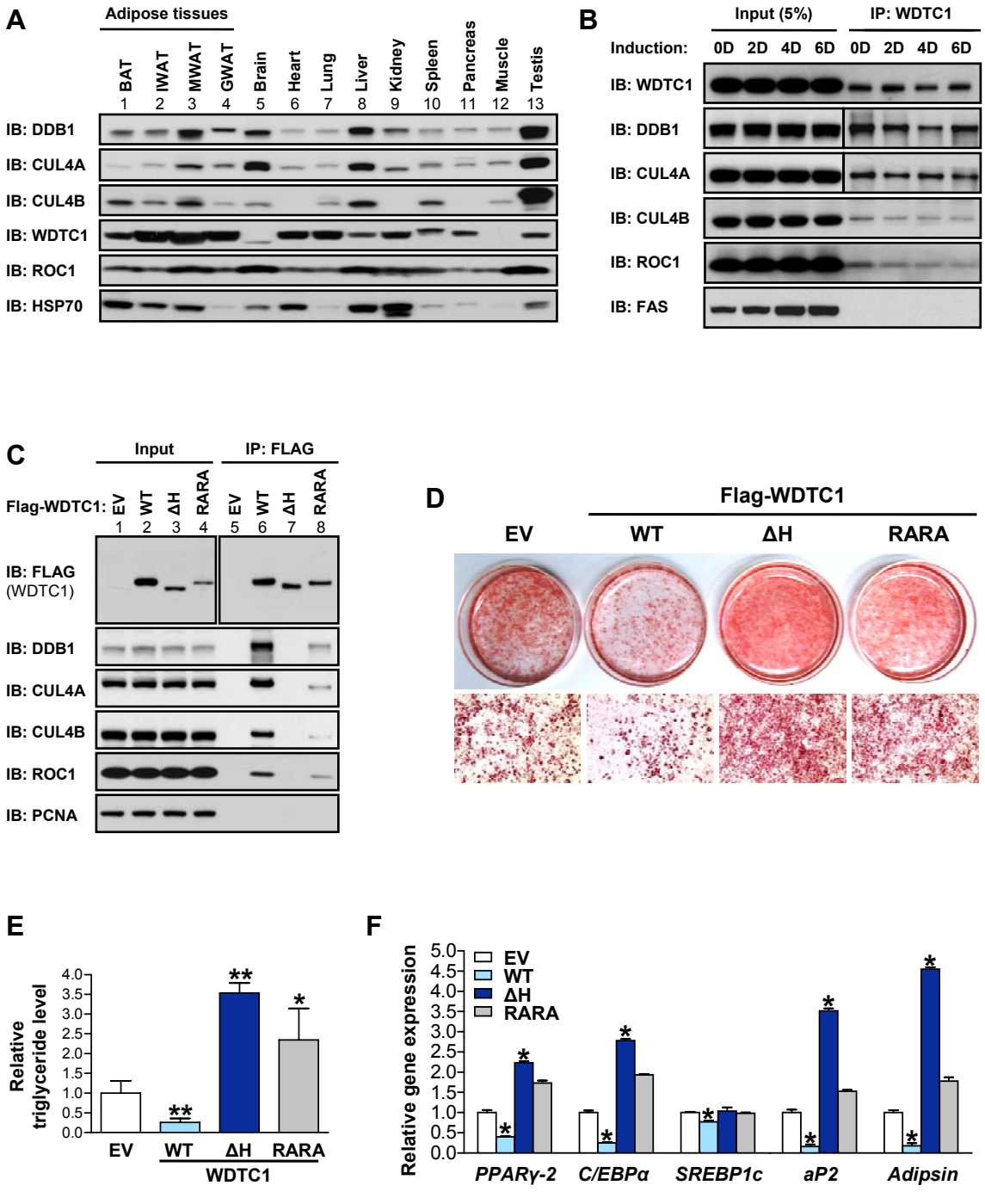

Figure 2.4. CUL4A and CUL4B RNAi phenotype cannot be clearly assessed in 3T3-L1 differentiation.

(A) 3T3-L1 preadipocytes were stably transfected with either retroviral-based shRNAs targeting GFP control or either *Cul4a* or *Cul4b*. Knockdown efficiency and the expression levels of various proteins were analyzed by immunoblotting as indicated.

(B) To measure proliferation, cells in (A) were plated at equal density ($1.5x10^5$). The cell number was counted every day for 7 days. An average from two experiments is plotted.

(C) To analyze cell cycle distribution, cells in (A) were plated at equal density ($1x10^6$). After 24 hours, cells were trypsinized and fixed overnight in 75% ethanol at 4 °C. Fixed cells were stained with propidium iodide and then analyzed by flow cytometry to measure DNA content.

(D) 3T3-L1 stable cells described in (A) were adipogenically induced. Their adipogenic potential was assessed by Oil Red O (ORO) staining; plate view (top) and microscopic view (bottom).

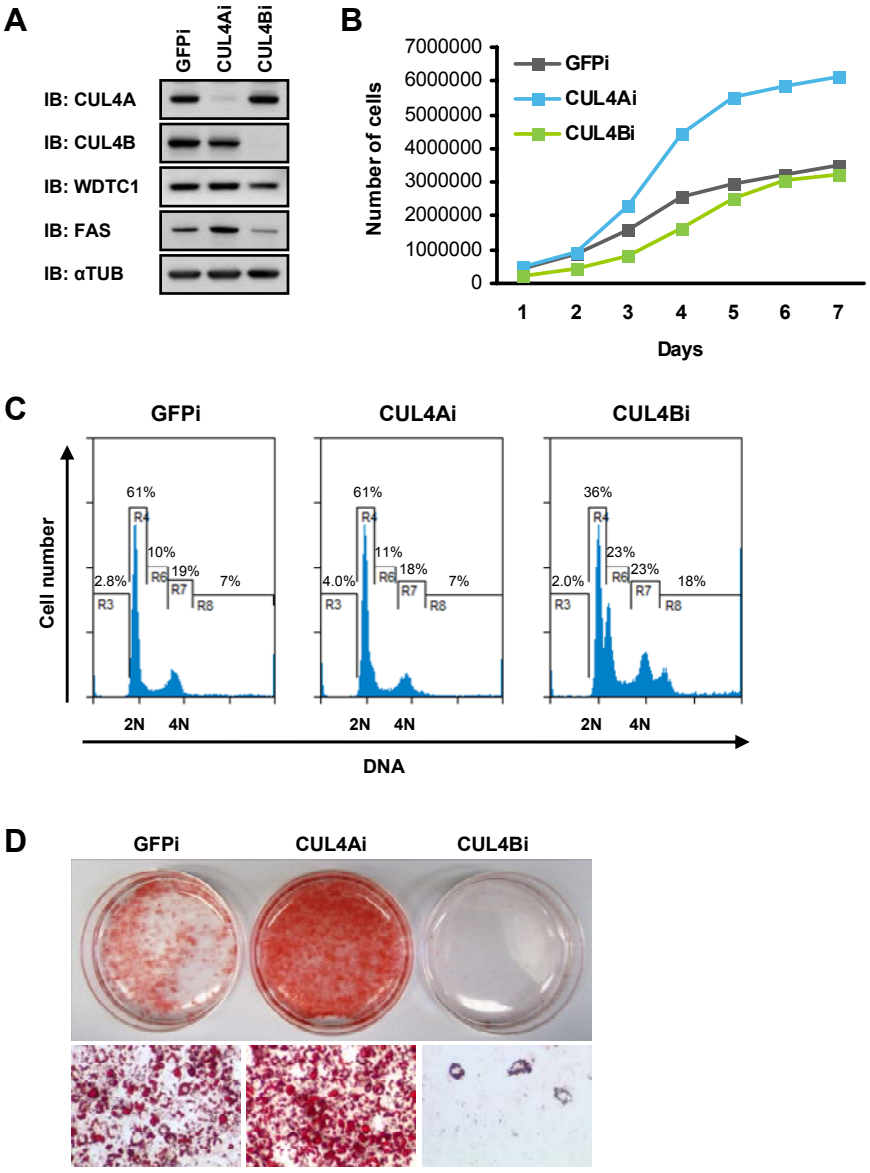

Figure 2.5. Wild-type WDTC1, but not CRL4 binding mutants, rescues the WDTC1 knockdown phenotype.

(A) Schematic of the WDTC1 knockdown-rescue lentiviral vector (top). 3T3-L1 preadipocytes were lentivirally transduced to generate stable cells expressing a non-specific (NS) control shRNA, shWDTC1 targeting endogenous *Wdtc1* mRNA, or cells simultaneously expressing shWDTC1 and shRNA refractory forms of *WDTC1* protein coding sequences. Bottom, depletion of endogenous *Wdtc1* mRNA by shWDTC1 was confirmed by real-time qPCR and expression of endogenous WDTC1 and ectopically expressed WDTC1 proteins were detected by immunoblotting with anti-WDTC1.

(B-D) 3T3-L1 stable cells described in (A) were adipogenically induced. Their adipogenic potential was assessed by ORO staining (B), triglyceride quantitation (C) and adipogenic gene expression (D). The data in (C) and (D) were derived from three replicate experiments and plotted as relative to NS control (mean ±SEM, **P*< 0.05, ***P*< 0.005, compared with cells expressing NS).

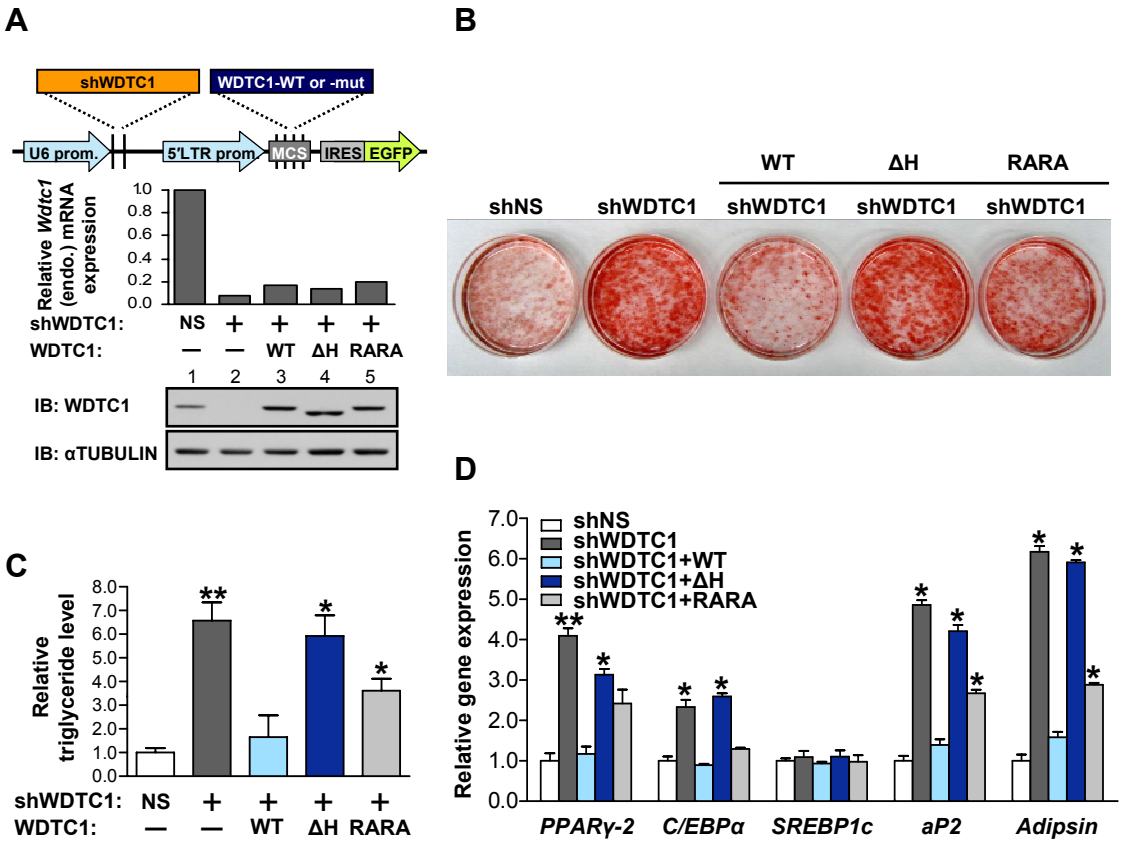

Figure 2.6. *Cul4a*$^{-/-}$ mice exhibit adipocyte hypertrophy and poor metabolic profiles.

(A) Lysates were prepared from gonadal and inguinal white adipose tissues (GWAT and IWAT, respectively) of wild-type (WT) or *Cul4a* knockout mice. Protein expression was evaluated by immunoblotting with antibodies as indicated.

(B) Average body weights of age-matched female WT (n = 4) and *Cul4a*$^{-/-}$ (n = 6) or male WT (n = 27) and *Cul4a*$^{-/-}$ (n = 18) mice.

(C) Photograph of representative GWAT and IWAT from two different WT (n = 7) and *Cul4a*$^{-/-}$ (n = 8) age-matched or littermate mice. Scale bar, 10 mm.

(D) Average weights of indicated tissues or organs of WT (n = 6) and *Cul4a*$^{-/-}$ (n = 4) age-matched or littermate mice.

(E) Histological analysis of representative GWAT and IWAT of WT and *Cul4a*$^{-/-}$ age-matched or littermate mice by HE stain. Scale bar, 0.05 mm.

(F) Analysis of indicated serum metabolites from age-matched or littermate controlled WT (n = 6) and *Cul4a*$^{-/-}$ (n = 8) mice (except insulin; n = 4 WT, n = 3 *Cul4a*$^{-/-}$).

The data in (B), (D) and (F) represent mean ±SEM, * P< 0.05 for *Cul4a*$^{-/-}$ compared with WT for each comparison; ns is non-significant.

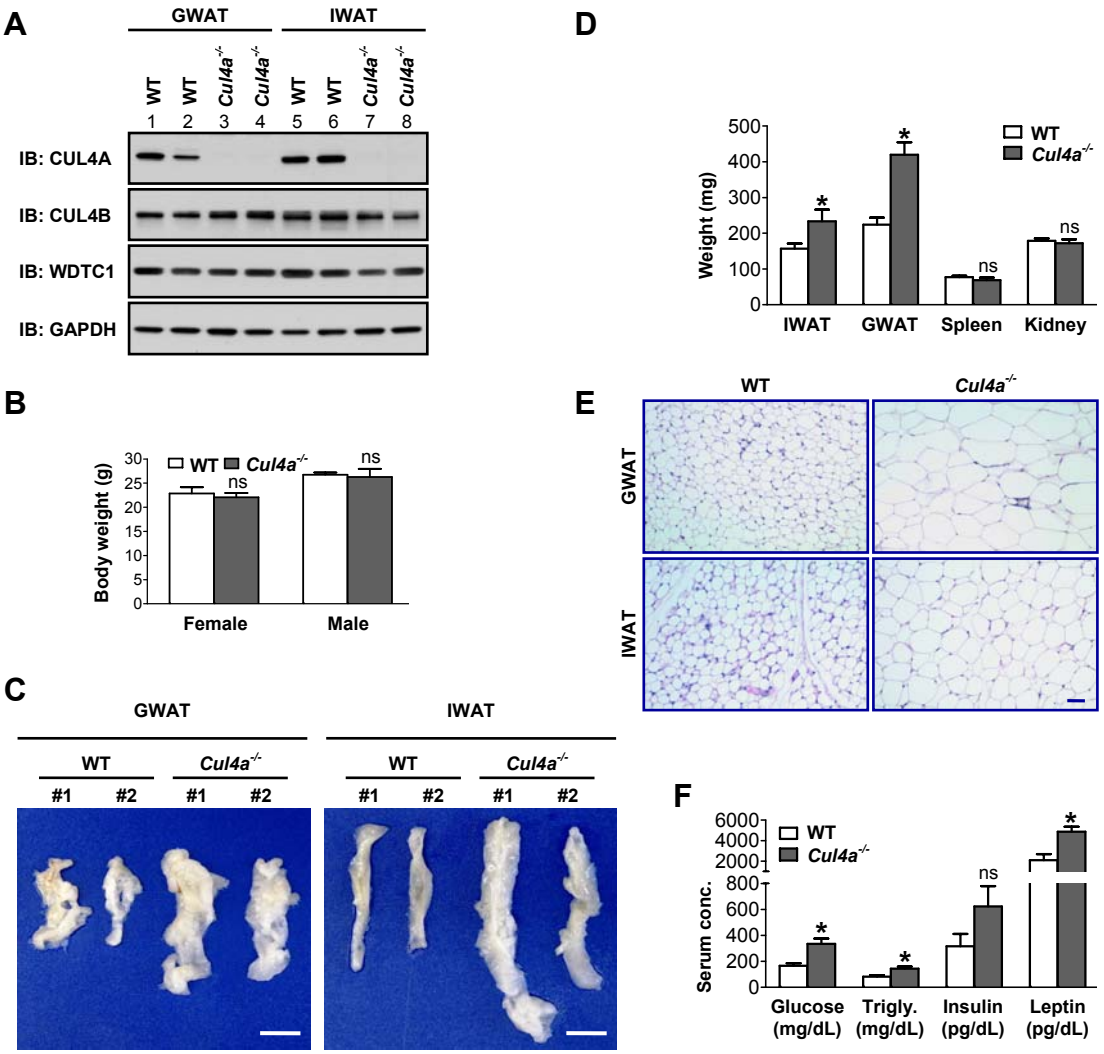

Figure 2.7. WDTC1 binds histones and promotes histone H2AK119 monoubiquitylation.

(A) 3T3-L1 cells stably expressing Flag-WDTC1 were subjected to subcellular fractionation. Chromatin-enriched fraction (S3*) was prepared by micrococcal nuclease (MNase) digestion to release mononucleosomes from insoluble nuclear fraction. Aliquots of total cell extract (TCE) and subcellular fractions were analyzed by immunoblotting (IB) with indicated antibodies; fraction purity was assessed by α-tubulin and histone H3 antibodies.

(B) Cells in (A) were fixed and protein localization was detected by immunofluorescence microscopy with an anti-FLAG antibody (red) and anti-DDB1 antibody (green). Nuclei were stained with DAPI and images were merged to show colocalization of WDTC1 and DDB1 in the cytoplasm and nucleus (yellow).

(C) Chromatin enriched nuclear extracts were prepared from HEK293T cells cotransfected with Flag-WDTC1 and HA-tagged core histones and immunoprecipitated (IP) with anti-FLAG and immunoblotted as indicated. The probable H2AK119ub band detected in nuclear extract is indicated by an asterisk.

(D) Soluble chromatin extracts were prepared as in (A) from preadipocyte or induced 3T3-L1 cells stably expressing control (EV) and Flag-WDTC1 proteins. Histone H2A monoubiquitylation was detected by H2AK119ub-specific antibody (anti-H2AK119ub) and total histone H2A served as loading control. Relative intensity represents ratio of H2AK119ub over total H2A signal normalized to EV; data derived from two (preadipocyte) or three (induced) independent experiments (mean ±SD, *P< 0.05 for WDTC1-WT or WDTC1-ΔH, compared with EV control).

(E) Chromatin extracts were prepared by MNase digestion from HEK293T cells transiently expressing either EV control or the indicated Flag-WDTC1 proteins. Histone H2AK119 levels were evaluated by immunoblotting with anti-H2AK119ub (H2Aub) and total histone H2A served as loading control.

(F) Chromatin extracts were prepared as in (E) from HCT116 cells transiently expressing EV control or Flag-WDTC1 proteins along with siRNAs against scramble (scrm) control or DDB1. Levels of H2AK119ub were assessed by immunoblotting as indicated.

(G) Nucleosomal proteins were released from insoluble chromatin preparation from cells in (D) by deoxyribonuclease (DNase) digestion and the resulting extract was used for immunoprecipitation by anti-FLAG and immunoprecipitated proteins were detected by immunoblotting as indicated.

Figure 2.7. (continued)

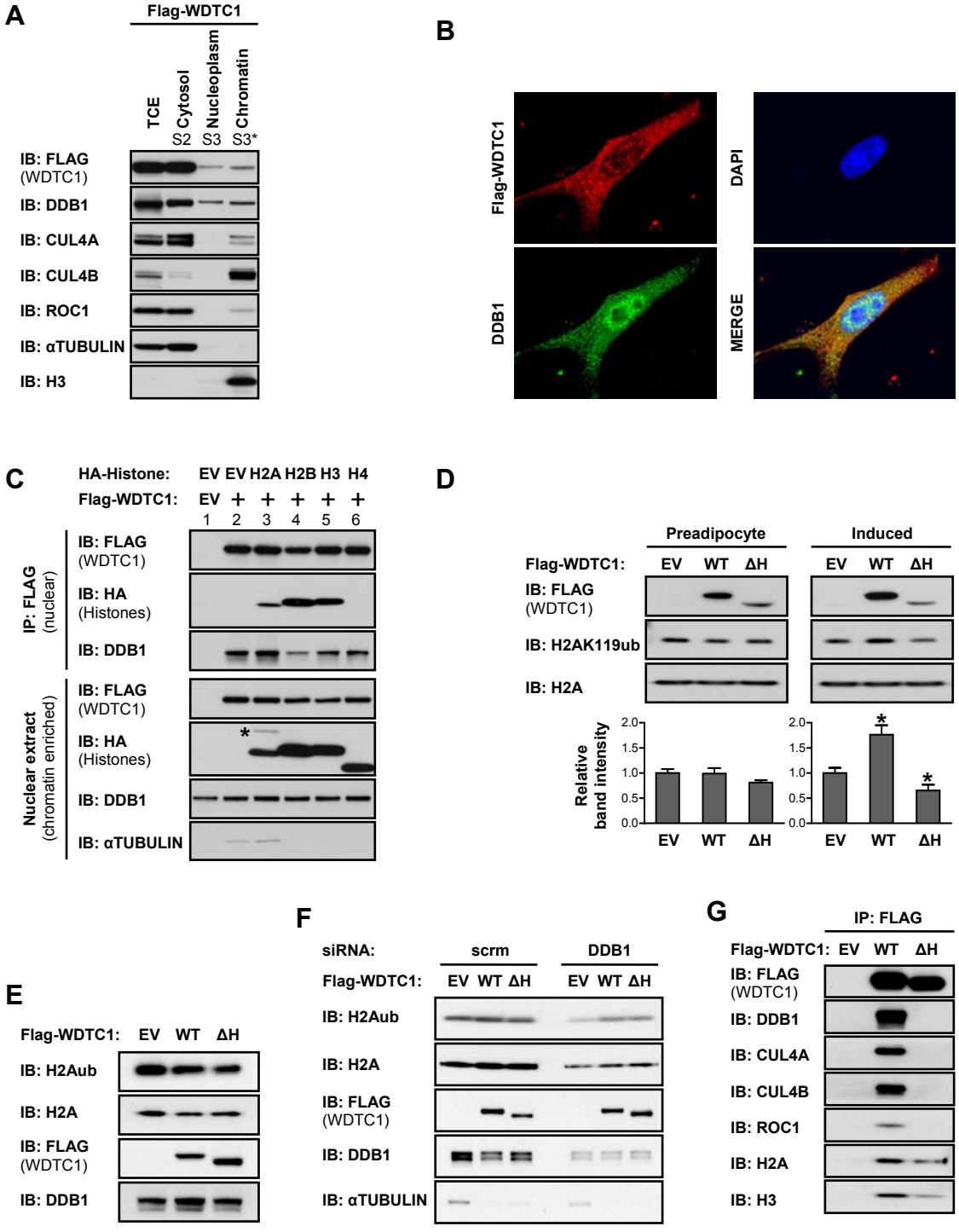

Figure 2.8. CRL4^{WDTC1} catalyzes histone H2AK119 monoubiquitylation in vitro.

(A) Immunoaffinity purification of Flag-WDTC1 complexes from HEK293T cells transiently expressing Flag-WDTC1-WT or Flag-WDTC1-ΔH. Cell lysates were immunopurified by anti-FLAG M2 resin and eluted with 3XFLAG peptide. The eluted fractions were resolved by SDS-PAGE followed by Coomassie staining and immunoblotting as indicated to confirm copurification of CRL4 proteins.

(B) In vitro ubiquitylation assay with recombinant histone and WDTC1 complexes purified in (A) as the source of E3 ligase. Reactions were incubated in a buffer containing ubiquitin, recombinant E1 (UBE1), E2 (UBE2D3) and ATP. Reaction products were resolved by SDS-PAGE. Ubiquitylated H2A was detected by anti-H2AK119ub.

(C) Lower exposure of lane 1 of H2A ubiquitylation blot in (B); scaling is preserved for ladder reference in (B) and monoubiquitylated H2A band is indicated.

(D) In vitro ubiquitylation assay with wild-type and mutant histone proteins. Assay details are described in (B). H2A ubiquitylation was assessed by immunoblotting with anti-ubiquitin and other antibodies as indicated. Substrate H2A was detected by anti-H2A.

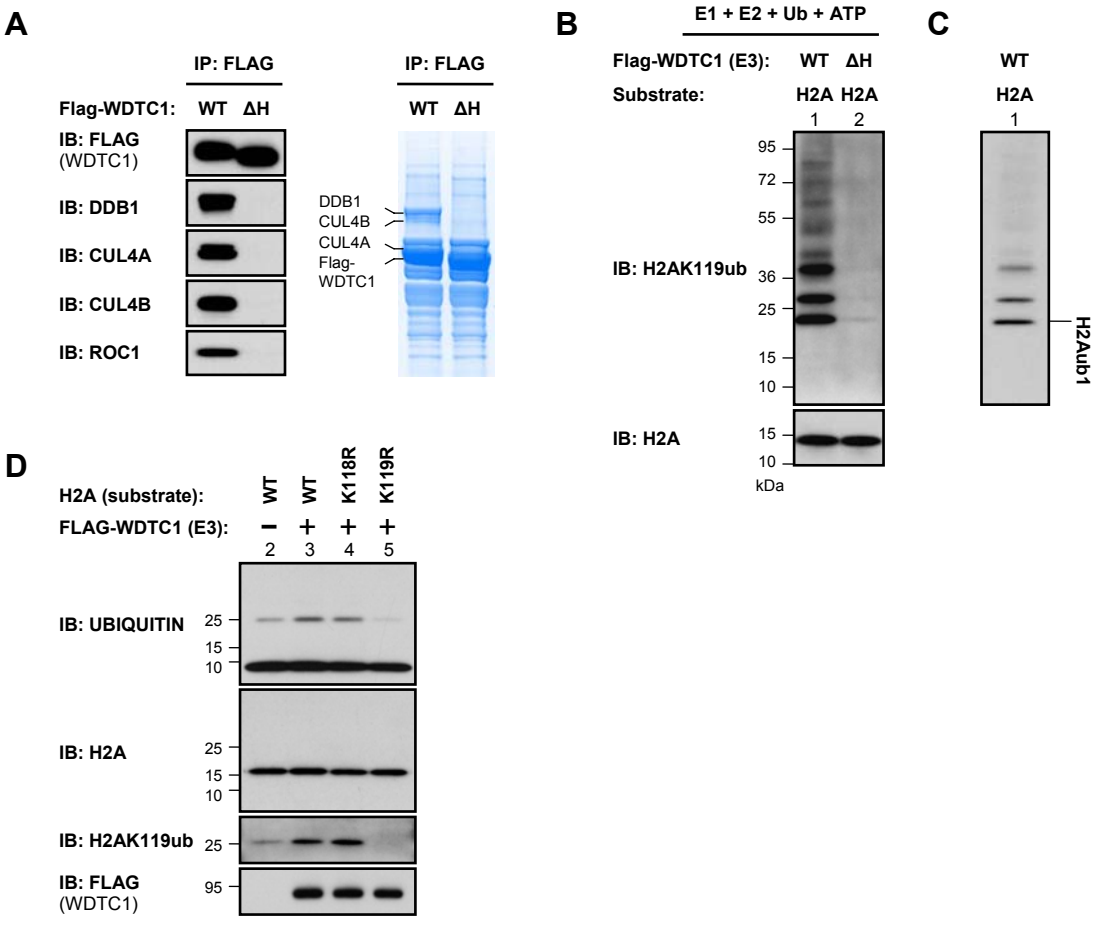

Figure 2.9. CRL4^{WDTC1}-dependent increase in H2AK119 monoubiquitylation is associated with reduced H3K4 trimethylation.

(A) Chromatin extracts from adipogenically induced 3T3-L1 cells stably expressing vector control (EV) or Flag-WDTC1 proteins were prepared by MNase digestion. The levels of various histone modifications were evaluated by immunoblotting with indicated antibodies.

(B) Chromatin extracts from adipogenically induced 3T3-L1 cells stably expressing control shRNA (GFPi) or two different *Wdtc1* shRNAs were prepared as in (A). Extracts were subjected to immunoblot analysis with indicated antibodies (Top). The specificity of the *Wdtc1* shRNAs was confirmed by ORO staining and immnoblotting with anti-WDTC1 (bottom).

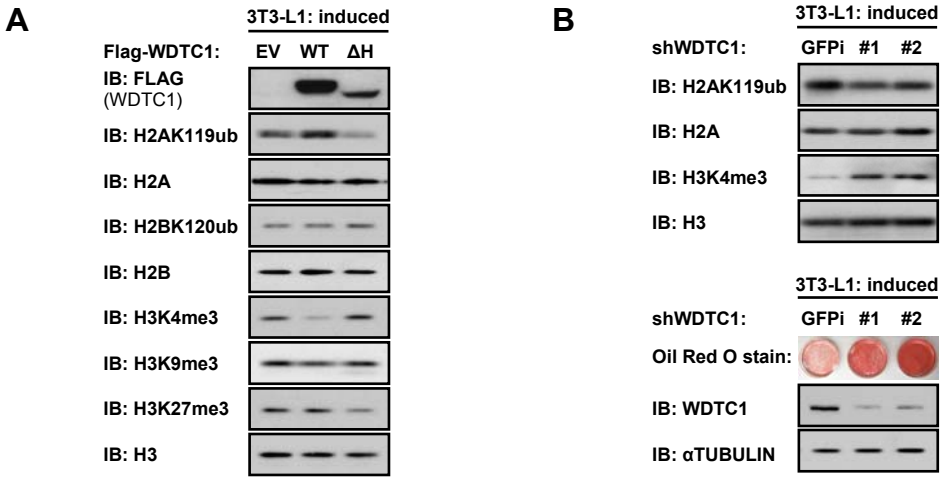

Figure 2.10. A model of CRL4^{WDTC1}-dependent transcriptional repression.

This model predicts CRL4^{WDTC1} E3 ligase negatively regulates adipogenesis through transcriptional repression. During adipogenesis, CRL4^{WDTC1} promotes H2AK119ub at a subset of proadipogenic gene promoters. H2AK119ub consequently prevents H3K4me3 at these promoters, thus maintaining transcriptional repression. To promote adipogenesis, an upstream signal inhibits CRL4^{WDTC1} E3 ligase activity. Subsequently, H2AK119ub silenced promoters are predicted to be antagonized by histone H2A deubiquitylases (DUBs), which remove H2AK119ub to facilitate histone methytransferase (HMT) activity, establishing H3K4me3 promoters. H3K4me3 in turn drives preinitiation complex (PIC) formation to activate transcription at CRL4^{WDTC1} repressed genes.

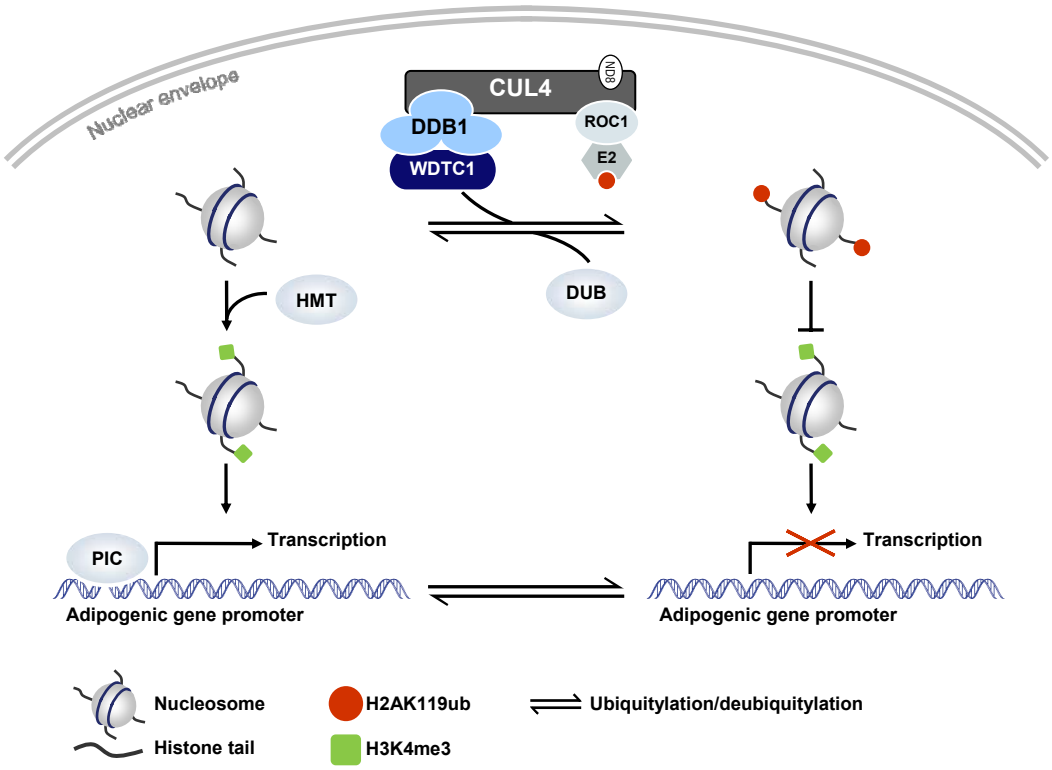

Figure 2.11. Schematic summary of experimental procedures performed with 3T3-L1 cells.

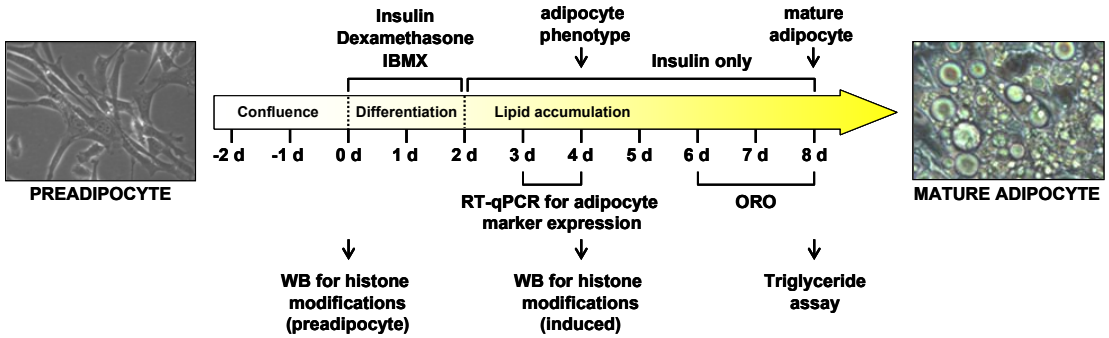

Table 2.1. List of oligos used in this study.

Gene	Oligo type	Sequence* (5′–3′)
Mouse *Wdtc1*-1	shRNA (pMKO.1)	GCTCTTCCTAAGGACCCTTTG
Mouse *Wdtc1*-2	shRNA (pMKO.1)	GGAGAGACACATAAGCCTTAC
Mouse *Cul4a*	shRNA (pMKO.1)	GCTTCTGTAAATCAGGTTTCT
Mouse *Cul4b*	shRNA (pMKO.1)	GCTGTAGCCATTGGATAAACT
Mouse *Wdtc1*-1	shRNA (pLL5.5)	GGGTGACACAATTGATTAA
Mouse *Wdtc1*-2	shRNA (pLL5.5)	GCACCATCTCATTGCTTTA
Non-specific (NS)	shRNA (pLL5.5)	GATCGACTTACGACGTTAT
Human *DDB1*	siRNA	CCUGUUGAUUGCCAAAAAC
Human *CUL4A*	siRNA	GAACUUCCGAGACAGACCU
Human *CUL4B*	siRNA	AAGCCUAAAUUACCAGAAA
Hs/ms *WDTC1*	qPCR forward	CTGCACCACAAGAAGCTGCT
Hs/ms *WDTC1*	qPCR reverse	ATGCGCTTCACCCGGTTTGTG
Mouse *Wdtc1*	qPCR forward	GGCGTCTGGTTCCGACGACC
Mouse *Wdtc1*	qPCR reverse	GCCGTGGCAATGCGCTTCAC
Mouse *PPARγ*	qPCR forward	GCATGGTGCCTTCGCTGA
Mouse *PPARγ*	qPCR reverse	TGGCATCTCTGTGTCAACCATG
Mouse *C/EBPα*	qPCR forward	CAAGAACAGCAACGAGTACCG
Mouse *C/EBPα*	qPCR reverse	GTCACTGGTCAACTCCAGCAC
Mouse *SREBP1c*	qPCR forward	CTGGCTGAGGCGGGATGA
Mouse *SREBP1c*	qPCR reverse	TACGGGCCACAAGAAGTAGA
Mouse *aP2*	qPCR forward	AAGGTGAAGAGCATCATAACCCT
Mouse *aP2*	qPCR reverse	TCACGCCTTTCATAACACATTCC
Mouse *Adipsin*	qPCR forward	CATGCTCGGCCCTACATGG
Mouse *Adipsin*	qPCR reverse	CACAGAGTCGTCATCCGTCAC
Mouse *TBP*	qPCR forward	ACCCTTCACCAATGACTCCTATG
Mouse *TBP*	qPCR reverse	TGACTGCAGCAAATCGCTTGG

*Only sense strands are shown for shRNA and siRNA oligos.

Table 2.2. List of antibodies used in this study.

Antibody	Provider	Catalog number
WDTC1	Abcam	174294
WDTC1	Abgent	AP4944b
CUL4A (mouse)	Abcam	ab72548
CUL4B	Sigma	HPA011880
FAS	Abcam	ab22759
GAPDH	Abcam	ab8245
α-TUBULIN	Thermo Sci.	MS-581
Ubiquitin	Dako	Z 0458
Ubiquityl-Histone H2A (Lys119) (D27C4)	Cell Signaling	8240
Ubiquityl-Histone H2B (Lys120) (D11)	Cell Signaling	5546
Tri-Methyl-Histone H3 (Lys4) (C42D8)	Cell Signaling	9751
Tri-Methyl-Histone H3 (Lys9)	Abcam	ab8898
Tri-Methyl-Histone H3 (Lys27) (C36B11)	Cell Signaling	9733
Histone H2A	Cell Signaling	12349
Histone H2B	Cell Signaling	8135
Histone H3	Cell Signaling	4499
HA-peroxidase (3F10)	Roche	12013819001
FLAG-peroxidase (M2)	Sigma	A8592

CHAPTER 3: PROTEOMIC SCREEN FOR CRL4^{WDTC1} SUBSTRATES

SUMMARY

WDTC1 gene, encoding a WD40 protein of undefined molecular function, has an evolutionarily conserved role in suppressing lipid accumulation in multicellular organisms. In the previous chapter, results demonstrated that WDTC1 protein is a substrate receptor of cullin 4 RING E3 ligase (CRL4) complexes. Central to WDTC1 function is its interaction with CRL4, suggesting WDTC1 may target a key proadipogenic substrate(s) to mediate adipogenic suppression. In this chapter, I aimed to characterize WDTC1 interacting proteins to search for candidate substrates of the CRL4^{WDTC1} complex using 3T3-L1 cell culture model of adipogenesis. Here I describe the results from two separate proteomic based screens for WDTC1 interactors using immunopurified wild-type and CRL4 binding mutant WDTC1 complexes. From these screens emerged a candidate substrate, fatty acid synthase (FAS), a key enzyme in lipid storage pathway. I characterized the interaction between WDTC1 and FAS, but ultimately the data conclusively show that FAS is not a substrate of the CRL4^{WDTC1} complex. However, I observed that while FAS expression is largely under transcriptional control, FAS ubiquitylation appears to be dynamically altered upon adipogenic induction. The functional consequence of FAS ubiquitylation is presently unclear but implicates that its activity maybe regulated posttranslationally by ubiquitylation.

BACKGROUND

Adipose tissues or depots, composed primarily of adipocytes, are energy reservoirs of vertebrate animals. Under metabolic homeostasis, adipocytes store excess energy in the form of triglycerides (lipogenesis), which is balanced by triglyceride release in the form of free fatty acids (lipolysis) to meet physiological energy requirements. By comparison, when energy consumption greatly exceeds expenditure or when other factors contribute to adipocyte dysfunction, total adipose tissue mass increases and can eventually lead to obesity and associated pathologies such as cardiovascular diseases and type 2 diabetes. Two factors can contribute to adipose tissue expansion: an increase in adipocyte size due to increased lipogenesis (hypertrophy) or an increase in adipocyte cell number due to deregulated differentiation of preadipocytes (hyperplasia), or both. Evidently, adipocyte hypertrophy underlies obesity, while the potential contribution of hyperplasia is still being debated (Sun et al., 2011). Adipocyte differentiation, preadipocyte to adipocyte transition, however has a critical role in adipose tissue maintenance as adult humans have a ~10% annual turnover rate, thus requiring continual replacement (Jiang et al., 2012b). In this chapter, adipogenesis is often used to generally refer to lipid accumulation, but in the strict sense, adipogenesis encompasses differentiation of preadipocytes and lipogenesis in mature adipocytes.

As with any biological process, adipogenesis is under complex regulation. Nutrition and hormone induced signaling cascades converge on transcriptional activation of key regulators of adipogenesis. While transcriptional mechanisms primarily regulate adipocyte function, posttranslational mechanisms such as ubiquitylation certainly play a role. Notably, the $CRL1^{FBXW7}$ complex targets two adipogenic transcription regulators for degradation: C/EBPα and SREBP1c transcriptional factors (Bengoechea-Alonso and Ericsson, 2010; Sundqvist et al., 2005). C/EBPα, together with PPARγ (master regulator of adipogenesis) transcription factor, is part of a feed-forward autoregulatory loop that is essential for adipocyte differentiation (Farmer, 2006). SREBP1c controls *de novo* lipid biosynthesis

through transcriptional activation of *fatty acid synthase* and also promotes *PPARγ* expression (Rosen and MacDougald, 2006). In 3T3-L1 cell culture, FBXW7 inactivation increases C/EBPα and SRBP1c protein stability, thus promoting adipogenesis as evidenced by increased adipogenic gene expression and lipid accumulation (Bengoechea-Alonso and Ericsson, 2010; Sundqvist et al., 2005). In both of these studies, the substrates were identified by a candidate approach based on their phosphorylation-dependent degradation and the presence of a FBXW7 phosphodegron, which mediates recognition and binding of phosphorylated substrates. The role of FBXW7 in adipocyte biology has not been examined in an animal model, but by targeting key proadipogenic substrates, these results minimally suggest FBXW7 is a negative regulator of adipogenesis.

WDTC1 has an established role in the negative regulation of lipid accumulation in multicellular organisms. To the best of my knowledge, it is the first factor that links CRL4 to adipocyte biology as uncovered in this study (Chapter 2). I demonstrated that adipogenic suppression by WDTC1 is dependent on its interaction with the CRL4 complex. Supporting an in vivo role for CRL4 in adipocyte biology, *Cul4a* knockout mice show adipocyte hypertrophy and metabolic defects similar to *Wdtc1*$^{+/-}$ mice. This also provided genetic support for their function in the same molecular pathway. Additionally, the discovery that CRL4^{WDTC1} promotes histone H2AK119ub in an adipocyte specific manner is in line with experiments showing that *Wdtc1* transgenic expression in mature adipocytes yielded leaner mice (Suh et al., 2007). This suggests WDTC1 mediates its anti-adipogenic effect in differentiated fat cells rather than by regulating the differentiation program itself. As such, I favor a model wherein CRL4^{WDTC1} targets a key proadipogenic protein(s) for degradation to mediate its anti-adipogenic function, at least in part. In chapter 2, I used a candidate approach to identify histone H2A as a CRL4^{WDTC1} substrate in vitro and showed that WDTC1 expression affects H2AK119ub levels in vivo. In this chapter, I used an unbiased proteomic based screen to identify candidate substrates to provide further mechanistic insights into CRL4^{WDTC1} function.

The interaction between a substrate and its E3 ligase is frequently weak, possibly to promote product release (Harper and Tan, 2012). Moreover, unlike CRL1 substrate receptors, which recognize substrates by phosphodegron motifs, whether CRL4 substrate receptors generally use targeting motifs is unclear, except CDT2 which targets PIP box proteins. Surely a large number of proteins may be identified in a proteomic screen and there has to be some means of selecting candidates. It was therefore a practical consideration to include a substrate trapping tool to maximize detection and aid selection of candidate substrates from contaminating proteins. As such, I immunopurified wild-type WDTC1 and CRL4 binding mutant WDTC1-ΔH complexes to obtain parallel analysis of their composition by mass spectrometry. Additionally, composition of WDTC1 complexes from two different 3T3-L1 cell states, undifferentiated and differentiated, was examined for comparison of differentiation-regulated interactions. Each screen included immunoprecipitates from control cells to eliminate nonspecific contaminants. Based on relevance to adipocyte biology and abundant interaction with WDTC1-ΔH, a candidate substrate emerged from this analysis: fatty acid synthase (FAS). FAS is a multifunctional enzyme that catalyzes the last step in *de novo* fatty acids synthesis from acetyl-CoA substrates, a process that contributes to adipocyte function—triglyceride storage (Jiang et al., 2012b). This chapter describes the results from the two screens and experiments to validate the interaction between WDTC1 and FAS.

RESULTS

WDTC1 interacting proteins in preadipocyte and induced 3T3-L1 cells

To search for WDTC1-associated proteins in 3T3-L1 uninduced cells, cells stably expressing an empty vector control (EV), or Flag-tagged wild-type WDTC1 (WDTC1-WT) and the CRL4 binding mutant WDTC1 (WDTC1-ΔH) were subjected to immunopurification followed by identification of associated proteins by mass spectrometry. The list of proteins associated with WDTC1-WT and WDTC1-ΔH complexes was manually refined by excluding

proteins that were indentified in the EV control sample and several ribosomal and cytoskeleton proteins that appeared to be common contaminants. This analysis revealed a large number of proteins in both WDTC1-WT and WDTC1-ΔH complexes (Figure 3.1A). The known interacting proteins, DDB1, CUL4A, CUL4B, ROC1 and the CRL4 associated COP9 signalosome complex and DDA1, were indentified in WDTC1-WT (Figure 3.1B) but not in WDTC1-ΔH complexes (Figure 3.1C), indicating the presence of cellular binding partners in purified WDTC1 complexes and the specificity of the screen. Although a larger number of WDTC1-WT associated proteins were identified, this is most likely due to the higher expression of WDTC1-WT than WDTC1-ΔH protein. Notably, WDTC1 does not appear to interact with any other protein complexes in 3T3-L1 cells and except histone H2A, WDTC1-WT associated proteins appeared to be unrelated to WDTC1 function in adipogenic suppression. Additionally, ~40% of the proteins in the WDTC1-ΔH complex overlapped with proteins identified in the WDTC1-WT complex, but no specific pathway enrichment is readily apparent either (Figure 3.1D). Quite remarkably, fatty acid synthase (FAS) was the most abundant protein in the WDTC1-ΔH complex (43 peptide spectrum matches, ~10% coverage) and it is clearly visible by silver stain (Figure 3.1E).

Similar to the search described above, I next immunopurified control and WDTC1 complexes from 3T3-L1 cells that were induced to undergo differentiation. In the first screen with uninduced cells, one problem that arose was high background from actin contamination in the purified complexes. Since the interacting proteins in purified complexes frequently range widely in abundance, it is likely that some low abundance proteins were missed in the previous screen due to signal masking from strong contaminants. To circumvent this problem, the protein complexes were fractionated by SDS-PAGE based on their molecular weight (Figure 3.2A) and in gel trypsin digestion was preformed for 43 gel slices which were then subjected to LC-MS. More than three times as many total number of proteins were identified in WDTC1-WT and WDTC1-ΔH complexes using this approach (Figure 3.2B). Notably, FAS was identified again with high confidence in WDTC1-ΔH complex but this time it was also

identified in the WDTC1-WT complex (Figure 3.2C). However, the total number of peptides (peptide spectral matches; PSM) and the number of unique FAS peptides (corresponding to ~30% coverage) revealed that while it was present abundantly in the WDTC1-ΔH complex, only one peptide was confidently indentified in the WDTC1-WT complex (Figure 3.2D). If FAS is a bona fide substrate of $CRL4^{WDTC1}$, this is indeed consistent with the notion that the interaction between the E3 ligase and substrate is intrinsically weak. Thus, perhaps reflecting the decreased probability of copurifying a substrate by WDTC1-WT, FAS is detected by immunoblotting in WDTC1-ΔH eluted fraction only (Figure 3.2E).

In summary, although a very large number of proteins were identified, a careful survey of the data sets yielded only one promising candidate that is clearly linked to adipogenesis. In addition, majority of the proteins that were identified are housekeeping proteins and due to their high abundance in the cell, these likely represent contaminants of the immunopurification process rather than physiologic binding partners. One notable absence from either screen was any other DWD proteins, consistent with the idea that WDTC1 binds CRL4 mutually exclusive of other substrate receptors to form a distinct complex. The one promising candidate that emerged from these screens is FAS. Because FAS activity is essential for lipid accumulation (lipogenesis) in maturing 3T3-L1 adipocytes, it fits well with the original hypothesis and may indeed be an adipogenic factor targeted by the $CRL4^{WDTC1}$ complex. In addition, since FAS was identified abundantly in the WDTC1-ΔH complex, it also fits with the dominant negative effect of WDTC1-ΔH. Since WDTC1-ΔH cannot bind CRL4, it may promote adipogenesis, at least in part, by sequestering a proadipogenic substrate such as FAS, and thereby prevent its ubiquitylation by CRL4 E3 ligase. I decided to further characterize the interaction between WDTC1 and FAS and determine whether it is indeed a CRL4 substrate.

Fatty acid synthase interacts with dominant negative WDTC1 but its protein level is not regulated by WDTC1

To begin to assess the functional significance of the interaction between WDTC1 and FAS, I first confirmed in vivo binding by immunoprecipitation and determined the effect of WDTC1 expression on FAS steady state protein levels by immunoblot analyses. In these experiments, I included the disrupted WDXR motifs mutant WDTC1-RARA which is defective in CRL4 binding and acts as a hypomorphic allele of WDTC1 (Chapter 2). In 3T3-L1 cells stably expressing Flag-WDTC1 proteins, immunoprecipitation by anti-FLAG revealed that endogenous FAS coimmunoprecipitated with WDTC1-ΔH mutant but not wild-type or WDTC1-RARA mutant (Figure 3.3A). I reasoned that if WDTC1-ΔH binds FAS nonspecifically, then in principle, spurious binding could also be detected in other cells that express FAS. However, FAS was not detected in WDTC1-ΔH complex from HCT116 cells (Figure 3.3B), suggesting that the interaction between WDTC1-ΔH and FAS is cell type specific. I next asked if WDTC1 regulates FAS protein stability in 3T3-L1 cells. While WDTC1 overexpression or knockdown did not appear to alter FAS protein levels in uninduced preadipocytes (Figures 3.3C and 3.3D), but after 3T3-L1 cells were induced to differentiate, FAS levels were decreased in WDTC1-WT cells and markedly increased in cells expressing mutant WDTC1 (Figure 3.3E), suggesting WDTC1 may regulate FAS stability in an adipocyte specific manner.

To better assess whether WDTC1 regulates FAS stability, I monitored FAS steady state protein levels over the course of 3T3-L1 differentiation. Indeed, this analysis revealed that FAS protein levels increased during differentiation and this increase was further enhanced in WDTC1 mutant expressing cells, especially WDTC1-ΔH cells (Figure 3.4A). To determine if this was indeed due to an increase in FAS protein stability rather than gene expression, I first looked at *Fasn* mRNA expression. It is evident from this experiment that the increase in FAS protein levels is related to a corresponding increase in *Fasn* mRNA expression (Figure 3.4B). In addition, FAS appears to be a very stable protein in 3T3-L1 cells

with a half-life longer than 12 hours, as estimated by cycloheximide chase experiment (Figure 3.4C). I learned later that FAS half-life is over 32 hours in 3T3-L1 cells (Student et al., 1980). In fact, these results are consistent with previous reports that increased *Fasn* mRNA expression directly correlates with FAS protein induction during 3T3-L1 differentiation (Moustaid and Sul, 1991; Student et al., 1980). It is therefore highly unlikely that WDTC1 regulates FAS stability during 3T3-L1 differentiation, and the increased FAS induction in cells expressing WDTC1 mutants likely reflects enhanced adipogenic potential of these cells (Chapter 2).

Fatty acid synthase is not a CRL4^{WDTC1} substrate

FAS is ubiquitylated by an as yet to be identified E3 ligase and its proteolytic degradation was demonstrated to be critical for promoting apoptosis in prostate cancer cells (Graner et al., 2004). Although WDTC1 does not appear to regulate FAS protein levels, I tested whether FAS is a nonproteolytic substrate of the CRL4^{WDTC1} complex. HCT116 cells were transiently transfected with HA-tagged ubiquitin and either WDTC1-WT or WDTC1-ΔH mutant. The level of FAS ubiquitylation was detected by immunoblotting following immunoprecipitation of FAS. While there was no detectable difference in FAS protein stability, FAS ubiquitylation was markedly enhanced by WDTC1-WT but not the CRL4 binding mutant WDTC1-ΔH (Figure 3.5A). Encouraged by this preliminary result, I predicted that if CRL4^{WDTC1} targets FAS ubiquitylation, then WDTC1 can only enhance FAS ubiquitylation in the presence of CRL4 core components. To test this idea, FAS ubiquitylation was evaluated in cells transfected with either control or DDB1 targeting siRNAs followed by cotransfection with HA-ubiquitin and Flag-WDTC1 plasmids. While FAS ubiquitylation was enhanced in WDTC1 overexpressing cells, its ubiquitylation was dramatically reduced in DDB1 depleted cells regardless of WDTC1 expression (Figure 3.5B; compare lanes 4 with 5 and 6). While this strongly supports the notion that CRL4^{WDTC1} mediates FAS ubiquitylation, there is one

major caveat. I found that HA-ubiquitin expression was not uniform across different cells and importantly, FAS ubiquitylation levels correlate with HA-ubiquitin expression levels.

I later discovered that the order of transfection matters for evaluating ubiquitylation with HA-ubiquitin in HCT116 cells. In the above experiment, I first transfected scramble or siDDB1 and then did the plasmid transfection the following day to achieve 72 hour knockdown and 48 hour plasmid expression. For reasons not entirely clear, I found that transfection efficiency is markedly reduced in HCT116 cells after DDB1 depletion (data not shown), perhaps this is related to impaired cell cycle control after DDB1 knockdown. Following this discovery, I evaluated FAS ubiquitylation by transfecting HA-ubiquitin in a single dish first and then splitting these cells into separate dishes for subsequent transfections. Using this approach, I found that FAS ubiquitylation was largely unaffected in cells overexpressing either WDTC1 or CUL4 proteins (Figure 3.5C). Consistent with this result, DDB1 or CUL4A depletion also did not have a significant effect on FAS ubiquitylation, although CUL4B depleted cells appeared to have slightly increased levels of ubiquitylated FAS (Figure 3.5D).

To conclude my study on FAS, I sought to determine whether endogenous FAS is ubiquitylated in 3T3-L1 cells as this could indicate FAS activity, localization or protein-protein interaction is potentially regulated by ubiquitylation. FAS ubiquitylation was evaluated over a 24 hour course of 3T3-L1 differentiation by immunoblotting with an antibody against ubiquitin following immunoprecipitation of FAS. FAS ubiquitylation appears to be quite dynamic as it declines hours post induction, but recovers within 24 hours (Figure 3.6A). Although the significance of this finding is unclear, it is possible that FAS ubiquitylation is cell cycle regulated since induced preadipocytes undergo several rounds of cell division before terminal differentiation into adipocytes. Another final consideration regarding FAS ubiquitylation is whether FAS is mono- or multi-monoubiquitylated or polyubiquitylated. Due to its high molecular weight, ubiquitylated FAS was not efficiently resolved by SDS-PAGE. A panel of HA-tagged ubiquitin mutants, each encoding a single lysine mutation or a no lysine

mutant (K0), was transfected in HCT116 cells to evaluate FAS ubiquitylation type. While the band corresponding to ubiquitylated FAS shows a characteristic smear in wild-type HA-ubiquitin transfected cells, a distinct FAS ubiquitylation band is detected in the HA-Ubiquitin-K0 mutant cells, indicating that FAS is polyubiquitylated (Figure 3.6B; compare lanes 2 and 3). The low expression level of HA-Ubiquitin-K48R mutant compared to other plasmids makes it difficult to conclude whether K48-linkage, associated primarily with proteasome mediated degradation, is important for FAS ubiquitylation. Interestingly, FAS ubiquitylation was significantly reduced in HA-Ubiquitin-K6R transfected cells (lane 4). Presently, the functional significance of K6-linkage is unknown but it has been linked to DNA repair and polyubiquitylation by this linkage may have a nonproteolytic role in the cell (Kulathu and Komander, 2012). Collectively, these results demonstrate that FAS is not a $CRL4^{WDTC1}$ substrate and although unlikely to regulate protein levels, FAS ubiquitylation in 3T3-L1 cells merits future investigation.

DISCUSSION

The results described in this chapter suggest WDTC1 potentially interacts with a large number of proteins. The proteomic based screen was designed to profile WDTC1 interacting proteins and hopefully identify candidate substrates. I characterized one candidate which was confidently identified in mutant WDTC1-ΔH complexes, FAS. As a critical and positive regulator of lipid accumulation, FAS appeared to be a perfect candidate that might have largely accounted for the anti-adipogenic function of the $CRL4^{WDTC1}$ complex. However, I have shown conclusively that WDTC1 does not regulate FAS protein levels or target it for ubiquitylation by the CRL4 E3 ligase. I favor the conclusion that nonspecific binding, possibly arising from the expression of a mutant protein in the cell, explains the interaction between FAS and WDTC1-ΔH.

FAS ubiquitylation is nevertheless interesting. Despite what appears to be a readily detectable modification (HCT116 and 3T3-L1 cells), FAS ubiquitylation is vastly unexplored

and not surprisingly, the presence of ubiquitylated FAS in 3T3-L1 cells has not been reported previously. That posttranslational regulation (phosphorylation) is critically important for the activity of two other key enzymes of *de novo* lipogenesis, ATP-citrate lyase (ACL) and Acetyl-CoA carboxylase (ACC), is well established. By comparison, the prevailing view that FAS is almost entirely, if not entirely, transcriptionally regulated in response to hormones or nutritional status remains largely unaltered (Liu et al., 2010; Semenkovich, 1997). Indeed, a recent study demonstrating that FAS is regulated by the ubiquitin-proteasome pathway in prostate cancer cells is a first (Graner et al., 2004). Separate from its anabolic function in energy storage, FAS is a metabolic oncogene as it confers growth and survival advantage to tumor cells by meeting their enhance lipid metabolism for energy and membrane biosynthesis (Menendez and Lupu, 2007). Search for proteins that interact with the prostate specific deubiquitinase USP2a led to FAS being identified as an USP2a substrate (Graner et al., 2004). USP2a, overexpressed in prostate cancer, prevents FAS proteasome-mediated degradation and in turn, enhanced FAS protein stability promotes tumor cell growth.

Does FAS ubiquitylation serve a regulatory role in 3T3-L1 cells or perhaps in other cells as well? It is interesting to note that around the same time that I was examining FAS ubiquitylation, its ubiquitylation was reported in two separate proteomic studies. In a global screen of the ubiquitin-modified proteome, FAS was found to be ubiquitylated but not stabilized by proteasome inhibition in HCT116 cells (Kim et al., 2011), consistent with my data showing that FAS ubiquitylation does not serve a proteolytic function in these cells. In the second paper, the authors utilized stable isotope labeling with amino acids in cell culture (SILAC) combined with pharmacological inactivation of cullin proteins by MLN4924 to identify proteins that are ubiquitylated by CRLs in HEK293T cells (Emanuele et al., 2011). Results from this study suggested that FAS is a candidate substrate of a CRL complex but unlikely to be a proteolytic substrate as changes in its ubiquitylation status does not correspond to a change in protein levels. Future studies may clarify the role of FAS ubiquitylation in different

cell types, but particularly in lipogenic cells such as 3T3-L1 cells where FAS function is not linked to cancer pathogenesis.

Since CRL4 was not previously linked to adipogenic control, my initial hope was to identify an adipogenic substrate(s) of $CRL4^{WDTC1}$ to further validate a role for this complex in a new biological process. I had hoped that eliminating interaction with the cognate E3 ligase would strengthen the binding between WDTC1 and a candidate substrate; instead it led to the false discovery of FAS in WDTC1-ΔH complex. While disappointing, FAS ubiquitylation may yet have an interesting role in 3T3-L1 adipogenesis. Ultimately, I was unable to identify any new potential substrates of the $CRL4^{WDTC1}$ complex. Clearly, future efforts will have to modify or change the approach I used: immunopurification of ectopically expressed WDTC1 complexes followed by identification of associated proteins by mass spectrometry. Michele Pagano's laboratory has reported success with identifying CRL1 substrates by straightforward immunoprecipitation of F-box substrate receptors followed by mass spectrometry (D'Angiolella et al., 2010; Kuchay et al., 2013). However, substrate assignment by this approach is rare given that substrate abundance is frequently low in the cell and the E3-substrate interaction is expected to be transient, thereby limiting copurification (Harper and Tan, 2012).

Despite considerable progress in identifying ubiquitylated proteins at a global level and mapping ubiquitylation sites (the two studies mentioned above, for example), systematic identification of E3 ligase and physiologic substrate pairs remains a challenge and likely no single method can efficiently tackle this task. I suggest an alternative approach for future efforts aimed at identifying $CRL4^{WDTC1}$ substrates: SILAC-based quantitation with mass spectrometry. By differentially labeling control cells and cells with altered WDTC1 expression, it may be possible to identify candidate substrates by quantitatively comparing changes in protein stability. A more direct method that would also help identify nonproteolytic substrates is enrichment of ubiquitylated proteins with an ubiquitin remnant antibody combined with SILAC. However, I suspect tedious validation may ensue and the general utility of this

method to identity candidate substrates is as yet uncertain. On a final note, if interaction based methods are to be utilized in the future, a minimum requirement for tandem affinity purification (TAP) is underscored by the vast number of apparently nonspecific interactions that were detected in this study.

EXPERIMENTAL PROCEDURES

Immunopurification and mass spectrometry

Details of generating stable cells, 3T3-L1 cell culture and induction can be found in Chapter 2 under Experimental procedures. WDTC1 associated proteins were isolated from cells stably expressing Flag-WDTC1-WT and Flag-WDTC1-ΔH proteins by FLAG affinity purification (Figure 3.7A-B). WDTC1 complexes were purified from uninduced 3T3-L1 preadipocytes and 3T3-L1 cells that were induced to undergo differentiation, representing two separate screens (Figure 3.7C). Cell stably transfected with an empty vector (EV) served as purification control in these experiments. Due to the lower expression of WDTC1-ΔH compared to WDTC1-WT, twice the number of cell plates were used for purifying associated proteins. Cells from five (EV and WDTC1-WT) or ten (WDTC1-ΔH) 15 cm plates were collected and cell pellets were stored in -80 °C until lysis. The general workflow is listed in (Figure 3.7D-E). Cell pellets were lysed for 30 min on a rotator at 4 °C in NP-40 lysis buffer [50 mM Tris (pH 8.0), 150 mM NaCl, 10% glycerol, 1 mM EDTA and 0.1% NP-40] supplemented with Halt^{TM} (Thermo Sci.) protease/phosphatase inhibitor cocktail. Cell extracts were clarified by centrifugation and the soluble fractions were incubated with anti-FLAG M2 agarose beads (Sigma) overnight on a rotating platform at 4 °C. Immunoprecipitated proteins were washed ten times by inverting tubes in 10 ml wash volumes; five times in NP-40 buffer followed by five times in PBS. Protein complexes were eluted with 50 µl of 3XFLAG peptide (200 µg/ml) for 5 min by shaking (800 rpm) on a Thermomixer (Eppendorf) at 37 °C; each sample was eluted three times and fractions were combined in a single tube on ice. A small amount of total purified protein (~2-5%) was resolved by SDS-PAGE and visualized by either silver staining or Coomassie Blue staining for confirmation. Eluted fractions were either in solution digested (uninduced cells) or in-gel digested (induced cells) at 37 °C using trypsin (Promega). Digested peptides were desalted and purified by C_{18} resin (C_{18} columns or Zip-Tip from Pierce or Millipore, respectively) following manufacturers' instructions. The identities of eluted proteins were determined by

mass spectrometry analysis carried out by Dr. Yanbao Yu (Xian Chen laboratory) at the UNC Proteomics Technology Development Core Facility using a LTQ-Velos-Orbitrap (Thermo Sci.) mass spectrometer coupled to a 2D nano ultra liquid chromatography system (Eksigent). Dr. Yu processed the data using MaxQuant software and searched the MS/MS data sets against UniProt mouse database.

Plasmids, antibodies, immunoblotting and in vivo ubiquitylation assay

A detailed description of reagents and additional experimental procedures can be found in Chapter 2 under experimental procedures. qPCR primers for *Fasn* (fwd: GCTGGCATTCGTGATGGAGTCGT; rev: AGGCCACCAGTGATGATGTAACTCT) was reported previously (Choi et al., 2010).

FIGURES

Figure 3.1. Proteomic analysis of WDTC1 interacting proteins in uninduced 3T3-L1 cells.

(A) Schematic representation of the number of unique and overlapping proteins that were identified in WDTC1-WT and WDTC1-ΔH complexes.

(B) List of proteins identified in WDTC1-WT complexes; CRL4 subunits and associated proteins are highlighted in bold, *CSN complex listed instead of individual subunits.

(C) List of proteins identified in WDTC1-ΔH complexes; FAS is highlighted in bold.

(D) List of overlapping proteins from both complexes; bait protein is highlighted in bold.

(E) DDB1 and FAS bands were visualized by silver staining in WDTC1-WT and WDTC1-ΔH immunoprecipitates, respectively; indicated by blue arrowheads.

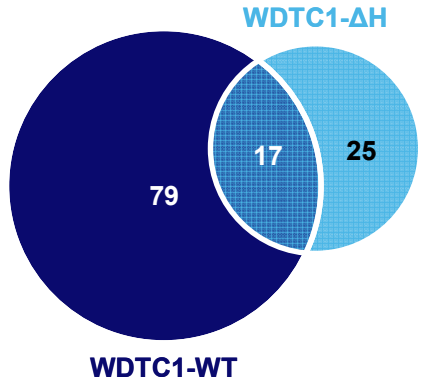

B

DDB1	CD003	SCML4	PEX5	TPC10
CUL4B	CL023	EKI1	SCNNB	PHLB1
CUL4A	THIO	IFT57	A16A1	MYOM3
ROC1	IFM3	OST48	HCN3	M3K4
CSN*	GMFG	PLVAP	CPT1A	SMCA2
DDA1	PPIA	PCOC1	AMPD3	P3C2A
SPTC2	SKP1	PRUNE	ACE2	ESPL1
ASPH	SSRD	IRAK4	K0562	RP1
H2A2C	SPAG7	MOT1	TRI37	PK1L3
EIF1	HDHD1	MDM2	AT1A1	SPTB1
GAPR1	F173B	SPAS2	IPO8	ACACA
GHC1	PSME3	FACR1	SEM6D	USMG5
SPTC1	MEMO1	KAD5	DI3L1	
4F2	SURF6	PSL1	ZCHC2	
FAK1	ST17B	RPN2	AEBP1	

C

FAS	DUS27	SESN3
RFX6	IL6RB	CHIP
PHLP	NDUS1	TBCD8
AMRA1	OBSCN	TAB3
ADCY2	FKBP8	CI14B
AP3M2	THMS1	
ERC6L	PCD15	
RD21L	DHX57	
RN133	GDIR1	
NKX26	SEM3G	

D

WDTC1	FKBPL
NUDC	TMOD2
SUGT1	MARHB
NDUA4	SYT10
CALU	NGEF
DDX3Y	MYOME
GBG12	BPA1
AIF1L	
SEP15	
SRSF2	

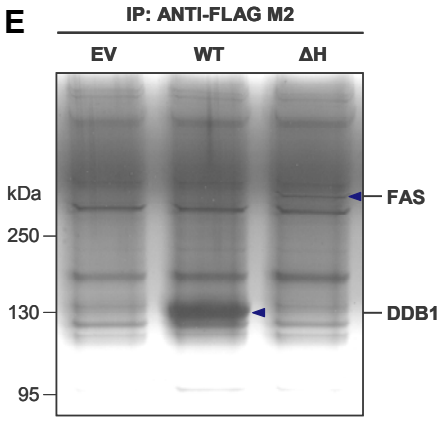

Figure 3.2. Proteomic analysis of WDTC1 interacting proteins in induced 3T3-L1 cells.

(A) Control and WDTC1 complexes were immunopurified by anti-FLAG, resolved by SDS-PAGE on a 4%-12% gradient gel and followed by Coomassie staining. Gel slices that were submitted for mass spectrometry are indicated.

(B) Schematic representation of the number of unique and overlapping proteins that were identified in WDTC1-WT and WDTC1-ΔH complexes.

(C) List of overlapping proteins identified in both complexes; bait protein and FAS are highlighted in bold.

(D) Comparison of FAS coverage, number of unique peptides and peptide spectrum matches (PSMs) between WDTC1-WT and WDTC1-ΔH complexes.

(E) Verification of FAS interaction by immunoblot analysis of eluted fractions from complexes analyzed.

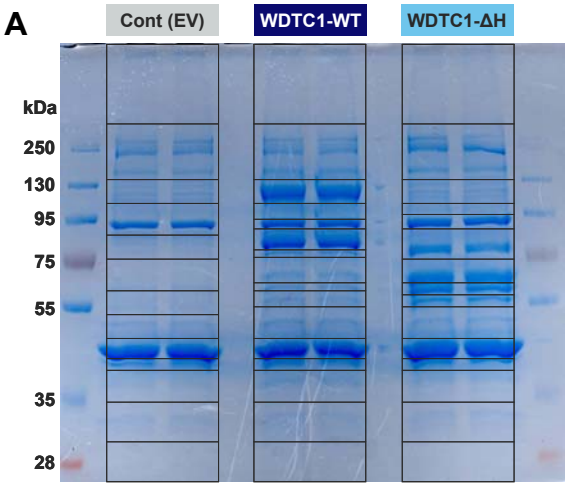

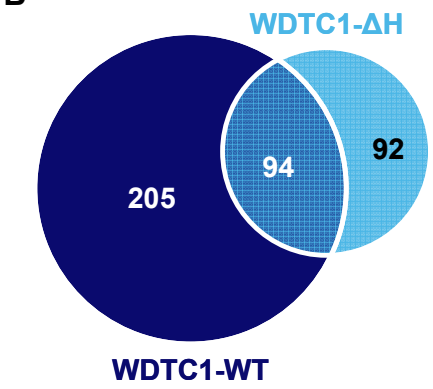

C

WDTC1	PRDX4	P5CR2	H2A2C	PUR6	PSA6	CSK22
FAS	MMP37	PP2AB	CHP1	MXRA8	ETFB	PDK3
NUDC	RBCC1	SG196	CHCH3	PYR5	CK074	TRP13
FKBP5	PFD3	RBBP7	TMM33	DDX6	MLF2	FNTB
SUGT1	CUL7	ODO2	PPP6	SYDC	HACD2	ODBA
IF4A1	ASPH	F115A	FAF2	SPD2A	P5CR3	TBG1
ATX10	ALDH2	PRDX3	CLIC1	UBP19	ITM2B	DC1L2
CHIP	PSA7	ERP44	HCD2	COPR5	DIC	SNTB2
GHC1	SFXN3	CSN2	RCD1	LSM12	PEX19	CP1B1
PPM1A	GOGA2	SC22B	CDK4	PSB2	PSMG1	WLS
NU155	OST48	DPM1	FBRL	BCL7C	ARM10	
AT1A1	ARL1	SRPRB	SEC13	RAB14	DCNL3	
CNN3	DHSB	MPCP	PCBP1	RPAB1	AIMP2	
GDIR1	ERGI1	SPTC1	GNAS2	GSTM1	GET4	

D

Bait	Protein	Coverage	Peptides	PSMs
WT	Fatty Acid Synthase	0.44	1	1
ΔH	Fatty Acid Synthase	27.4	50	111

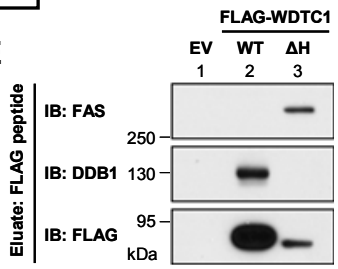

Figure 3.3. Dominant negative WDTC1 binds FAS and WDTC1 expression alters FAS protein expression in adipogenically induced 3T3-L1 cells.

(A) Flag-WDTC1 complexes were isolated from 3T3-L1 cell lysates by immunoprecipitation with anti-FLAG and associated proteins were detected by immunoblotting as indicated; EV, empty vector control.

(B) Flag-tagged WDTC1 proteins were transiently expressed in HCT116 cells and immunoprecipitated with anti-FLAG and associated proteins were detected by immunoblotting as indicated.

(C-D) Cell lystates were prepared from uninduced 3T3-L1 preadipocytes that stably expressed Flag-WDTC1 (C) or shRNA targeting WDTC1 (D), and FAS protein levels were detected by immunoblotting as indicated.

(E) 3T3-L1 preadipocytes stably expressing Flag-WDTC1 proteins were adipogenically induced to differentiate and cell lysates were prepared to detect FAS protein levels by immunoblotting as indicated.

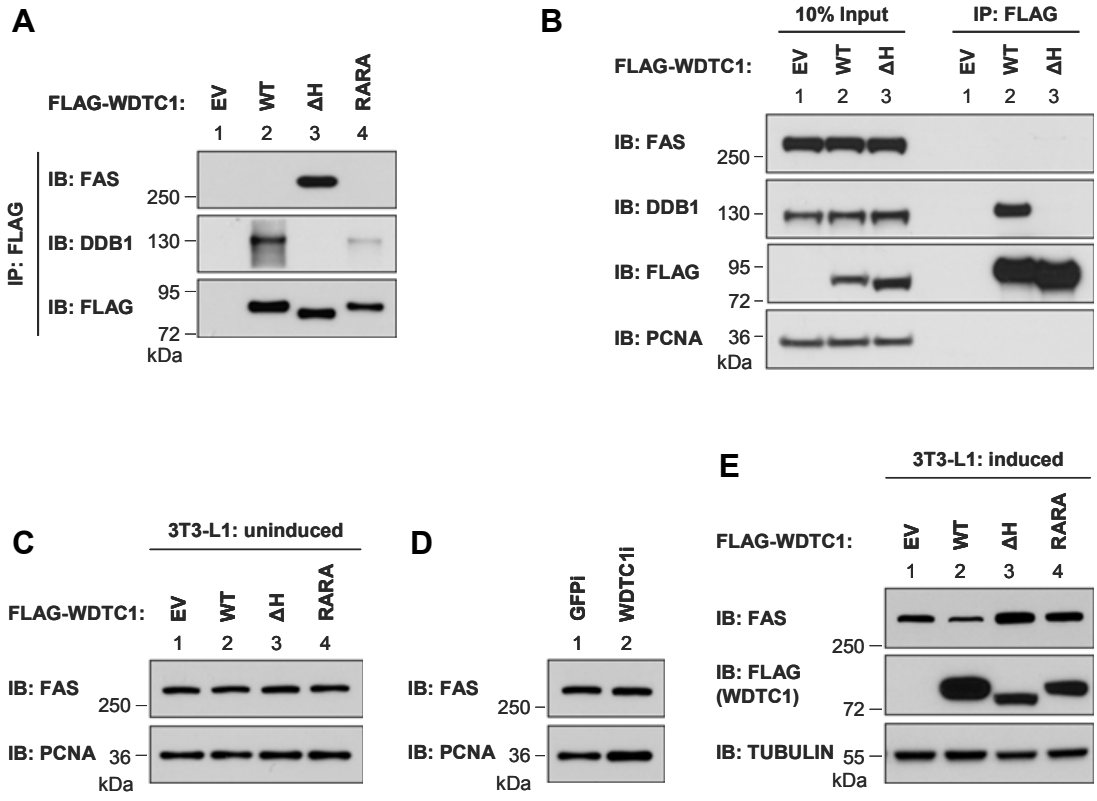

Figure 3.4. FAS protein expression is transcriptionally regulated in 3T3-L1 cells.

(A-B) 3T3-L1 preadipocytes stably expressing empty vector (EV) control and Flag-WDTC1 proteins were adipogenically induced to differentiate. Cells were collected at zero time point (0D) and at indicated days post induction to prepare cell extracts and isolate mRNAs. FAS protein levels and *Fasn* mRNA expression were monitored by immunoblot analyses with indicated antibodies (A) and real-time qPCR analysis (B), respectively.

(C) 3T3-L1 cells were treated with 50 μg/ml protein synthesis inhibitor cycloheximide (CHX) in the absence or presence of 10 μM protease inhibitor (MG132) for 0, 4, 8 and 12 hours. Cell extracts were prepared and protein levels were analyzed by immunoblotting as indicated (left) and quantified by normalizing to α-tubulin and plotted as relative to 0 h (right).

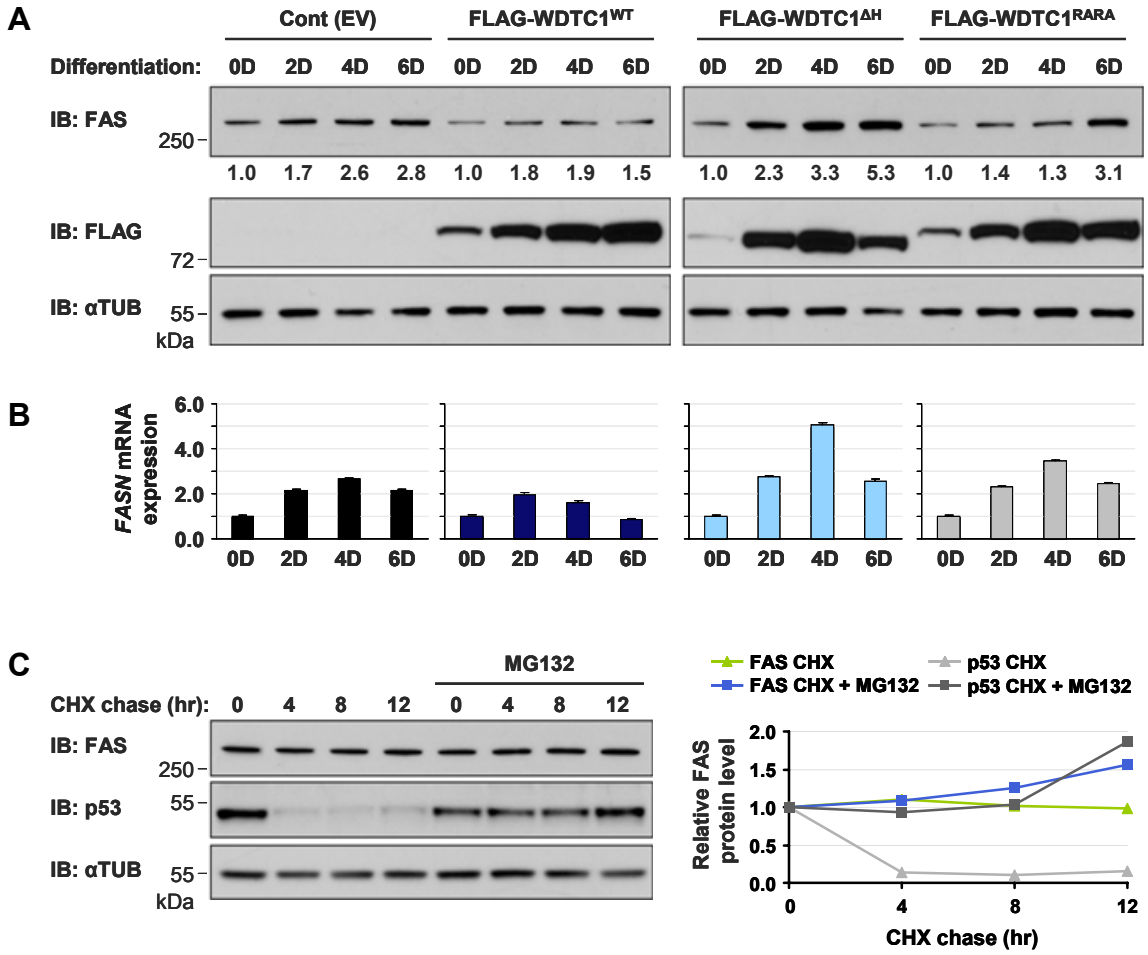

Figure 3.5. FAS is not a $CRL4^{WDTC1}$ substrate.

(A) Empty vector (EV) control and Flag-tagged WDTC1-WT and WDTC1-ΔH along with HA-ubiquitin were transiently expressed in HCT116 cells for 48 h. Cells were lysed under denaturing conditions (1% SDS), cell extracts were immunoprecipitated by anti-FAS and FAS ubiquitylation was evaluated by immunoblotting with indicated antibodies.

(B) HCT116 cells were transfected by scramble (scrm) control or DDB1 targeting siRNAs. These cells were transfected again after a 24 h interval with HA-ubiquitin plasmid along various combinations of control and Flag-WDTC1-WT plasmids. Levels of FAS ubiquitylation were evaluated same as (A).

(C) HCT116 cells were first transfected with HA-ubiquitin plasmid in a single dish, split ~10 h later to carry out subsequent transfections. Following 24 h after first transfection, cells were transfected again along with various combinations of control and expression plasmids. Levels of FAS ubiquitylation were evaluated as in (A).

(D) Same as (C) except cells were transfected with siRNAs targeting CRL4 subunits following transient transfection of HA-ubiquitin plasmid. Levels of FAS ubiquitylation were evaluated as in (A).

Figure 3.5 (continued)

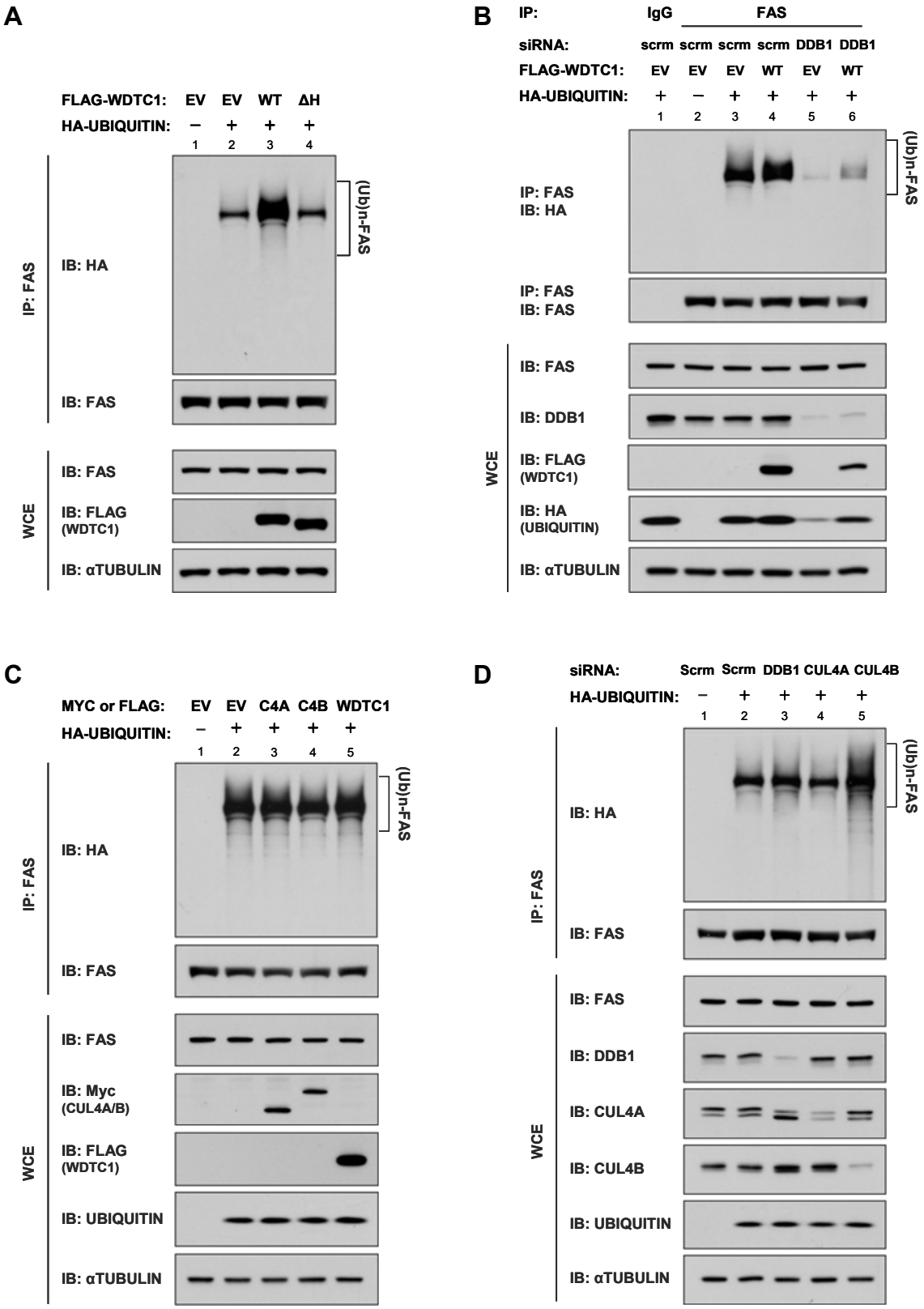

Figure 3.6. FAS polyubiquitylation is rapidly altered following 3T3-L1 induction.

(A) 3T3-L1 preadipocytes were adipogenically induced and cells were collected within a 24 hour time course of differentiation, including an uninduced control at 0 h. Cell lysates were prepared under denaturing conditions and subjected to immunoprecipitation using anti-FAS. FAS ubiquitylation was evaluated by anti-ubiquitin antibody. FAS protein expression and equal loading were confirmed by immunoblotting of whole cell extract (WCE) as indicated.

(B) Empty vector (EV) control, and HA-tagged wild-type ubiquitin (WT), no lysine ubiquitin (K0) and various single lysine ubiquitin mutants were transiently expressed in HCT116 cells. Cell lysates were prepared under denaturing conditions and subjected to immunoprecipitation by anti-FAS. Levels of FAS ubiquitylation was evaluated by immunoblotting with indicated antibodies.

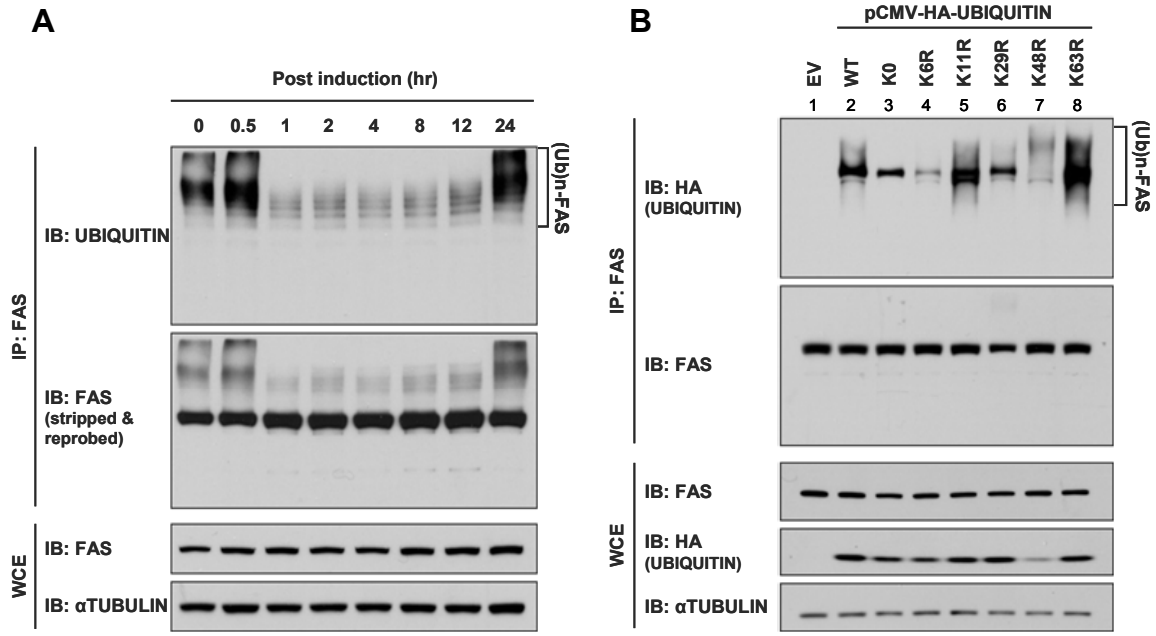

Figure 3.7. Experimental overview of proteomic based screen for WDTC1 interacting proteins.

(A) Schematic representation of Flag-tagged WDTC1-WT and WDTC1-ΔH proteins depicted in the context of CRL4 binding.

(B) Elution check for WDTC1 complexes using 1XFLAG or 3XFLAG peptides by immunoblotting. Greater elution efficiency was obtained with 3XFLAG peptide as indicated by less protein retention on beads (lanes 4 and 8).

(C) Schematic representation of 3T3-L1 differentiation with time points of uninduced and induced cell collection times circled.

(D-E) Outline of workflow for mass spectrometry based identification of WDTC1 interacting proteins from uninduced and induced 3T3-L1 cells by in solution or in gel trypsin digest, respectively.

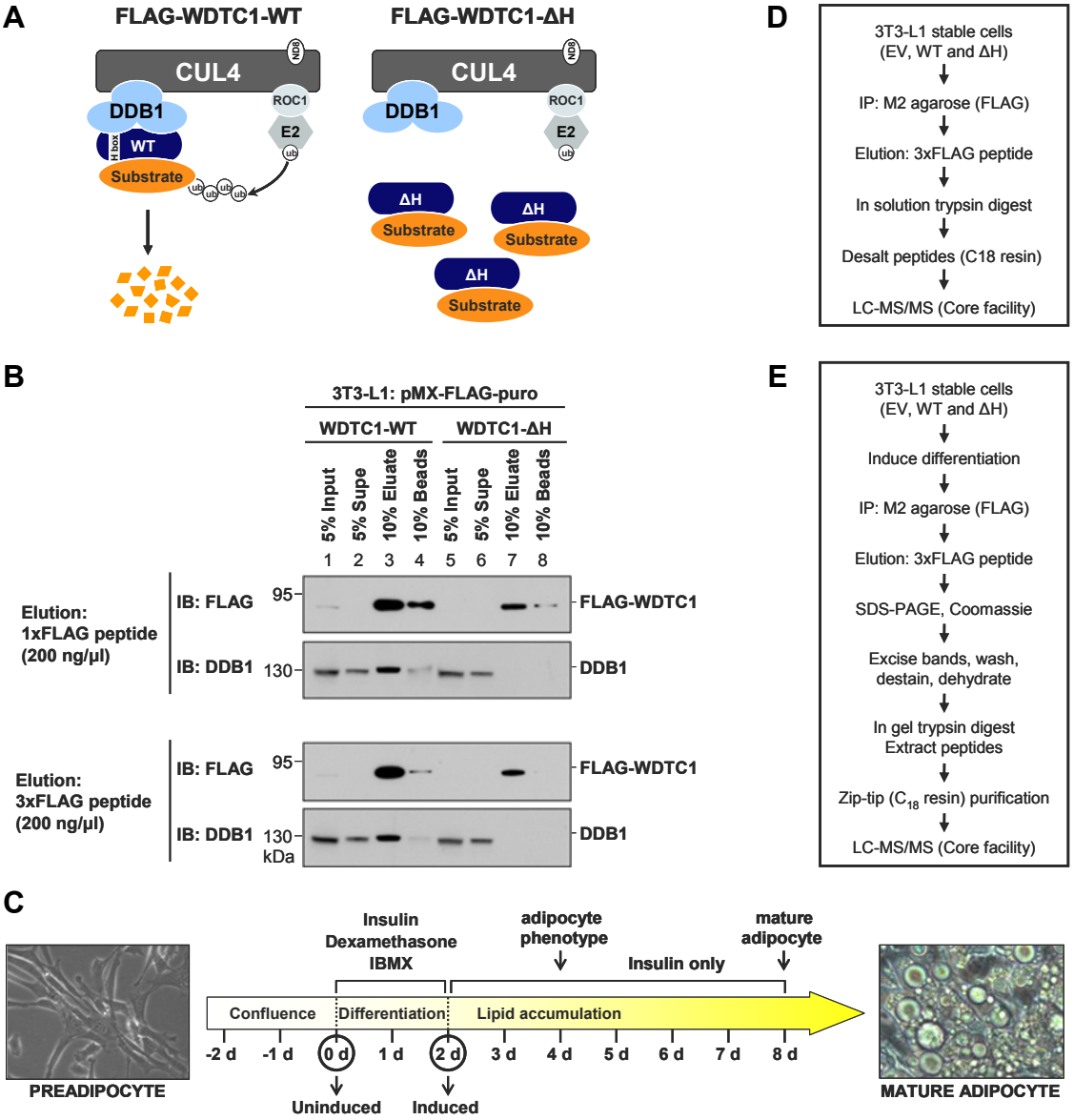

CHAPTER 4: CONCLUSIONS AND PERSPECTIVES

Summary

When I started my dissertation research in Dr. Yue Xiong's laboratory, the substrate targeting mechanism of CRL4 complexes had already been elucidated and the focus of the field shifted to functionally characterizing distinct CRL4 complexes, identifying associated cellular pathways and substrates. Among the vast majority of DWD proteins that remained uncharacterized, I chose to characterize WDTC1. Besides the potential therapeutic relevance of WDTC1 in suppressing fat accumulation, I was intrigued by its unique structural organization. The latter played a key role in my exploration of a nuclear function for $CRL4^{WDTC1}$. I document two main findings in this dissertation: WDTC1 mediates adipogenic suppression through a CRL4 complex and histone H2A is a $CRL4^{WDTC1}$ substrate in vitro, suggesting a role in transcriptional repression may underlie the biochemical function of $CRL4^{WDTC1}$ in vivo. Given that virtually nothing was known about the molecular action of WDTC1, the work presented here provides the first mechanistic insight into its function. This study also prompts new and exciting questions for future research. In this final chapter, I discuss some outstanding questions in WDTC1 research and suggest future directions that may be pursued for this fascinating protein.

Is WDTC1 the mammalian ortholog of yeast TUP1-SSN6 transcriptional repressor?

From the very beginning, the unique structure of WDTC1 held a fascination for me. So when I began to explore mechanisms underlying WDTC1 function, I considered transcriptional repression by WDTC1 a possibility since the only example of WD40 and TPR domains functioning collectively is in transcriptional corepression by the well characterized yeast TUP1 (WD40 domain) and SSN6 (TPR domain) heterodimer (Malave and Dent, 2006). TUP1 and SSN6 do not have homologs in higher eukaryotes, and given the structural parallel between WDTC1 and TUP1-SSN6, I hypothesized that WDTC1 may function as a vertebrate counterpart. In retrospect, extending the TUP1-SSN6 corepressor analogy to WDTC1 was not only conceptually satisfying, but this idea has support in a number of observations: (1) WDTC1 expression is associated with decreased adipogenic gene expression (Suh et al., 2007 and my data in Chapter 2), (2) nuclear exclusion of WDTC1 mimics functional loss of WDTC1 (Suh et al., 2007), (3) WDTC1 is a histone binding protein (Figures 2.7C and 2.7G; Angers et al., 2006; Suh et al., 2007), (4) WDTC1 expression is associated with increased histone H2AK119ub (Figure 2.7D), (5) $CRL4^{WDTC1}$ ubiquitylates histone H2A in vitro (Figures 2.8B and 2.8D), (6) WDTC1 exhibits intrinsic transcription repressive activity in luciferase reporter gene assays (Suh et al., 2007), and finally, (7) the reported interactions between WDTC1 and HDAC3 histone deacetylase (Suh et al., 2007), and the association of WDTC1 with transcription regulators in screen studies (Krebs et al., 2010; Nakayama et al., 2002). Below I expand on the idea that WDTC1 potentially represents an evolutionarily conserved mechanism of transcriptional corepression by WD40 and TPR domains in mammals.

TUP1-SSN6 heterodimer functions in the global corepression pathway since it regulates the expression of a diverse get of genes (Malave and Dent, 2006). Its promoter specificity is conferred by sequence-specific DNA binding proteins as neither subunit possesses intrinsic DNA binding activity. The TPR containing SSN6 protein is thought to mediate the interaction with DNA binding protein while the WD40 containing TUP1

possesses the transcription repressive activity. Sequences N-terminal to the WD40 β-propeller of TUP1 binds histone tail regions whereas the TPR motifs of SSN6 mediate interaction with HDACs. Once targeted to a specific promoter, the exact mechanism of repression is unclear. However, mutational analyses firmly established that histone binding and recruitment of histone deacetylases are critical to transcriptional repression by TUP1-SSN6 (Davie et al., 2002; Edmondson et al., 1996; Watson et al., 2000). TUP1-SSN6 colocalize with hypoacetylated histones at targeted promoters and loss of HDAC activity results in enriched histone acetylation and a loss of TUP1-SSN6-dependent gene repression. Thus the available evidence indicates that TUP1-SSN6 mediated transcriptional repression involves the establishment of a repressive chromatin state through reinforced binding and recruitment of other transcriptional repressors, HDACs.

Although TUP1and SSN6 proteins do not have sequence homologs in higher organisms, there is precedence for evolutionary conservation through structurally similar proteins. The strongest candidate for a homolog is *D. melanogaster* Groucho (Gro) protein and its mammalian homologs, transducin-like Enhancer of split (TLE) proteins. Gro and TLE are global repressors that regulate a number of developmental pathways and share few key features of TUP1-SSN6 mediated repression: (1) recruited to target promoters by sequence specific DNA binding proteins, (2) histone binding is critical for function, and (3) histone deacetylation likely plays a role in their mechanism of repression (Flores-Saaib and Courey, 2000; Malave and Dent, 2006). Although Gro and TLEs have WD40 domains but not TPR motifs, TLE1 has demonstrated ability to interact with yeast SSN6 in mammalian cells and mediate transcriptional repression in luciferase reporter gene assays (Grbavec et al., 1999). While this suggests functional conservation of WD40 and TPR domains in transcriptional repression, how exactly Gro/TLEs inhibit transcription remains unclear and likely involves multiple mechanisms that are unrelated to that of TUP1-SSN6 (Jennings and Ish-Horowicz, 2008). It is interesting to note, however, that TLE proteins are putative substrate receptors

for CRL4 complexes and may offer additional opportunities for studying CRL4 function in the regulation of gene expression.

Like TUP1-SSN6, WDTC1 binds histones and was found to interact with HDAC3. However, histone ubiquitylation does not appear to contribute to TUP1-SSN6 mediated repression (Malave and Dent, 2006). On the basis of structural resemblance and the noted similarities, I believe it is possible that WDTC1 represents an evolutionarily conserved factor that mediates gene repression via WD40 and TRP domains but acquired distinct functional mechanisms through specific interactions, CRL4 in this case. It remains formally possible that WDTC1 may share functional properties with TUP1-SSN6; I did not examine the effect of WDTC1 expression on histone acetylation in 3T3-L1 differentiation. However, exploring the evolutionary relationship between $CRL4^{WDTC1}$ and TUP1-SSN6 complexes may provide important insight into the proposed transcription repressor role of the $CRL4^{WDTC1}$ complex. Importantly, number of key questions will have to be addressed experimentally regarding this proposed role. First, while $CRL4^{WDTC1}$ has an effect on H2AK119ub and H3K4me3 in cells, one critical question concerns whether the $CRL4^{WDTC1}$ complex directly catalyzes histone H2AK119ub to inhibit transcription in vivo and what are the target genes? Second, WDTC1 appears to bind histones independent of DDB1 (Figure 2.7G) and it does not have an apparent DNA binding domain, therefore, how is WDTC1 recruited to chromatin? On a related note, it will be important to determine if WDTC1 mutations that abolish histone binding negatively impact transcriptional inhibition and consequently, adipogenic suppression. Lastly, does $CRL4^{WDTC1}$ interact with other histone modifiers such as histone deacetylases and methyltransferases to establish transcriptionally silent chromatin through crosstalk? These and other associated questions will be discussed in more detail below.

Regulation of adipogenesis through H2AK119ub

Upon induction of differentiation, preadipocyte to adipocyte transition is controlled by coordinated expression of adipocyte-specific genes. While much is known about the complex

cascade of transcription factors that activate their gene expression programs, very little is known about the chromatin states underlying transcriptional activation or repression. However, details of epigenetic mechanisms that control adipocyte differentiation are beginning to emerge. Results from genome-wide studies indicate the presence of an epigenomic transition state, which refers to dynamic alterations in localization of transcriptional regulators, DNA methylation and histone modifications during differentiation (Cristancho and Lazar, 2011). Histone modifications driving adipocyte-specific gene expression, primarily histone H3 acetylation and methylation marks, have received the most attention in the literature (Mikkelsen et al., 2010; Steger et al., 2010). Consequently, the role of many histone modifying enzymes such as methyltransferases, acetyltransferases and deacetylases has also come into focus (Fu et al., 2005; Lee et al., 2008; Picard et al., 2004; Steger et al., 2010; Wang et al., 2010; Wang et al., 2013). By comparison, epigenomic alterations that block transcriptional activation, thereby adipogenesis, remain poorly understood. Notably, the functional significance of H2AK119ub in adipogenesis is virtually unknown.

The data I presented here suggest adipogenic suppression by $CRL4^{WDTC1}$ is mediated through histone H2AK119ub, and to the best of my knowledge, demonstrate the first link between H2AK119ub and adipogenesis (Chapter 2). Despite firmly established role in transcriptional silencing, how exactly H2AK119ub inhibits transcription is unclear. At least three non-mutually exclusive models have been proposed: (1) H2AK119ub alters chromatin structure and limits accessibly of transcription regulators to underlying DNA, (2) ubiquitin acts as a platform for recruitment of downstream repressors, possibly containing ubiquitin binding domains, and (3) H2AK119ub impacts other histone modifications to reinforce gene silencing, referred to as crosstalk (Hammond-Martel et al., 2012). Although I did not test all three proposed mechanisms, my data is consistent with crosstalk being a contributing factor. In fact, the interaction between CRL4 and histone methyltransferases in yeast and mammalian cells implicates crosstalk is critical to CRL4 mediated transcriptional regulation (Chapter 1).

I observed that the effect of $CRL4^{WDTC1}$ on H2AK119ub inversely correlated with H3K4me3, suggesting H2AK119ub blocks transcription initiation (Figures 2.9A and 2.9B). While this could be an indirect effect, in vitro evidence supports a crosstalk between H2AK119 and H3K4me3. In vitro transcription assays on reconstituted chromatin templates showed that H2AK119ub inhibits transcription initiation by blocking modifications associated with promoter activation, MLL3-catalyzed histone H3K4me2/3, but does not appear to have an effect on H3K9 or H3K27 methylation (Nakagawa et al., 2008). Their data suggested that blocking H3K4 methylation prevents preinitiation complex formation, but this inhibition on transcription initiation is relived by the addition of the USP21 deubiquitinase. While correlative, my results predict a model whereby $CRL4^{WDTC1}$ E3 ligase complex represses a subset of adipogenic genes through H2AK119ub, which then prevents H3K4me3 and thus transcriptional activation and adipogenesis (Figure 2.10). In vivo support for this model will require a few critical pieces of evidence; below I suggest possible experiments to test this model.

A key question concerns the relative contribution of H2AK119ub to the adipogenic suppression mediated by $CRL4^{WDTC1}$. Does $CRL4^{WDTC1}$-catalyzed H2AK119ub account for transcriptional repression of adipogenic genes in vivo? Presently, it cannot be ruled out that the altered levels of H2AK119ub and H3K4me3, resulting from the modulation of WDTC1 expression, is not secondary to altered adipogenesis. I suggest comprehensive chromatin immunoprecipitation and sequencing (ChIP-Seq) analyses combined with microarray analyses for quantitative gene expression profiling to conclusively ascertain the anti-adipogenic function of $CRL4^{WDTC1}$ through epigenetic modulation. First, the effect of WDTC1 expression on the genome-wide profile of H2AK119ub and H3K4me3 should be obtained to determine the in vivo targets of $CRL4^{WDTC1}$. It will also be important to determine WDTC1 localization to identify specific genes that are targeted and to compare with H2AK119ub and H3K4me3 enrichment profiles. Lastly, the effect of $CRL4^{WDTC1}$ activity on specific gene promoters should be evaluated by gene expression profiling experiments. Other key

remaining questions that may be addressed by future studies is how WDTC1 is targeted to specific promoters and what other corepressor complexes $CRL4^{WDTC1}$ potentially interact with to contribute to distinct transcriptional repression. Additionally, the identity of deubiquitinases that activate adipogenic gene transcription is another important consideration. In summary, although my research has progressed our understanding of WDTC1 molecular function, the extent to which the model I favor or alternative mechanisms explain the anti-adipogenic function of $CRL4^{WDTC1}$ remains to be experimentally determined.

How many histone H2AK119ub E3 ligases are there?

Since the initial discovery of a ubiquitylated protein (Goldknopf et al., 1975), histone H2AK119ub now represents one of the most abundant post translational modifications in higher eukaryotes (~5-15% of total H2A). At least three different H2A E3 ligases have been linked to transcriptional regulation: RING1B of Polycomb repressive complex PRC1 (Wang et al., 2004), 2A-HUB (Zhou et al., 2008), and most recently, $CRL4B^{RBBP4/7}$ (Hu et al., 2012). RING1B is the first identified and best characterized E3 ligase for H2AK119ub, and is linked to heritable gene silencing and X-inactivation (de Napoles et al., 2004; Wang et al., 2004). Recruited by the NCoR/HDAC1/3 corepressor complex, 2A-HUB appears to function in a lineage specific manner. In response to TLR activation in macrophages, 2A-HUB ubiquitylates H2A at a subset of chemokine gene promoters, which blocks transcriptional elongation (Zhou et al., 2008). $CRL4B^{RBBP4/7}$ on the other hand interacts with PRC2 complex to repress cell growth and migration genes through possible crosstalk between H2AK119ub and H3K27me3, although the specific details are unclear (Hu et al., 2012).

While *Ring1b* deletion results in a dramatic loss of H2AK119ub in mouse ES cells and mouse embryonic fibroblasts (van der Stoop et al., 2008) and RING1B protein is present in two additional protein complexes besides PRC1, E2F6.com-1 and FBXL10-BcoR (Zhou et al., 2009), it is unclear how and whether a single E3 ligase regulates all biological processes involving H2AK119ub. Following the discovery of 2A-HUB, it has been proposed that distinct

H2A E3 ligases, through their selective interactions with different corepressor complexes, target specific gene promoters (Zhou et al., 2009). In addition to $CRL4B^{RBBP4/7}$, my data that $CRL4^{WDTC1}$ promotes H2AK119ub in vivo and possesses E3 ligase activity in vitro not only supports the notion that distinct H2A E3 ligases are present in cells, but raises the possibility that additional CRL4-based H2AK119 E3 ligases may exist. $CRL4^{WDTC1}$ and $CRL4B^{RBBP4/7}$ only differ in the DWD subunit and given the ~90 estimated DWD proteins in humans, it is tempting to speculate that additional DWD may function analogously. Testing this hypothesis for DWD proteins associated with gene regulation could potentially strengthen our mechanistic understanding of CRL4 complexes in chromatin related processes.

Additional cellular substrates and functions of $CRL4^{WDTC1}$ E3 ligase

I speculate WDTC1 may target additional substrates to regulate adipogenesis or other biological processes, or both. I base this prediction on two pieces of evidence: (1) WDTC1 is present in both CRL4A and CRL4B complexes (Figures 2.2A and 3.1B), and (2) WDTC1 is primarily localized in the cytoplasm (Figures 2.7A and 2.7B). In this study, a distinction was not made regarding whether CUL4A or its paralog CUL4B is the physiologically relevant cullin scaffold interacting with WDTC1 to regulate adipogenesis. Structurally, CRL4A and CRL4B are nearly indistinguishable except for an N-terminal unstructured region in CUL4B that contains a nuclear localization signal and forms the basis for its preferential localization in the nucleus (Fischer et al., 2011; Nakagawa and Xiong, 2011; Zou et al., 2009). Functionally, CUL4A and CUL4B are not completely redundant as *Cul4a*$^{-/-}$ mice are viable but *Cul4b*$^{-/-}$ mice are embryonic lethal, indicating CUL4A cannot fully compensate the loss of CUL4B (Jackson and Xiong, 2009). That a single substrate receptor can target multiple substrates to the CRL4 catalytic core is well known and best exemplified by CDT1 and DDB2 (Table 1.1). However, since a distinction has rarely been made in the literature, it is unclear whether distinct CUL4A and CUL4B complexes regulate different cellular pathways. The available evidence indicates CRL4A and CRL4B complexes function

redundantly in many processes. In the case of NER, both $CRL4A^{DDB2}$ and $CRL4B^{DDB2}$ complexes ubiquitylate histone H2A, but CUL4B exhibits greater efficiency in in vitro ubiquitylation assays with purified H2A (Guerrero-Santoro et al., 2008; Kapetanaki et al., 2006). Similarly, CDT1 degradation is mediated by both CUL4A and CUL4B since both isoforms have to be codepleted to detect CDT1 accumulation (Higa et al., 2006a; Hu et al., 2004). In contrast, WDR5 (Nakagawa and Xiong, 2011), cyclin E (Zou et al., 2009) and PDRX3 (Li et al., 2011) are solely targeted by CRL4B. While WDR5 is itself a DWD protein, the CRL4B substrate receptors for cyclin E and PDRX3 are currently unknown, thus whether their corresponding substrate receptors also form CRL4A complexes is currently unknown. The relative contribution of H2AK119ub to the $CRL4^{WDTC1}$-dependent adipogenic suppression and the molecular mechanism underlying the adipocyte-specific defect in *Cul4a*$^{-/-}$ mice should help clarify whether WDTC1 functions in different CRL4 complexes, and potentially identify additional cellular targets.

I focused exclusively on the anti-adipogenic function of WDTC1 in this study. But does WDTC1 play a role in other biological pathways, and utilize similar or different mechanisms? This is indeed a strong possibility based on two lines of evidence: (1) partial embryonic lethality of the WDTC1 knockout mice (Suh et al., 2007), and (2) WDTC1 is broadly expressed in flies, mice and humans. Although the adipose tissue starts to develop in late gestation, the real expansion does not occur until after birth (MacDougald and Lane, 1995). Therefore, it can be inferred from the partial embryonic lethality that WDTC1 has adipocyte-independent roles and minimally in embryogenesis. Because *Wdtc1*$^{+/-}$ mice have not been fully characterized yet, it remains to be determined whether additional cellular phenotypes are associated with altered WDTC1 expression. Although correlative, WDTC1 expression in both adipogenic and non-adipogenic tissues of adult mice (Figure 2.3A and Suh et al., 2007) is consistent with its involvement in diverse cellular processes. If *Wdtc1*$^{+/-}$ mice have additional phenotypes, then targeted *Wdtc1* deletion in specific tissues should

circumvent the partial embryonic lethality and enable linking WDTC1 to different cellular functions, and potentially identify downstream effector proteins through molecular analyses.

A final consideration regarding WDTC1 is whether it has CRL4-independent function. While it is probable, I favor a model wherein CRL4 activity underlies the primary function of WDTC1 in anti-adipogenic suppression and potentially in other cellular process as well. Given the limited knowledge we have of WDTC1 biology, I base this on the absence of WDTC1 in protein complexes other than CRL4, as revealed by the screen for WDTC1 interacting proteins through mass spectrometry analyses (Chapter 3). It is also of note that WDTC1 was readily detected in DDB1 and CUL4 immunocomplexes from three separate studies (Angers et al., 2006; Bennett et al., 2010; Jin et al., 2006), indicating that WDTC1 containing CRL4 complexes are frequently assembled in cells. I suggest an as yet to be identified CRL4-independent function plays a minor role in WDTC1-dependent adipogenic suppression.

REFERENCES

Abbas, T., Shibata, E., Park, J., Jha, S., Karnani, N., and Dutta, A. (2010). CRL4(Cdt2) regulates cell proliferation and histone gene expression by targeting PR-Set7/Set8 for degradation. Mol Cell *40*, 9-21.

Angers, S., Li, T., Yi, X., MacCoss, M. J., Moon, R. T., and Zheng, N. (2006). Molecular architecture and assembly of the DDB1-CUL4A ubiquitin ligase machinery. Nature *443*, 590-593.

Arias, E. E., and Walter, J. C. (2006). PCNA functions as a molecular platform to trigger Cdt1 destruction and prevent re-replication. Nat Cell Biol *8*, 84-90.

Bai, C., Sen, P., Hofmann, K., Ma, L., Goebl, M., Harper, J. W., and Elledge, S. J. (1996). SKP1 connects cell cycle regulators to the ubiquitin proteolysis machinery through a novel motif, the F-box. Cell *86*, 263-274.

Bengoechea-Alonso, M. T., and Ericsson, J. (2010). The ubiquitin ligase Fbxw7 controls adipocyte differentiation by targeting C/EBPalpha for degradation. Proc Natl Acad Sci U S A *107*, 11817-11822.

Bennett, E. J., Rush, J., Gygi, S. P., and Harper, J. W. (2010). Dynamics of cullin-RING ubiquitin ligase network revealed by systematic quantitative proteomics. Cell *143*, 951-965.

Bosu, D. R., and Kipreos, E. T. (2008). Cullin-RING ubiquitin ligases: global regulation and activation cycles. Cell Div *3*, 7.

Cai, L., Marshall, T. W., Uetrecht, A. C., Schafer, D. A., and Bear, J. E. (2007). Coronin 1B coordinates Arp2/3 complex and cofilin activities at the leading edge. Cell *128*, 915-929.

Cang, Y., Zhang, J., Nicholas, S. A., Bastien, J., Li, B., Zhou, P., and Goff, S. P. (2006). Deletion of DDB1 in mouse brain and lens leads to p53-dependent elimination of proliferating cells. Cell *127*, 929-940.

Cao, R., Tsukada, Y., and Zhang, Y. (2005). Role of Bmi-1 and Ring1A in H2A ubiquitylation and Hox gene silencing. Mol Cell *20*, 845-854.

Chartron, J. W., Gonzalez, G. M., and Clemons, W. M., Jr. (2011). A structural model of the Sgt2 protein and its interactions with chaperones and the Get4/Get5 complex. J Biol Chem *286*, 34325-34334.

Chiu, Y. H., Sun, Q., and Chen, Z. J. (2007). E1-L2 activates both ubiquitin and FAT10. Mol Cell *27*, 1014-1023.

Choi, J. H., Banks, A. S., Estall, J. L., Kajimura, S., Bostrom, P., Laznik, D., Ruas, J. L., Chalmers, M. J., Kamenecka, T. M., Bluher, M.*, et al.* (2010). Anti-diabetic drugs inhibit obesity-linked phosphorylation of PPARgamma by Cdk5. Nature *466*, 451-456.

Chu, G., and Chang, E. (1988). Xeroderma pigmentosum group E cells lack a nuclear factor that binds to damaged DNA. Science *242*, 564-567.

Cope, G. A., and Deshaies, R. J. (2006). Targeted silencing of Jab1/Csn5 in human cells downregulates SCF activity through reduction of F-box protein levels. BMC Biochem *7*, 1.

Cope, G. A., Suh, G. S., Aravind, L., Schwarz, S. E., Zipursky, S. L., Koonin, E. V., and Deshaies, R. J. (2002). Role of predicted metalloprotease motif of Jab1/Csn5 in cleavage of Nedd8 from Cul1. Science *298*, 608-611.

Cristancho, A. G., and Lazar, M. A. (2011). Forming functional fat: a growing understanding of adipocyte differentiation. Nat Rev Mol Cell Biol *12*, 722-734.

D'Angiolella, V., Donato, V., Vijayakumar, S., Saraf, A., Florens, L., Washburn, M. P., Dynlacht, B., and Pagano, M. (2010). SCF(Cyclin F) controls centrosome homeostasis and mitotic fidelity through CP110 degradation. Nature *466*, 138-142.

Davie, J. K., Trumbly, R. J., and Dent, S. Y. (2002). Histone-dependent association of Tup1-Ssn6 with repressed genes in vivo. Mol Cell Biol *22*, 693-703.

Day, T. A., Palle, K., Barkley, L. R., Kakusho, N., Zou, Y., Tateishi, S., Verreault, A., Masai, H., and Vaziri, C. (2010). Phosphorylated Rad18 directs DNA polymerase eta to sites of stalled replication. J Cell Biol *191*, 953-966.

de Napoles, M., Mermoud, J. E., Wakao, R., Tang, Y. A., Endoh, M., Appanah, R., Nesterova, T. B., Silva, J., Otte, A. P., Vidal, M.*, et al.* (2004). Polycomb group proteins Ring1A/B link ubiquitylation of histone H2A to heritable gene silencing and X inactivation. Dev Cell *7*, 663-676.

Deshaies, R. J., and Joazeiro, C. A. (2009). RING domain E3 ubiquitin ligases. Annu Rev Biochem *78*, 399-434.

Doane, W. W. (1960a). Developmental physiology of the mutant female sterile(2)adipose of Drosophila melanogaster. I. Adult morphology, longevity, egg production, and egg lethality. J Exp Zool *145*, 1-21.

Doane, W. W. (1960b). Developmental physiology of the mutant female sterile(2)adipose of Drosophila melanogaster. II. Effects of altered environment and residual genome on its expression. J Exp Zool *145*, 23-41.

Duda, D. M., Borg, L. A., Scott, D. C., Hunt, H. W., Hammel, M., and Schulman, B. A. (2008). Structural insights into NEDD8 activation of cullin-RING ligases: conformational control of conjugation. Cell *134*, 995-1006.

Edmondson, D. G., Smith, M. M., and Roth, S. Y. (1996). Repression domain of the yeast global repressor Tup1 interacts directly with histones H3 and H4. Genes Dev *10*, 1247-1259.

El-Mahdy, M. A., Zhu, Q., Wang, Q. E., Wani, G., Praetorius-Ibba, M., and Wani, A. A. (2006). Cullin 4A-mediated proteolysis of DDB2 protein at DNA damage sites regulates in vivo lesion recognition by XPC. J Biol Chem *281*, 13404-13411.

Emanuele, M. J., Elia, A. E., Xu, Q., Thoma, C. R., Izhar, L., Leng, Y., Guo, A., Chen, Y. N., Rush, J., Hsu, P. W.*, et al.* (2011). Global identification of modular cullin-RING ligase substrates. Cell *147*, 459-474.

Farmer, S. R. (2006). Transcriptional control of adipocyte formation. Cell Metab *4*, 263-273.

Feldman, R. M., Correll, C. C., Kaplan, K. B., and Deshaies, R. J. (1997). A complex of Cdc4p, Skp1p, and Cdc53p/cullin catalyzes ubiquitination of the phosphorylated CDK inhibitor Sic1p. Cell *91*, 221-230.

Fischer, E. S., Scrima, A., Bohm, K., Matsumoto, S., Lingaraju, G. M., Faty, M., Yasuda, T., Cavadini, S., Wakasugi, M., Hanaoka, F.*, et al.* (2011). The molecular basis of CRL4DDB2/CSA ubiquitin ligase architecture, targeting, and activation. Cell *147*, 1024-1039.

Fiser, A., and Sali, A. (2003). Modeller: generation and refinement of homology-based protein structure models. Methods Enzymol *374*, 461-491.

Flores-Saaib, R. D., and Courey, A. J. (2000). Analysis of Groucho-histone interactions suggests mechanistic similarities between Groucho- and Tup1-mediated repression. Nucleic Acids Res *28*, 4189-4196.

Fu, M., Rao, M., Bouras, T., Wang, C., Wu, K., Zhang, X., Li, Z., Yao, T. P., and Pestell, R. G. (2005). Cyclin D1 inhibits peroxisome proliferator-activated receptor gamma-mediated adipogenesis through histone deacetylase recruitment. J Biol Chem *280*, 16934-16941.

Furukawa, M., He, Y. J., Borchers, C., and Xiong, Y. (2003). Targeting of protein ubiquitination by BTB-Cullin 3-Roc1 ubiquitin ligases. Nat Cell Biol *5*, 1001-1007.

Gagne, J. M., Downes, B. P., Shiu, S. H., Durski, A. M., and Vierstra, R. D. (2002). The F-box subunit of the SCF E3 complex is encoded by a diverse superfamily of genes in Arabidopsis. Proc Natl Acad Sci U S A *99*, 11519-11524.

Galgani, J. E., Kelley, D. E., Albu, J. B., Krakoff, J., Smith, S. R., Bray, G. A., and Ravussin, E. (2013). Adipose tissue expression of adipose (WDTC1) gene is associated with lower fat mass and enhanced insulin sensitivity in humans. Obesity (Silver Spring).

Geyer, R., Wee, S., Anderson, S., Yates, J., and Wolf, D. A. (2003). BTB/POZ domain proteins are putative substrate adaptors for cullin 3 ubiquitin ligases. Mol Cell *12*, 783-790.

Goldenberg, S. J., Cascio, T. C., Shumway, S. D., Garbutt, K. C., Liu, J., Xiong, Y., and Zheng, N. (2004). Structure of the Cand1-Cul1-Roc1 complex reveals regulatory mechanisms for the assembly of the multisubunit cullin-dependent ubiquitin ligases. Cell *119*, 517-528.

Goldknopf, I. L., and Busch, H. (1977). Isopeptide linkage between nonhistone and histone 2A polypeptides of chromosomal conjugate-protein A24. Proc Natl Acad Sci U S A *74*, 864-868.

Goldknopf, I. L., Taylor, C. W., Baum, R. M., Yeoman, L. C., Olson, M. O., Prestayko, A. W., and Busch, H. (1975). Isolation and characterization of protein A24, a "histone-like" non-histone chromosomal protein. J Biol Chem *250*, 7182-7187.

Graner, E., Tang, D., Rossi, S., Baron, A., Migita, T., Weinstein, L. J., Lechpammer, M., Huesken, D., Zimmermann, J., Signoretti, S., and Loda, M. (2004). The isopeptidase USP2a regulates the stability of fatty acid synthase in prostate cancer. Cancer Cell *5*, 253-261.

Grbavec, D., Lo, R., Liu, Y., Greenfield, A., and Stifani, S. (1999). Groucho/transducin-like enhancer of split (TLE) family members interact with the yeast transcriptional co-repressor SSN6 and mammalian SSN6-related proteins: implications for evolutionary conservation of transcription repression mechanisms. Biochem J *337 (Pt 1)*, 13-17.

Green, H., and Meuth, M. (1974). An established pre-adipose cell line and its differentiation in culture. Cell *3*, 127-133.

Groettrup, M., Pelzer, C., Schmidtke, G., and Hofmann, K. (2008). Activating the ubiquitin family: UBA6 challenges the field. Trends Biochem Sci *33*, 230-237.

Groisman, R., Kuraoka, I., Chevallier, O., Gaye, N., Magnaldo, T., Tanaka, K., Kisselev, A. F., Harel-Bellan, A., and Nakatani, Y. (2006). CSA-dependent degradation of CSB by the ubiquitin-proteasome pathway establishes a link between complementation factors of the Cockayne syndrome. Genes Dev *20*, 1429-1434.

Groisman, R., Polanowska, J., Kuraoka, I., Sawada, J., Saijo, M., Drapkin, R., Kisselev, A. F., Tanaka, K., and Nakatani, Y. (2003). The ubiquitin ligase activity in the DDB2 and CSA complexes is differentially regulated by the COP9 signalosome in response to DNA damage. Cell *113*, 357-367.

Guerrero-Santoro, J., Kapetanaki, M. G., Hsieh, C. L., Gorbachinsky, I., Levine, A. S., and Rapic-Otrin, V. (2008). The cullin 4B-based UV-damaged DNA-binding protein ligase binds to UV-damaged chromatin and ubiquitinates histone H2A. Cancer Res *68*, 5014-5022.

Hader, T., Muller, S., Aguilera, M., Eulenberg, K. G., Steuernagel, A., Ciossek, T., Kuhnlein, R. P., Lemaire, L., Fritsch, R., Dohrmann, C*., et al.* (2003). Control of triglyceride storage by a WD40/TPR-domain protein. EMBO Rep *4*, 511-516.

Hammond-Martel, I., Yu, H., and Affar el, B. (2012). Roles of ubiquitin signaling in transcription regulation. Cell Signal *24*, 410-421.

Harper, J. W., and Tan, M. K. (2012). Understanding cullin-RING E3 biology through proteomics-based substrate identification. Mol Cell Proteomics *11*, 1541-1550.

He, Y. J., McCall, C. M., Hu, J., Zeng, Y., and Xiong, Y. (2006). DDB1 functions as a linker to recruit receptor WD40 proteins to CUL4-ROC1 ubiquitin ligases. Genes Dev *20*, 2949-2954.

Hershko, A. (1983). Ubiquitin: roles in protein modification and breakdown. Cell *34*, 11-12.

Hicke, L. (2001). Protein regulation by monoubiquitin. Nat Rev Mol Cell Biol *2*, 195-201.

Higa, L. A., Banks, D., Wu, M., Kobayashi, R., Sun, H., and Zhang, H. (2006a). L2DTL/CDT2 interacts with the CUL4/DDB1 complex and PCNA and regulates CDT1 proteolysis in response to DNA damage. Cell Cycle *5*, 1675-1680.

Higa, L. A., Wu, M., Ye, T., Kobayashi, R., Sun, H., and Zhang, H. (2006b). CUL4-DDB1 ubiquitin ligase interacts with multiple WD40-repeat proteins and regulates histone methylation. Nat Cell Biol *8*, 1277-1283.

Higa, L. A., and Zhang, H. (2007). Stealing the spotlight: CUL4-DDB1 ubiquitin ligase docks WD40-repeat proteins to destroy. Cell Div *2*, 5.

Hori, T., Osaka, F., Chiba, T., Miyamoto, C., Okabayashi, K., Shimbara, N., Kato, S., and Tanaka, K. (1999). Covalent modification of all members of human cullin family proteins by NEDD8. Oncogene *18*, 6829-6834.

Horn, P. J., Bastie, J. N., and Peterson, C. L. (2005). A Rik1-associated, cullin-dependent E3 ubiquitin ligase is essential for heterochromatin formation. Genes Dev *19*, 1705-1714.

Hu, H., Yang, Y., Ji, Q., Zhao, W., Jiang, B., Liu, R., Yuan, J., Liu, Q., Li, X., Zou, Y.*, et al.* (2012). CRL4B catalyzes H2AK119 monoubiquitination and coordinates with PRC2 to promote tumorigenesis. Cancer Cell *22*, 781-795.

Hu, J., McCall, C. M., Ohta, T., and Xiong, Y. (2004). Targeted ubiquitination of CDT1 by the DDB1-CUL4A-ROC1 ligase in response to DNA damage. Nat Cell Biol *6*, 1003-1009.

Hu, J., Zacharek, S., He, Y. J., Lee, H., Shumway, S., Duronio, R. J., and Xiong, Y. (2008). WD40 protein FBW5 promotes ubiquitination of tumor suppressor TSC2 by DDB1-CUL4-ROC1 ligase. Genes Dev *22*, 866-871.

Husnjak, K., and Dikic, I. (2012). Ubiquitin-binding proteins: decoders of ubiquitin-mediated cellular functions. Annu Rev Biochem *81*, 291-322.

Hwang, J. W., Min, K. W., Tamura, T. A., and Yoon, J. B. (2003). TIP120A associates with unneddylated cullin 1 and regulates its neddylation. FEBS Lett *541*, 102-108.

Ivan, M., Kondo, K., Yang, H., Kim, W., Valiando, J., Ohh, M., Salic, A., Asara, J. M., Lane, W. S., and Kaelin, W. G., Jr. (2001). HIFalpha targeted for VHL-mediated destruction by proline hydroxylation: implications for O2 sensing. Science *292*, 464-468.

Jackson, S., and Xiong, Y. (2009). CRL4s: the CUL4-RING E3 ubiquitin ligases. Trends Biochem Sci *34*, 562-570.

Jennings, B. H., and Ish-Horowicz, D. (2008). The Groucho/TLE/Grg family of transcriptional co-repressors. Genome Biol *9*, 205.

Jia, S., Kobayashi, R., and Grewal, S. I. (2005). Ubiquitin ligase component Cul4 associates with Clr4 histone methyltransferase to assemble heterochromatin. Nat Cell Biol *7*, 1007-1013.

Jiang, B., Zhao, W., Yuan, J., Qian, Y., Sun, W., Zou, Y., Guo, C., Chen, B., Shao, C., and Gong, Y. (2012a). Lack of Cul4b, an E3 ubiquitin ligase component, leads to embryonic lethality and abnormal placental development. PLoS One *7*, e37070.

Jiang, Y., Jo, A. Y., and Graff, J. M. (2012b). SnapShot: adipocyte life cycle. Cell *150*, 234-234 e232.

Jin, J., Arias, E. E., Chen, J., Harper, J. W., and Walter, J. C. (2006). A family of diverse Cul4-Ddb1-interacting proteins includes Cdt2, which is required for S phase destruction of the replication factor Cdt1. Mol Cell *23*, 709-721.

Jin, J., Li, X., Gygi, S. P., and Harper, J. W. (2007). Dual E1 activation systems for ubiquitin differentially regulate E2 enzyme charging. Nature *447*, 1135-1138.

Jonnalagadda, S., Butt, T. R., Monia, B. P., Mirabelli, C. K., Gotlib, L., Ecker, D. J., and Crooke, S. T. (1989). Multiple (alpha-NH-ubiquitin)protein endoproteases in cells. J Biol Chem *264*, 10637-10642.

Kamura, T., Conrad, M. N., Yan, Q., Conaway, R. C., and Conaway, J. W. (1999a). The Rbx1 subunit of SCF and VHL E3 ubiquitin ligase activates Rub1 modification of cullins Cdc53 and Cul2. Genes Dev *13*, 2928-2933.

Kamura, T., Koepp, D. M., Conrad, M. N., Skowyra, D., Moreland, R. J., Iliopoulos, O., Lane, W. S., Kaelin, W. G., Jr., Elledge, S. J., Conaway, R. C*., et al.* (1999b). Rbx1, a component of the VHL tumor suppressor complex and SCF ubiquitin ligase. Science *284*, 657-661.

Kamura, T., Maenaka, K., Kotoshiba, S., Matsumoto, M., Kohda, D., Conaway, R. C., Conaway, J. W., and Nakayama, K. I. (2004). VHL-box and SOCS-box domains determine binding specificity for Cul2-Rbx1 and Cul5-Rbx2 modules of ubiquitin ligases. Genes Dev *18*, 3055-3065.

Kapetanaki, M. G., Guerrero-Santoro, J., Bisi, D. C., Hsieh, C. L., Rapic-Otrin, V., and Levine, A. S. (2006). The DDB1-CUL4ADDB2 ubiquitin ligase is deficient in xeroderma pigmentosum group E and targets histone H2A at UV-damaged DNA sites. Proc Natl Acad Sci U S A *103*, 2588-2593.

Kerscher, O., Felberbaum, R., and Hochstrasser, M. (2006). Modification of proteins by ubiquitin and ubiquitin-like proteins. Annu Rev Cell Dev Biol *22*, 159-180.

Kim, W., Bennett, E. J., Huttlin, E. L., Guo, A., Li, J., Possemato, A., Sowa, M. E., Rad, R., Rush, J., Comb, M. J*., et al.* (2011). Systematic and quantitative assessment of the ubiquitin-modified proteome. Mol Cell *44*, 325-340.

Kipreos, E. T., Lander, L. E., Wing, J. P., He, W. W., and Hedgecock, E. M. (1996). cul-1 is required for cell cycle exit in C. elegans and identifies a novel gene family. Cell *85*, 829-839.

Komander, D., and Rape, M. (2012). The ubiquitin code. Annu Rev Biochem *81*, 203-229.

Kopanja, D., Stoyanova, T., Okur, M. N., Huang, E., Bagchi, S., and Raychaudhuri, P. (2009). Proliferation defects and genome instability in cells lacking Cul4A. Oncogene *28*, 2456-2465.

Kotake, Y., Cao, R., Viatour, P., Sage, J., Zhang, Y., and Xiong, Y. (2007). pRB family proteins are required for H3K27 trimethylation and Polycomb repression complexes binding to and silencing p16INK4alpha tumor suppressor gene. Genes Dev *21*, 49-54.

Kouzarides, T. (2007). Chromatin modifications and their function. Cell *128*, 693-705.

Krebs, A. R., Demmers, J., Karmodiya, K., Chang, N. C., Chang, A. C., and Tora, L. (2010). ATAC and Mediator coactivators form a stable complex and regulate a set of non-coding RNA genes. EMBO Rep *11*, 541-547.

Kuchay, S., Duan, S., Schenkein, E., Peschiaroli, A., Saraf, A., Florens, L., Washburn, M. P., and Pagano, M. (2013). FBXL2- and PTPL1-mediated degradation of p110-free p85beta regulatory subunit controls the PI(3)K signalling cascade. Nat Cell Biol *15*, 472-480.

Kulathu, Y., and Komander, D. (2012). Atypical ubiquitylation - the unexplored world of polyubiquitin beyond Lys48 and Lys63 linkages. Nat Rev Mol Cell Biol *13*, 508-523.

Kurz, T., Chou, Y. C., Willems, A. R., Meyer-Schaller, N., Hecht, M. L., Tyers, M., Peter, M., and Sicheri, F. (2008). Dcn1 functions as a scaffold-type E3 ligase for cullin neddylation. Mol Cell *29*, 23-35.

Lai, C. Q., Parnell, L. D., Arnett, D. K., Garcia-Bailo, B., Tsai, M. Y., Kabagambe, E. K., Straka, R. J., Province, M. A., An, P., Borecki, I. B.*, et al.* (2009). WDTC1, the ortholog of Drosophila adipose gene, associates with human obesity, modulated by MUFA intake. Obesity (Silver Spring) *17*, 593-600.

Lee, J., Saha, P. K., Yang, Q. H., Lee, S., Park, J. Y., Suh, Y., Lee, S. K., Chan, L., Roeder, R. G., and Lee, J. W. (2008). Targeted inactivation of MLL3 histone H3-Lys-4 methyltransferase activity in the mouse reveals vital roles for MLL3 in adipogenesis. Proc Natl Acad Sci U S A *105*, 19229-19234.

Lee, P. C., Dodart, J. C., Aron, L., Finley, L. W., Bronson, R. T., Haigis, M. C., Yankner, B. A., and Harper, J. W. (2013). Altered social behavior and neuronal development in mice lacking the Uba6-Use1 ubiquitin transfer system. Mol Cell *50*, 172-184.

Li, T., Chen, X., Garbutt, K. C., Zhou, P., and Zheng, N. (2006). Structure of DDB1 in complex with a paramyxovirus V protein: viral hijack of a propeller cluster in ubiquitin ligase. Cell *124*, 105-117.

Li, T., Robert, E. I., van Breugel, P. C., Strubin, M., and Zheng, N. (2010). A promiscuous alpha-helical motif anchors viral hijackers and substrate receptors to the CUL4-DDB1 ubiquitin ligase machinery. Nat Struct Mol Biol *17*, 105-111.

Li, X., Lu, D., He, F., Zhou, H., Liu, Q., Wang, Y., Shao, C., and Gong, Y. (2011). Cullin 4B protein ubiquitin ligase targets peroxiredoxin III for degradation. J Biol Chem *286*, 32344-32354.

Liu, H., Liu, J. Y., Wu, X., and Zhang, J. T. (2010). Biochemistry, molecular biology, and pharmacology of fatty acid synthase, an emerging therapeutic target and diagnosis/prognosis marker. Int J Biochem Mol Biol *1*, 69-89.

Liu, J., Furukawa, M., Matsumoto, T., and Xiong, Y. (2002). NEDD8 modification of CUL1 dissociates p120(CAND1), an inhibitor of CUL1-SKP1 binding and SCF ligases. Mol Cell *10*, 1511-1518.

Liu, L., Lee, S., Zhang, J., Peters, S. B., Hannah, J., Zhang, Y., Yin, Y., Koff, A., Ma, L., and Zhou, P. (2009). CUL4A abrogation augments DNA damage response and protection against skin carcinogenesis. Mol Cell *34*, 451-460.

Lyapina, S., Cope, G., Shevchenko, A., Serino, G., Tsuge, T., Zhou, C., Wolf, D. A., Wei, N., and Deshaies, R. J. (2001). Promotion of NEDD-CUL1 conjugate cleavage by COP9 signalosome. Science *292*, 1382-1385.

MacDougald, O. A., and Lane, M. D. (1995). Transcriptional regulation of gene expression during adipocyte differentiation. Annu Rev Biochem *64*, 345-373.

Malave, T. M., and Dent, S. Y. (2006). Transcriptional repression by Tup1-Ssn6. Biochem Cell Biol *84*, 437-443.

Mathias, N., Johnson, S. L., Winey, M., Adams, A. E., Goetsch, L., Pringle, J. R., Byers, B., and Goebl, M. G. (1996). Cdc53p acts in concert with Cdc4p and Cdc34p to control the G1-to-S-phase transition and identifies a conserved family of proteins. Mol Cell Biol *16*, 6634-6643.

McDowell, G. S., and Philpott, A. (2013). Non-canonical ubiquitylation: Mechanisms and consequences. Int J Biochem Cell Biol *45*, 1833-1842.

Mendez, J., and Stillman, B. (2000). Chromatin association of human origin recognition complex, cdc6, and minichromosome maintenance proteins during the cell cycle: assembly of prereplication complexes in late mitosis. Mol Cell Biol *20*, 8602-8612.

Menendez, J. A., and Lupu, R. (2007). Fatty acid synthase and the lipogenic phenotype in cancer pathogenesis. Nat Rev Cancer *7*, 763-777.

Metzger, M. B., Hristova, V. A., and Weissman, A. M. (2012). HECT and RING finger families of E3 ubiquitin ligases at a glance. J Cell Sci *125*, 531-537.

Mikkelsen, T. S., Xu, Z., Zhang, X., Wang, L., Gimble, J. M., Lander, E. S., and Rosen, E. D. (2010). Comparative epigenomic analysis of murine and human adipogenesis. Cell *143*, 156-169.

Min, K. W., Hwang, J. W., Lee, J. S., Park, Y., Tamura, T. A., and Yoon, J. B. (2003). TIP120A associates with cullins and modulates ubiquitin ligase activity. J Biol Chem *278*, 15905-15910.

Moustaid, N., and Sul, H. S. (1991). Regulation of expression of the fatty acid synthase gene in 3T3-L1 cells by differentiation and triiodothyronine. J Biol Chem *266*, 18550-18554.

Nag, A., Bondar, T., Shiv, S., and Raychaudhuri, P. (2001). The xeroderma pigmentosum group E gene product DDB2 is a specific target of cullin 4A in mammalian cells. Mol Cell Biol *21*, 6738-6747.

Nakagawa, T., Kajitani, T., Togo, S., Masuko, N., Ohdan, H., Hishikawa, Y., Koji, T., Matsuyama, T., Ikura, T., Muramatsu, M., and Ito, T. (2008). Deubiquitylation of histone H2A activates transcriptional initiation via trans-histone cross-talk with H3K4 di- and trimethylation. Genes Dev *22*, 37-49.

Nakagawa, T., and Xiong, Y. (2011). X-linked mental retardation gene CUL4B targets ubiquitylation of H3K4 methyltransferase component WDR5 and regulates neuronal gene expression. Mol Cell *43*, 381-391.

Nakayama, M., Kikuno, R., and Ohara, O. (2002). Protein-protein interactions between large proteins: two-hybrid screening using a functionally classified library composed of long cDNAs. Genome Res *12*, 1773-1784.

Nickel, B. E., and Davie, J. R. (1989). Structure of polyubiquitinated histone H2A. Biochemistry *28*, 964-968.

Nishitani, H., Shiomi, Y., Iida, H., Michishita, M., Takami, T., and Tsurimoto, T. (2008). CDK inhibitor p21 is degraded by a proliferating cell nuclear antigen-coupled Cul4-DDB1Cdt2 pathway during S phase and after UV irradiation. J Biol Chem *283*, 29045-29052.

O'Connell, B. C., and Harper, J. W. (2007). Ubiquitin proteasome system (UPS): what can chromatin do for you? Curr Opin Cell Biol *19*, 206-214.

Ohta, T., Michel, J. J., Schottelius, A. J., and Xiong, Y. (1999). ROC1, a homolog of APC11, represents a family of cullin partners with an associated ubiquitin ligase activity. Mol Cell *3*, 535-541.

Osaka, F., Saeki, M., Katayama, S., Aida, N., Toh, E. A., Kominami, K., Toda, T., Suzuki, T., Chiba, T., Tanaka, K., and Kato, S. (2000). Covalent modifier NEDD8 is essential for SCF ubiquitin-ligase in fission yeast. EMBO J *19*, 3475-3484.

Oshikawa, K., Matsumoto, M., Yada, M., Kamura, T., Hatakeyama, S., and Nakayama, K. I. (2003). Preferential interaction of TIP120A with Cul1 that is not modified by NEDD8 and not associated with Skp1. Biochem Biophys Res Commun *303*, 1209-1216.

Pelzer, C., Kassner, I., Matentzoglu, K., Singh, R. K., Wollscheid, H. P., Scheffner, M., Schmidtke, G., and Groettrup, M. (2007). UBE1L2, a novel E1 enzyme specific for ubiquitin. J Biol Chem *282*, 23010-23014.

Petroski, M. D. (2008). The ubiquitin system, disease, and drug discovery. BMC Biochem *9 Suppl 1*, S7.

Petroski, M. D., and Deshaies, R. J. (2005). Function and regulation of cullin-RING ubiquitin ligases. Nat Rev Mol Cell Biol *6*, 9-20.

Picard, F., Kurtev, M., Chung, N., Topark-Ngarm, A., Senawong, T., Machado De Oliveira, R., Leid, M., McBurney, M. W., and Guarente, L. (2004). Sirt1 promotes fat mobilization in white adipocytes by repressing PPAR-gamma. Nature *429*, 771-776.

Pickart, C. M. (2001a). Mechanisms underlying ubiquitination. Annu Rev Biochem *70*, 503-533.

Pickart, C. M. (2001b). Ubiquitin enters the new millennium. Mol Cell *8*, 499-504.

Pickart, C. M. (2004). Back to the future with ubiquitin. Cell *116*, 181-190.

Pickart, C. M., and Eddins, M. J. (2004). Ubiquitin: structures, functions, mechanisms. Biochim Biophys Acta *1695*, 55-72.

Pierce, N. W., Lee, J. E., Liu, X., Sweredoski, M. J., Graham, R. L., Larimore, E. A., Rome, M., Zheng, N., Clurman, B. E., Hess, S.*, et al.* (2013). Cand1 promotes assembly of new SCF complexes through dynamic exchange of F box proteins. Cell *153*, 206-215.

Pintard, L., Willems, A., and Peter, M. (2004). Cullin-based ubiquitin ligases: Cul3-BTB complexes join the family. EMBO J *23*, 1681-1687.

Pintard, L., Willis, J. H., Willems, A., Johnson, J. L., Srayko, M., Kurz, T., Glaser, S., Mains, P. E., Tyers, M., Bowerman, B., and Peter, M. (2003). The BTB protein MEL-26 is a substrate-specific adaptor of the CUL-3 ubiquitin-ligase. Nature *425*, 311-316.

Ralph, E., Boye, E., and Kearsey, S. E. (2006). DNA damage induces Cdt1 proteolysis in fission yeast through a pathway dependent on Cdt2 and Ddb1. EMBO Rep *7*, 1134-1139.

Rapic-Otrin, V., Navazza, V., Nardo, T., Botta, E., McLenigan, M., Bisi, D. C., Levine, A. S., and Stefanini, M. (2003). True XP group E patients have a defective UV-damaged DNA binding protein complex and mutations in DDB2 which reveal the functional domains of its p48 product. Hum Mol Genet *12*, 1507-1522.

Rodrigo-Brenni, M. C., Foster, S. A., and Morgan, D. O. (2010). Catalysis of lysine 48-specific ubiquitin chain assembly by residues in E2 and ubiquitin. Mol Cell *39*, 548-559.

Rosen, E. D., and MacDougald, O. A. (2006). Adipocyte differentiation from the inside out. Nat Rev Mol Cell Biol *7*, 885-896.

Rotin, D., and Kumar, S. (2009). Physiological functions of the HECT family of ubiquitin ligases. Nat Rev Mol Cell Biol *10*, 398-409.

Saha, A., and Deshaies, R. J. (2008). Multimodal activation of the ubiquitin ligase SCF by Nedd8 conjugation. Mol Cell *32*, 21-31.

Sansam, C. L., Shepard, J. L., Lai, K., Ianari, A., Danielian, P. S., Amsterdam, A., Hopkins, N., and Lees, J. A. (2006). DTL/CDT2 is essential for both CDT1 regulation and the early G2/M checkpoint. Genes Dev *20*, 3117-3129.

Sarikas, A., Hartmann, T., and Pan, Z. Q. (2011). The cullin protein family. Genome Biol *12*, 220.

Schuettengruber, B., and Cavalli, G. (2009). Recruitment of polycomb group complexes and their role in the dynamic regulation of cell fate choice. Development *136*, 3531-3542.

Scrima, A., Konickova, R., Czyzewski, B. K., Kawasaki, Y., Jeffrey, P. D., Groisman, R., Nakatani, Y., Iwai, S., Pavletich, N. P., and Thoma, N. H. (2008). Structural basis of UV DNA-damage recognition by the DDB1-DDB2 complex. Cell *135*, 1213-1223.

Semenkovich, C. F. (1997). Regulation of fatty acid synthase (FAS). Prog Lipid Res *36*, 43-53.

Seol, J. H., Feldman, R. M., Zachariae, W., Shevchenko, A., Correll, C. C., Lyapina, S., Chi, Y., Galova, M., Claypool, J., Sandmeyer, S.*, et al.* (1999). Cdc53/cullin and the essential Hrt1 RING-H2 subunit of SCF define a ubiquitin ligase module that activates the E2 enzyme Cdc34. Genes Dev *13*, 1614-1626.

Shibutani, S. T., de la Cruz, A. F., Tran, V., Turbyfill, W. J., 3rd, Reis, T., Edgar, B. A., and Duronio, R. J. (2008). Intrinsic negative cell cycle regulation provided by PIP box- and Cul4Cdt2-mediated destruction of E2f1 during S phase. Dev Cell *15*, 890-900.

Shiyanov, P., Nag, A., and Raychaudhuri, P. (1999). Cullin 4A associates with the UV-damaged DNA-binding protein DDB. J Biol Chem *274*, 35309-35312.

Skaar, J. R., Pagan, J. K., and Pagano, M. (2009). SnapShot: F box proteins I. Cell *137*, 1160-1160 e1161.

Skowyra, D., Craig, K. L., Tyers, M., Elledge, S. J., and Harper, J. W. (1997). F-box proteins are receptors that recruit phosphorylated substrates to the SCF ubiquitin-ligase complex. Cell *91*, 209-219.

Soding, J. (2005). Protein homology detection by HMM-HMM comparison. Bioinformatics *21*, 951-960.

Soucy, T. A., Smith, P. G., Milhollen, M. A., Berger, A. J., Gavin, J. M., Adhikari, S., Brownell, J. E., Burke, K. E., Cardin, D. P., Critchley, S.*, et al.* (2009). An inhibitor of NEDD8-activating enzyme as a new approach to treat cancer. Nature *458*, 732-736.

Steger, D. J., Grant, G. R., Schupp, M., Tomaru, T., Lefterova, M. I., Schug, J., Manduchi, E., Stoeckert, C. J., Jr., and Lazar, M. A. (2010). Propagation of adipogenic signals through an epigenomic transition state. Genes Dev *24*, 1035-1044.

Student, A. K., Hsu, R. Y., and Lane, M. D. (1980). Induction of fatty acid synthetase synthesis in differentiating 3T3-L1 preadipocytes. J Biol Chem *255*, 4745-4750.

Sugasawa, K., Okuda, Y., Saijo, M., Nishi, R., Matsuda, N., Chu, G., Mori, T., Iwai, S., Tanaka, K., and Hanaoka, F. (2005). UV-induced ubiquitylation of XPC protein mediated by UV-DDB-ubiquitin ligase complex. Cell *121*, 387-400.

Suh, J. M., Zeve, D., McKay, R., Seo, J., Salo, Z., Li, R., Wang, M., and Graff, J. M. (2007). Adipose is a conserved dosage-sensitive antiobesity gene. Cell Metab *6*, 195-207.

Sun, K., Kusminski, C. M., and Scherer, P. E. (2011). Adipose tissue remodeling and obesity. J Clin Invest *121*, 2094-2101.

Sundqvist, A., Bengoechea-Alonso, M. T., Ye, X., Lukiyanchuk, V., Jin, J., Harper, J. W., and Ericsson, J. (2005). Control of lipid metabolism by phosphorylation-dependent degradation of the SREBP family of transcription factors by SCF(Fbw7). Cell Metab *1*, 379-391.

Tan, M., Davis, S. W., Saunders, T. L., Zhu, Y., and Sun, Y. (2009). RBX1/ROC1 disruption results in early embryonic lethality due to proliferation failure, partially rescued by simultaneous loss of p27. Proc Natl Acad Sci U S A *106*, 6203-6208.

Tan, P., Fuchs, S. Y., Chen, A., Wu, K., Gomez, C., Ronai, Z., and Pan, Z. Q. (1999). Recruitment of a ROC1-CUL1 ubiquitin ligase by Skp1 and HOS to catalyze the ubiquitination of I kappa B alpha. Mol Cell *3*, 527-533.

Tarpey, P. S., Raymond, F. L., O'Meara, S., Edkins, S., Teague, J., Butler, A., Dicks, E., Stevens, C., Tofts, C., Avis, T.*, et al.* (2007). Mutations in CUL4B, which encodes a ubiquitin E3 ligase subunit, cause an X-linked mental retardation syndrome associated with aggressive outbursts, seizures, relative macrocephaly, central obesity, hypogonadism, pes cavus, and tremor. Am J Hum Genet *80*, 345-352.

Teague, B. D., Clark, A. G., and Doane, W. W. (1986). Developmental analysis of lipids from wild-type and adipose60 mutants of Drosophila melanogaster. J Exp Zool *240*, 95-104.

Uetrecht, A. C., and Bear, J. E. (2009). Golgi polarity does not correlate with speed or persistence of freely migrating fibroblasts. Eur J Cell Biol *88*, 711-717.

van der Stoop, P., Boutsma, E. A., Hulsman, D., Noback, S., Heimerikx, M., Kerkhoven, R. M., Voncken, J. W., Wessels, L. F., and van Lohuizen, M. (2008). Ubiquitin E3 ligase Ring1b/Rnf2 of polycomb repressive complex 1 contributes to stable maintenance of mouse embryonic stem cells. PLoS One *3*, e2235.

Varshavsky, A. (2006). The early history of the ubiquitin field. Protein Sci *15*, 647-654.

Vissers, J. H., Nicassio, F., van Lohuizen, M., Di Fiore, P. P., and Citterio, E. (2008). The many faces of ubiquitinated histone H2A: insights from the DUBs. Cell Div *3*, 8.

Wang, H., Wang, L., Erdjument-Bromage, H., Vidal, M., Tempst, P., Jones, R. S., and Zhang, Y. (2004). Role of histone H2A ubiquitination in Polycomb silencing. Nature *431*, 873-878.

Wang, H., Zhai, L., Xu, J., Joo, H. Y., Jackson, S., Erdjument-Bromage, H., Tempst, P., Xiong, Y., and Zhang, Y. (2006). Histone H3 and H4 ubiquitylation by the CUL4-DDB-ROC1 ubiquitin ligase facilitates cellular response to DNA damage. Mol Cell *22*, 383-394.

Wang, L., Jin, Q., Lee, J. E., Su, I. H., and Ge, K. (2010). Histone H3K27 methyltransferase Ezh2 represses Wnt genes to facilitate adipogenesis. Proc Natl Acad Sci U S A *107*, 7317-7322.

Wang, L., Xu, S., Lee, J. E., Baldridge, A., Grullon, S., Peng, W., and Ge, K. (2013). Histone H3K9 methyltransferase G9a represses PPARgamma expression and adipogenesis. EMBO J *32*, 45-59.

Watson, A. D., Edmondson, D. G., Bone, J. R., Mukai, Y., Yu, Y., Du, W., Stillman, D. J., and Roth, S. Y. (2000). Ssn6-Tup1 interacts with class I histone deacetylases required for repression. Genes Dev *14*, 2737-2744.

Wertz, I. E., O'Rourke, K. M., Zhang, Z., Dornan, D., Arnott, D., Deshaies, R. J., and Dixit, V. M. (2004). Human De-etiolated-1 regulates c-Jun by assembling a CUL4A ubiquitin ligase. Science *303*, 1371-1374.

Xu, L., Wei, Y., Reboul, J., Vaglio, P., Shin, T. H., Vidal, M., Elledge, S. J., and Harper, J. W. (2003). BTB proteins are substrate-specific adaptors in an SCF-like modular ubiquitin ligase containing CUL-3. Nature *425*, 316-321.

Yang, X., Zhou, J., Sun, L., Wei, Z., Gao, J., Gong, W., Xu, R. M., Rao, Z., and Liu, Y. (2007). Structural basis for the function of DCN-1 in protein Neddylation. J Biol Chem *282*, 24490-24494.

Ye, Y., and Rape, M. (2009). Building ubiquitin chains: E2 enzymes at work. Nat Rev Mol Cell Biol *10*, 755-764.

Yu, X., Yu, Y., Liu, B., Luo, K., Kong, W., Mao, P., and Yu, X. F. (2003). Induction of APOBEC3G ubiquitination and degradation by an HIV-1 Vif-Cul5-SCF complex. Science *302*, 1056-1060.

Zhang, Y. (2003). Transcriptional regulation by histone ubiquitination and deubiquitination. Genes Dev *17*, 2733-2740.

Zheng, J., Yang, X., Harrell, J. M., Ryzhikov, S., Shim, E. H., Lykke-Andersen, K., Wei, N., Sun, H., Kobayashi, R., and Zhang, H. (2002a). CAND1 binds to unneddylated CUL1 and regulates the formation of SCF ubiquitin E3 ligase complex. Mol Cell *10*, 1519-1526.

Zheng, N., Schulman, B. A., Song, L., Miller, J. J., Jeffrey, P. D., Wang, P., Chu, C., Koepp, D. M., Elledge, S. J., Pagano, M*., et al.* (2002b). Structure of the Cul1-Rbx1-Skp1-F boxSkp2 SCF ubiquitin ligase complex. Nature *416*, 703-709.

Zhong, W., Feng, H., Santiago, F. E., and Kipreos, E. T. (2003). CUL-4 ubiquitin ligase maintains genome stability by restraining DNA-replication licensing. Nature *423*, 885-889.

Zhou, W., Wang, X., and Rosenfeld, M. G. (2009). Histone H2A ubiquitination in transcriptional regulation and DNA damage repair. Int J Biochem Cell Biol *41*, 12-15.

Zhou, W., Zhu, P., Wang, J., Pascual, G., Ohgi, K. A., Lozach, J., Glass, C. K., and Rosenfeld, M. G. (2008). Histone H2A monoubiquitination represses transcription by inhibiting RNA polymerase II transcriptional elongation. Mol Cell *29*, 69-80.

Zou, Y., Mi, J., Cui, J., Lu, D., Zhang, X., Guo, C., Gao, G., Liu, Q., Chen, B., Shao, C., and Gong, Y. (2009). Characterization of nuclear localization signal in the N terminus of CUL4B and its essential role in cyclin E degradation and cell cycle progression. J Biol Chem *284*, 33320-33332.